



2022

Biofilms on Plastic Litter: Community Composition and Activity and the Effects on Ecosystem Processes

Raul F. Lazcano

Follow this and additional works at: https://ecommons.luc.edu/luc_theses



Part of the [Biology Commons](#)

Recommended Citation

Lazcano, Raul F., "Biofilms on Plastic Litter: Community Composition and Activity and the Effects on Ecosystem Processes" (2022). *Master's Theses*. 4460.

https://ecommons.luc.edu/luc_theses/4460

This Thesis is brought to you for free and open access by the Theses and Dissertations at Loyola eCommons. It has been accepted for inclusion in Master's Theses by an authorized administrator of Loyola eCommons. For more information, please contact ecommons@luc.edu.



This work is licensed under a [Creative Commons Attribution-Noncommercial-No Derivative Works 3.0 License](#).
Copyright © 2022 Raul F Lazcano

LOYOLA UNIVERSITY CHICAGO

BIOFILMS ON PLASTIC LITTER:
COMMUNITY COMPOSITION AND ACTIVITY
AND THE EFFECTS ON ECOSYSTEM PROCESSES

A DISSERTATION SUBMITTED TO
THE FACULTY OF THE GRADUATE SCHOOL
IN CANDIDACY FOR THE DEGREE OF
MASTER OF SCIENCE

PROGRAM IN BIOLOGY

BY

RAÚL F. LAZCANO

CHICAGO, IL

DECEMBER 2022

Copyright by Raúl F. Lazcano, 2022
All rights reserved.

ACKNOWLEDGMENTS

This research was funded by the National Science Foundation Career grant (DEB1552825) as well as grants to Chelsea Rochman from the Department of Fisheries and Oceans National Contaminants Advisory Group and Environment and Climate Change Canada. I would like to thank my thesis advisor, Timothy Hoellein, and committee members John Kelly and Martin Berg for their guidance and advise. Thank you to Denise Bruesewitz, Kennedy Bucci, Rachel Cable, Audrey Eros, Ella Janson, Desiree Langenfeld, Rachel McNamee, Phil Nicodemus, David Richardson, Cody Veneruzzo, Nick Wesley, and Lauren Wisbrock for their assistance in the field and in the lab. Thank you to our collaborators Cyndy Desjardis, Lauren Hayhurst, Scott Higgins, Matthew Hoffman, Ken Jeffries, John Neall, Diane Orihel, Michael Paterson, Jennifer Provencher, Michael Rennie, and Chelsea Rochman. Thank you to REI Lincoln Park for allowing us to use their dock. Finally, thank you to all my professors in the Biology Department at Loyola University Chicago who inspired my love for Biology.

To my cat, Athena

TABLE OF CONTENTS

| | |
|---|------|
| ACKNOWLEDGMENTS | iii |
| LIST OF TABLES | vi |
| LIST OF FIGURES | viii |
| ABSTRACT | xi |
| CHAPTER I: INTRODUCTION | 1 |
| CHAPTER II: COMMUNITY COMPOSITION AND ACTIVITY OF BIOFILMS ON PLASTIC LITTER | 10 |
| Introduction | 10 |
| Methods | 13 |
| Results | 28 |
| Discussion | 69 |
| CHAPTER III: THE EFFECTS OF MICROPLASTIC ON ECOSYSTEM PROCESSES | 81 |
| Introduction | 81 |
| Methods | 83 |
| Results | 95 |
| Discussion | 115 |
| REFERENCE LIST | 126 |
| VITA | 145 |

LIST OF TABLES

| | |
|--|----|
| Table 1. Dimensions of each substrate of each size. | 19 |
| Table 2. Summary of physical and chemical measurements on the deployment date and each collection date. | 19 |
| Table 3. Aligned-rank-transform comparisons for each measurement type for each size. | 37 |
| Table 4. Results from 2-way ANOVA for bacterial ASV richness and ASV Shannon diversity and from ART for small ASV richness among material type and week for each size. | 42 |
| Table 5. Results from 2-way ANOVA for bacterial ASV richness and Shannon diversity among size and week for each material type. | 45 |
| Table 6. Results from full PERMANOVA on bacterial communities. | 48 |
| Table 7. Differentially abundant bacterial families between plastic and wood substrates in week 1 and the mean relative abundance (%). | 51 |
| Table 8. Differentially abundant bacterial families between plastic and wood substrates in week 3 and the mean relative abundance (%). | 53 |
| Table 9. Differentially abundant bacterial families between plastic and wood substrates in week 6 and the mean relative abundance (%). | 55 |
| Table 10. Results from 2-way ANOVA for algal large and medium ASV richness and ASV Shannon diversity and ART on algal small ASV richness and large and small ASV Shannon diversity among material type and week for each size. | 57 |
| Table 11. Results from 2-way ANOVA for bacterial ASV richness and Shannon diversity among size and week for each material type. | 60 |
| Table 12. Results from full PERMANOVA on algal communities as well as pairwise. | 63 |

| | |
|---|-----|
| Table 13. Differentially abundant algal families between plastic and wood substrates in week 1 and the mean relative abundance (%). | 66 |
| Table 14. Differentially abundant algal families between plastic and wood substrates in week 3 and the mean relative abundance (%). | 67 |
| Table 15. Differentially abundant algal families between plastic and wood substrates in week 6 and the mean relative abundance (%). | 68 |
| Table 16. Mass (g) and number of particles of PS, PET, and PE microplastic added to each mesocosm to reach the desired microplastic concentration (particles L ⁻¹) as well as the number of yellow perch (<i>Perca flavescens</i>) at the beginning and end of the study. | 94 |
| Table 17. Percent (%) chemical composition of each polymer type including additives. | 95 |
| Table 18. 1-way ANOVA results for ecosystem metabolism estimates, physical data in the mesocosm. | 99 |
| Table 19. 2-way ANOVA results for mesocosm abiotic N ₂ flux, mesocosm biotic N ₂ flux, and open water biotic N ₂ flux. ART results for mesocosm and open-water N ₂ concentration. | 100 |

LIST OF FIGURES

| | |
|---|----|
| Figure 1. Our predictions for biofilm community composition for: A) substrate type and B) substrate size. | 12 |
| Figure 2. Wood, rigid low-density polyethylene (LDPE), and foamed polystyrene (left to right) substrates of each size within mesh ‘sandwiches’ secured by zip ties. | 16 |
| Figure 3. Assembled raft showing randomized placements of substrates, the PVC pipe frame, and yellow floats. | 17 |
| Figure 4. Deployed raft showing substrates submerged near the water surface, attached to the seawall. | 18 |
| Figure 5. Timeseries of A) water temperature (°C) and B) illuminance (lx) measured by the HOBO logger attached to the raft for the entire range of the study. | 36 |
| Figure 6. Mean (\pm SE) respiration rates ($\text{mg O}_2 \text{ cm}^{-2} \text{ h}^{-1}$) over six-week period on A) large, B) medium and C) small substrates | 38 |
| Figure 7. Mean (\pm SE) optical density (cm^{-2}) of crystal violet (biomass) over six-week period on A) large, B) medium and C) small substrates. | 39 |
| Figure 8. Mean (\pm SE) chlorophyll concentration ($\mu\text{g cm}^{-2}$) over six-week period on A) large, B) medium and C) small substrates. | 40 |
| Figure 9. Mean (\pm SE) Nitrogen flux ($\mu\text{g N}_2 \text{ cm}^{-2} \text{ hr}^{-1}$) over six-week period on A) large, B) medium and C) small substrates. | 41 |
| Figure 10. Mean (\pm SE) bacterial ASV Richness on each material type for weeks 1, 3 and 6 on A) large, B) medium, and C) small substrates. | 43 |
| Figure 11. Mean (\pm SE) bacterial ASV Shannon diversity on each material type for weeks 1, 3 and 6 on A) large, B) medium, and C) small substrates. | 44 |
| Figure 12. Mean (\pm SE) bacterial ASV Richness on each material type for weeks 1, 3 and 6 on A) film, B) foam, C) rigid, and D) wood substrates. | 46 |

| | |
|---|-----|
| Figure 13. Mean (\pm SE) bacterial ASV Shannon diversity on each material type for weeks 1, 3 and 6 on A) film, B) foam, C) rigid, and D) wood substrates. | 47 |
| Figure 14. Nonmetric multidimensional scaling (NMDS) ordination of bacterial communities (Bray-Curtis dissimilarity) from substrates of four different material types and three different sizes in weeks 1, 3 and 6. | 48 |
| Figure 15. Mean relative abundance (%) of the top 20 bacterial families on each material type for weeks 1, 3 and 6. | 50 |
| Figure 16. Mean (\pm SE) algal ASV Richness on each material type for weeks 1, 3 and 6 on A) large, B) medium, and C) small substrates. | 58 |
| Figure 17. Mean (\pm SE) algal ASV Shannon diversity on each material type for weeks 1, 3 and 6 on A) large, B) medium, and C) small substrates. | 59 |
| Figure 18. Mean (\pm SE) algal ASV Richness on each material type for weeks 1, 3 and 6 on A) film, B) foam, C) rigid, and D) wood substrates. | 61 |
| Figure 19. Mean (\pm SE) algal ASV Richness on each material type for weeks 1, 3 and 6 on A) film, B) foam, C) rigid, and D) wood substrates. | 62 |
| Figure 20. Nonmetric multidimensional scaling (NMDS) ordination of algal communities (Bray-Curtis dissimilarity) from substrates of four different material types and three different sizes in weeks 1, 3 and 6. | 63 |
| Figure 21. Mean relative abundance (%) of the top 20 algal families on each material type for weeks 1, 3 and 6. | 65 |
| Figure 22. Timeseries from June 3 through August 10, 2021 of A) wind speed (m s^{-1}) and B) PAR ($\mu\text{mol m}^{-2} \text{s}^{-1}$). | 101 |
| Figure 23. Timeseries of physical data from June 3 through August 10, 2021, in each mesocosm. A) observed DO ($\text{mg O}_2 \text{L}^{-1}$), B) DO at 100% saturation ($\text{mg O}_2 \text{L}^{-1}$), C) O_2 transfer velocity (m day^{-1}), and D) water temperature ($^{\circ}\text{C}$). | 102 |
| Figure 24. Violin plots with boxplots for each mesocosm of A) observed DO ($\text{mg O}_2 \text{L}^{-1}$), B) DO at 100% saturation ($\text{mg O}_2 \text{L}^{-1}$), C) O_2 transfer velocity (m day^{-1}), and D) water temperature ($^{\circ}\text{C}$). | 103 |
| Figure 25. Timeseries from June 3 through August 10, 2021 of A) GPP ($\text{mg O}_2 \text{L}^{-1} \text{day}^{-1}$), B) R ($\text{mg O}_2 \text{L}^{-1} \text{day}^{-1}$), and C) NEP ($\text{mg O}_2 \text{L}^{-1} \text{day}^{-1}$). | 104 |
| Figure 26. Violin plots with boxplots ecosystem metabolism estimates for each mesocosm. | |

| | |
|---|-----|
| A) GPP ($\text{mg O}_2 \text{L}^{-1} \text{day}^{-1}$), B) R ($\text{mg O}_2 \text{L}^{-1} \text{day}^{-1}$), and C) NEP ($\text{mg O}_2 \text{L}^{-1} \text{day}^{-1}$). | 105 |
| Figure 27. Timeseries of measured N_2 concentration and N_2 concentration at saturation (mg L^{-1}), recorded hourly from August 3, 9:00 through August 4, 2021 9:00 for three mesocosms. A) mesocosm B (0 particles L^{-1}), B) mesocosm I (1710 particles L^{-1}), and C) mesocosm D (29240 particles L^{-1}). | 106 |
| Figure 28. Boxplots of N_2 concentration and flux at three mesocosms. A) Measured N_2 concentration and N_2 concentration at saturation (mg L^{-1}), B) abiotic N_2 flux by day and night and, C) biotic N_2 flux by day and night ($\text{mg N}_2 \text{L}^{-1} \text{hr}^{-1}$). | 107 |
| Figure 29. Boxplots of the difference between measured N_2 concentration and N_2 concentration at saturation ($\text{mg N}_2 \text{L}^{-1}$) in each mesocosm. | 108 |
| Figure 30. Temperature ($^{\circ}\text{C}$) profile of lake 378 by 1 m depth increments from 1 m to 15 m from May 11 through October 26, 2021. | 108 |
| Figure 31. Whole-lake timeseries of physical data from May,11 through September 22, 2021. | 109 |
| Figure 32. Violin plots with boxplots of physical data for the whole lake. A) observed DO ($\text{mg O}_2 \text{L}^{-1}$), B) DO at 100% saturation ($\text{mg O}_2 \text{L}^{-1}$), C) O_2 transfer velocity (m day^{-1}), and D) water temperature ($^{\circ}\text{C}$). | 110 |
| Figure 33. Whole-lake timeseries from May 12 through September 19, 2021 of A) GPP ($\text{mg O}_2 \text{L}^{-1} \text{day}^{-1}$), B) R ($\text{mg O}_2 \text{L}^{-1} \text{day}^{-1}$), and C) NEP ($\text{mg O}_2 \text{L}^{-1} \text{day}^{-1}$). | 111 |
| Figure 34. Violin plots with boxplots of ecosystem metabolism estimates for the whole lake. A) GPP ($\text{mg O}_2 \text{L}^{-1} \text{day}^{-1}$), B) R ($\text{mg O}_2 \text{L}^{-1} \text{day}^{-1}$), and C) NEP ($\text{mg O}_2 \text{L}^{-1} \text{day}^{-1}$). | 112 |
| Figure 35. Timeseries of measured N_2 concentration and N_2 concentration at saturation (mg L^{-1}), recorded hourly from August 3 9:00 through August 4, 2021 9:00 in A) the epilimnion and B) the hypolimnion. | 113 |
| Figure 36. Boxplots of N_2 concentration and flux at the two lake layers. A) Measured N_2 concentration and N_2 concentration at saturation (mg L^{-1}), B) abiotic N_2 flux by day and night and, C) biotic N_2 flux by day and night ($\text{mg N}_2 \text{L}^{-1} \text{hr}^{-1}$). | 114 |
| Figure 37. Boxplot of the difference between measured N_2 concentration and N_2 concentration at saturation ($\text{mg N}_2 \text{L}^{-1}$) at each lake layer. | 115 |

ABSTRACT

The rapid increase of plastic production and disposal has resulted in plastic pollution becoming a global problem. In aquatic ecosystems, plastic litter is a substrate for biofilms, but little research has simultaneously assessed the effects of plastic litter on biofilm activity, community composition, and ecosystem processes. Our objectives were to: (1) measure biofilm activity and community composition on plastic litter relative to a natural surface in an urban river and (2) assess the impact of microplastic pollution on ecosystem metabolism and N_2 flux in an oligotrophic lake. For objective (1) we incubated three common plastics with distinct physical and chemical properties and wood at three sizes. Biofilm activity was similar among substrates, except respiration was greater on wood. Bacterial and algal richness and diversity were highest on foam and wood substrates compared to film and firm polyethylene. Bacterial biofilm community composition was distinct between wood and plastic substrates while the algal community was distinct on both foam and wood. Substrate size had no influence on either algal or bacterial community composition. Overall, results demonstrate polymer properties influence biofilm alpha and beta diversity, which may affect transport and distribution of plastic pollution and associated microbes, as well as biogeochemical processes in urban streams. For objective (2), we added microplastics to pelagic mesocosms at a range of concentrations. Ecosystem metabolism rates were low, as expected for an oligotrophic lake, and similar across microplastic treatments. N_2 was undersaturated in all treatments and showed no differences by microplastic concentration. Our results suggested minimal impact of microplastic on ecosystem metabolism

and N₂ flux in an oligotrophic lake. These data will be combined with results from collaborators on the larger project that assessed the role of microplastics at other levels of organization, including water chemistry, plankton, and fish. This study provides valuable insights into the effects of substrate on biofilm characteristics, the ecological impacts of plastic pollution in urban rivers, and is a novel addition to the literature as an assessment of the impacts of microplastic pollution on ecosystem-scale processes through *in situ* microplastic addition.

CHAPTER I

INTRODUCTION

Plastic Pollution

Plastics are hydrocarbon polymers derived from fossil fuels that can be made into flexible or rigid items as well as adhesives, foams, and fibers (Napper & Thompson, 2020). Since the 1950s, plastic production has been increasing at a compound rate of 8.4% per year (Geyer et al., 2017) and in 2021 annual plastic production reached 367 Mt (Plastics Europe 2021). This accelerating rate of production is due to plastics low production cost, durability, low weight, versatility, and malleability (Andrady & Neal, 2009; Napper & Thompson, 2020). In addition, the plastic industry generates substantial economic benefits. In the United States alone the plastic industry provided 945,300 jobs and generated \$394.7 billion from plastic shipments in 2020 (PLASTICS 2021). Key use sectors of plastic include packaging, textiles, and consumer products (Geyer et al., 2017). However, the benefits plastics have provided modern society have not been without consequence.

Plastic pollution has become a major concern across the world. After its use, plastic can be recycled, incinerated, or discarded in landfills or the environment (Geyer et al., 2017). Approximately 79% of plastic waste produced since 1950 was discarded to landfills or the environment. The durability and recalcitrance of plastic make its degradation in the environment very slow (Chamas et al., 2020; Gewert et al., 2015). Though these properties may be beneficial

in an industrial context, they allow plastic to persist in the environment and be transported great distances (Barnes et al., 2009; Ryan et al., 2009; Vincent & Hoellein, 2021). Microplastics are a major component of the field of study that focuses on plastic pollution. Microplastics are typically defined as synthetic particles ranging in size from 1 μm to 5 mm (Frias & Nash, 2019). Microplastics can be a range of shapes including fibers, fragments, microbeads, and pellets. Microplastic origin can be either primary or secondary (Frias & Nash, 2019; Rochman et al., 2019). Primary microplastics include production pellets which are used to make larger plastic items and microbeads which are used in personal care products (Rochman et al., 2019). Secondary microplastics result from the fragmentation of larger plastics by physical, biological, or chemical processes (Rochman et al., 2019).

Plastic Pollution in Freshwater

Plastic litter enters freshwater through a range of sources, including effluent from wastewater, stormwater run-off, combined sewer outfalls and atmospheric deposition (Lebreton et al., 2017; Windsor et al., 2019). Freshwater near urban areas can accumulate high concentrations of plastic litter that can then be either transported or retained (Horton et al., 2017; McCormick & Hoellein, 2016). Each year approximately 1.15-2.41 million tons of plastic enter the world's oceans through rivers, a component of the global plastic budget that is expected to increase in the coming decades (Lebreton et al., 2017; Mai et al., 2020). Besides acting as conduits of plastic to downstream ecosystems, rivers can also retain plastic, which facilitates biological interactions between plastic litter and freshwater organisms (Windsor et al., 2019). Whether plastic litter is moving or retained in freshwater systems it will interact with the

chemical and biological components of freshwater ecosystems (Hoellein et al., 2017a; Hoellein & Rochman, 2021; Vincent & Hoellein, 2021).

In freshwater, plastic pollution interacts with aquatic organisms through numerous mechanisms. Aquatic organisms can become entangled in plastic pollution which can impede their movement and respiration (Blettler & Wantzen, 2019; Gregory, 2009). Animals can ingest plastic litter (Gil-Delgado et al., 2017; E. R. Holland et al., 2016; Sanchez et al., 2014) which poses a direct threat through negative effects on feeding and reproduction (Foley et al., 2018; Horton et al., 2017; Lei et al., 2018). Additives to plastic such as bisphenol-A, phthalates, colorants, flame retardants and metals can be released into water or when plastic litter is in the digestive tract, which exposes aquatic organisms to them (Nakashima et al., 2012; Rochman et al., 2019). Additives such as phthalates and bisphenol-A are biologically active and act as endocrine disruptors (Mills & Chichester, 2005). Plastic litter can also serve as a habitat for a range of taxa, including animals, algae, and bacteria (Gregory, 2009).

Plastic Pollution and Biofilms

Plastic litter provides a novel substrate that is well colonized by microbial biofilms in freshwater ecosystems (Harrison et al., 2018; Hoellein et al., 2017b; McCormick et al., 2016). Biofilms are aggregates of microbial cells (i.e., bacteria, algae, fungi, and protozoa) in a matrix of extracellular polymeric substances (EPS) that usually exist at a solid-liquid interface such as on the surface of a rock in a stream (Battin et al., 2016; Flemming & Wingender, 2010). In rivers, biofilms form the base of food webs and are active sites for nutrient cycling processes, including respiration and primary production (Battin et al., 2016). Plastic litter is abundant in freshwater ecosystems and is colonized by biofilms (Harrison et al., 2018; McCormick et al.,

2016) but the effect of plastic litter on biofilm community structure and activity is not commonly studied.

Biofilm communities are diverse and dynamic. Successional change in biofilm community composition is driven by many factors such as time since initial colonization, resource availability, competition, and life history strategies. In general, species richness is high at early stages of succession, declines due to competition in the early-middle stages, and then increases again as more niches become available and more specialized microbial populations emerge (Jackson, 2003; Lyautey et al., 2005). Biofilm colonization and growth is influenced by the chemical and physical properties of the surface it grows on, including plastic (Cazzaniga et al., 2015; Donlan, 2016).

Previous studies have demonstrated biofilm communities on plastic litter may differ from those in the surrounding environment, have lower taxa richness, and can harbor potentially hydrocarbon degrading bacteria (Amaral-Zettler et al., 2020; Barros & Seena, 2021; Oberbeckmann & Labrenz, 2020). Biogeography appears to be the most influential factor in shaping biofilm communities on plastic litter (Amaral-Zettler et al., 2020; Oberbeckmann & Labrenz, 2020; Vincent et al., 2022). Across polymer types, the individual physical and chemical properties of plastic particles may act as forces of selection that lead to taxonomically distinct biofilm communities and or differences in activity (Rummel et al., 2021), although evidence in the literature for this is mixed (Amaral-Zettler et al., 2015; Coons et al., 2021; Debroas et al., 2017; Oberbeckmann et al., 2018). Thus, more research is needed to understand the impact of plastic pollution on biofilm community composition, activity, and biofilm-mediated ecosystem processes in freshwaters (Amaral-Zettler et al., 2020; Harrison et al., 2018; Wright et al., 2021),

especially in relation to biofilm communities on natural surfaces that exist in the same habitat as the plastic particles under investigation.

The buoyancy and persistence of microplastics offer a novel habitat for colonization by biofilms (McCormick et al., 2016; Wright et al., 2020). The unique properties and abundance of microplastics suggest that they may influence microbially-mediated processes in aquatic ecosystems. Considering the relevance of biofilms to carbon and nutrient cycling (Battin et al., 2003; Chen et al., 2020), high levels of plastic pollution provide additional substrate for biofilm growth that would increase overall microbial biomass, which may impact microbially-mediated processes at larger spatial scales.

Inputs of both microplastic and larger plastic are increasing in freshwaters. This provides a novel substrate for biofilm growth and could increase mass on plastic particles that could facilitate the permanent retention of plastic litter. In addition, this could increase overall microbial biomass and alter food web dynamics and ecosystem processes. However, addressing this gap in knowledge is challenging, as it requires *in situ* experiments with microplastic addition, which presents methodological and permitting obstacles.

Ecosystem Processes

The transfer and exchange of nutrients and energy within an ecosystem constitute ecosystem processes (Lyons et al., 2005). Ecosystem processes are influenced by the biological, chemical, and physical processes and conditions within an ecosystem (Lyons et al., 2005). Examples of ecosystem processes include biomass production, nutrient cycling (e.g., phosphorus (P) and nitrogen (N) transformations), gross primary production (GPP) and respiration (R) (Lyons et al., 2005). Measurements of ecosystem processes integrate the activity of many

different organisms and can be used to assess an ecosystem's health and response to stress (Fu et al., 2013). In streams and lakes, biofilms are key sites for many ecosystem processes such as nutrient cycling, decomposition, and ecosystem metabolism.

Ecosystem metabolism integrates two ecosystem processes, the production of organic matter through photosynthesis (i.e., gross primary production; GPP) and the oxidation of organic matter through aerobic respiration (R), where the balance between the processes is net ecosystem productivity (NEP) (Odum, 1956). Rates of ecosystem metabolism can be calculated from direct measurements of dissolved oxygen (DO), which are attributable to biological and physical processes (Staeher et al., 2010). During the day DO may increase due to photosynthesis and decrease at night when respiration consumes O₂. Ecosystem metabolism is a highly integrative metric that aggregates multiple biological and physical dynamics (Staeher et al., 2010). Thus, metabolism can be used to assess how environmental changes affect ecosystem conditions for both natural variation (i.e., seasonality, biomes) and anthropogenic stressors (e.g., climate change and pollution) (Jankowski et al., 2021).

N cycling metrics (e.g., nitrification, denitrification, and nitrogen fixation), also integrate the activity of many organisms and can be used to infer ecosystem response to environmental changes at large spatial scales (Loeks-Johnson & Cotner, 2020; McCarthy et al., 2007a). N-fixation is the conversion of dinitrogen gas (N₂) into biologically available forms of N, and conversely, denitrification and anaerobic ammonium oxidation (anammox) generate N₂ (Bernhard, 2010). As with O₂, continuous measurements of N₂ in aquatic ecosystems can be used to estimate physical and biological processes which drive N₂ concentration over time (Reisinger et al., 2016) illustrating relative impacts on N₂ uptake and generation. The use of time intensive

N₂ measurements to infer underlying ecological processes which drive N₂ flux is at an early stage, as there is no automated N₂ sensor to collect the data (as can be done for oxygen). Thus, there is much to learn about the environmental conditions and anthropogenic stressors that control diel patterns in net N₂ flux from aquatic environments. Thus, measuring factors that drive the balance between those processes (i.e., net N₂ flux) is important as N can be a key limiting nutrient for ecosystem production, and in eutrophic ecosystems, N₂ flux out of the environment is critical for mitigating N pollution (Hoellein & Zarnoch, 2014; McCarthy et al., 2007b; Mulholland et al., 2008; Schindler, 1974).

If microplastic pollution in a freshwater ecosystem enhances the overall surface area for biofilm growth, microplastics may affect ecosystem processes at larger spatial scales. However, studies on the influence of plastic litter on ecosystem processes are newly emerging and are most commonly laboratory studies (López-Rojo et al., 2020; Seeley et al., 2020). Robust, in situ assessments of microplastic impacts on biofilm-mediated ecosystem processes are needed.

Thesis Objectives

The objectives of this thesis were to understand the impacts of plastic pollution on biofilms and ecosystem processes in freshwaters. In chapter II I sought to determine how biofilm activity and composition differ across three common plastic polymers (with different chemical and physical properties) relative to those on a natural surface. I incubated plastics with different physical and chemical characteristics, and a gradient of sizes in a large urban river, to further understand the potential impact of plastic material types and sizes on biofilm community composition and activity. I hypothesized that the activity of biofilms would be similar across different plastic types whereas biofilms on wood would be more active. We also predicted

microbial community assemblage would be different across all substrate types, with the community on wood showing the most diversity relative to plastic. Lastly, I predicted a positive relationship between substrate size and taxonomic richness and diversity across all substrate types since larger habitats sustain greater species richness and diversity (Wilson & MacArthur, 1967).

Chapter III consisted of my participation in the 'pELAstic project' at the International Institute for Sustainable Development's Experimental Lakes Area (IISD-ELA) in Ontario, Canada. This is a 10+ year project focusing on the fate and effects of microplastics in freshwater. This project began in 2018 with a baseline assessment of microplastic in the study lakes. Our experiment is part of the second phase of the pELAstic project where pelagic (i.e., open water) mesocosms in an experimental lake were deployed and dosed with microplastics at a range of concentrations. A direct addition of microplastics to a natural lake is unprecedented and will allow many factors to be studied including effects on microbes, plankton, fish, and ecosystem processes. The objectives of the pELAstic project were to determine: 1) the physical, chemical, and biological fate of microplastics in lakes and their watersheds; 2) how microplastic affects aquatic ecosystems at all levels of biological organization; 3) how microplastic affects ecosystem processes; 4) how ecosystems recover after microplastic exposure. My thesis project was related to objective 3. The objective was to measure how microplastics influence ecosystem metabolism and diel N₂ flux in large, in situ lake mesocosms. In addition, we measured ecosystem metabolism and diel N₂ flux at the whole-lake scale (in the absence of microplastic addition) to place mesocosm-based measurements in context. I predicted microplastics would serve as a novel and abundant surface for biofilm colonization that would increase GPP and R, with the

greatest impact at the highest microplastic concentrations. We also predicted that biofilm colonization of microplastics would impact N_2 flux rates, by increasing N_2 uptake (i.e., N-fixation) during the day, conducted by cyanobacteria that colonize microplastics. At the whole-lake scale, we expected relatively low rates of metabolism overall as is typical for oligotrophic lakes. In addition, we predicted that the epilimnion of the lake would show net N_2 uptake (i.e., under saturation) and the hypolimnion to show net N_2 production (super saturation) due to the relative impact of N-fixation and anaerobic respiration pathways that affect N_2 in the water column and sediment respectively.

The results from this thesis will expand the understanding of plastic-attached biofilms by comparing the results to a natural surface which riverine biofilms colonize and determining whether the impacts of microplastic pollution are reflected in ecosystem-scale processes or limited to individual ecological and biological components. This will help inform policy makers on how to manage plastic pollution and its impacts.

CHAPTER II

COMMUNITY COMPOSITION AND ACTIVITY OF BIOFILMS ON PLASTIC LITTER

Introduction

Since the onset of large-scale plastic production in 1950, plastic production has been increasing at a compound rate of 8.4% per year (Geyer et al., 2017). Of all plastic waste generated from 1950-2015, about 79% has been discarded in landfills or the environment (Geyer et al., 2017). In addition, the chemical and physical properties of plastic allow it to persist in the environment for long time periods (Chamas et al., 2020). Each year, approximately 1.15-2.41 million tons of plastic enter the world's oceans through rivers (Lebreton et al., 2017). Rivers are also key sites of plastic retention, leading to interactions between plastic litter and freshwater organisms (Windsor et al., 2019).

In aquatic environments, plastic litter is immediately colonized by biofilms (Wright et al., 2020; Zobell, 1943). Biofilms are aggregates of microbial cells (i.e., bacteria, algae, fungi, and protozoa) in a matrix of extracellular polymeric substances that usually exist at a solid-liquid interface (Battin et al., 2016; Flemming & Wingender, 2010). In rivers, biofilms form the base of food webs and are sites for nutrient cycling processes, (Battin et al., 2016). In addition to being centers of metabolic activity, biofilms are also highly diverse and dynamic (Battin et al., 2016).

Plastic litter provides a novel substrate that is well colonized by microbial biofilms in freshwater ecosystems (Harrison et al., 2018; Hoellein et al., 2017b; McCormick et al., 2016). Biofilm colonization and growth is influenced by the chemical and physical properties

of surfaces, including plastic (Cazzaniga et al., 2015; Donlan, 2016). The individual physical and chemical properties of plastic particles may act as forces of selection that lead to taxonomically distinct biofilm communities and or differences in activity (Rummel et al., 2021), although evidence in the literature for this is mixed (Amaral-Zettler et al., 2015; Coons et al., 2021; Debroas et al., 2017; Oberbeckmann et al., 2018). Therefore, more research is needed to understand the impact of plastic pollution on biofilm community composition, activity, and biofilm-mediated ecosystem processes in freshwaters (Amaral-Zettler et al., 2020; Harrison et al., 2018; Wright et al., 2021).

Plastic litter spans a gradient of material types and a wide range of particle sizes (Rochman et al., 2019) that could impact the composition and activity of biofilm communities. For example, particles with high surface area to volume ratios have greater biofilm biomass per unit area than particles with low surface area to volume ratios (Chen et al., 2019). Thus, biofilms may have a stronger impact on particle movement and aggregation (i.e., ‘stickiness’) for small plastic particles relative to larger ones. In addition, a central tenant of community ecology is that larger habitats sustain greater species richness and diversity (Wilson & MacArthur, 1967). Larger plastic particles might therefore support greater richness and diversity of microbial organisms than smaller particles, although this has not previously been tested. Overall, studies on biofilm community composition and activity, which span a gradient of plastic particle sizes and conducted under the same incubation conditions, are needed to better estimate the role of particle size on biofilm attributes.

In this study, we asked the following question: how does biofilm activity and composition differ across three common plastic polymers (with different chemical and physical

properties) relative to those on a natural surface? We incubated three plastic types for six weeks in the North Branch Chicago River in Chicago, IL, USA during summer 2021. We measured biofilm attributes (i.e., biomass and chlorophyll concentration) and activity (i.e., respiration and flux of nitrogen gas) weekly. We used next-generation sequencing to determine the bacterial and algal community composition in weeks 1, 3 and 6. We predicted that the activity of biofilms would be similar across different plastic types whereas biofilms on wood would be more active (e.g., higher rates of respiration) and have more biomass. We also predicted microbial community assemblage would be different across all substrate types, with the community on wood showing the most diversity relative to plastic (Fig 1A). Finally, we incubated all 4 substrate types at three different sizes. We predicted a positive relationship between substrate size, taxonomic richness, and diversity across all substrate types (Fig. 1B).

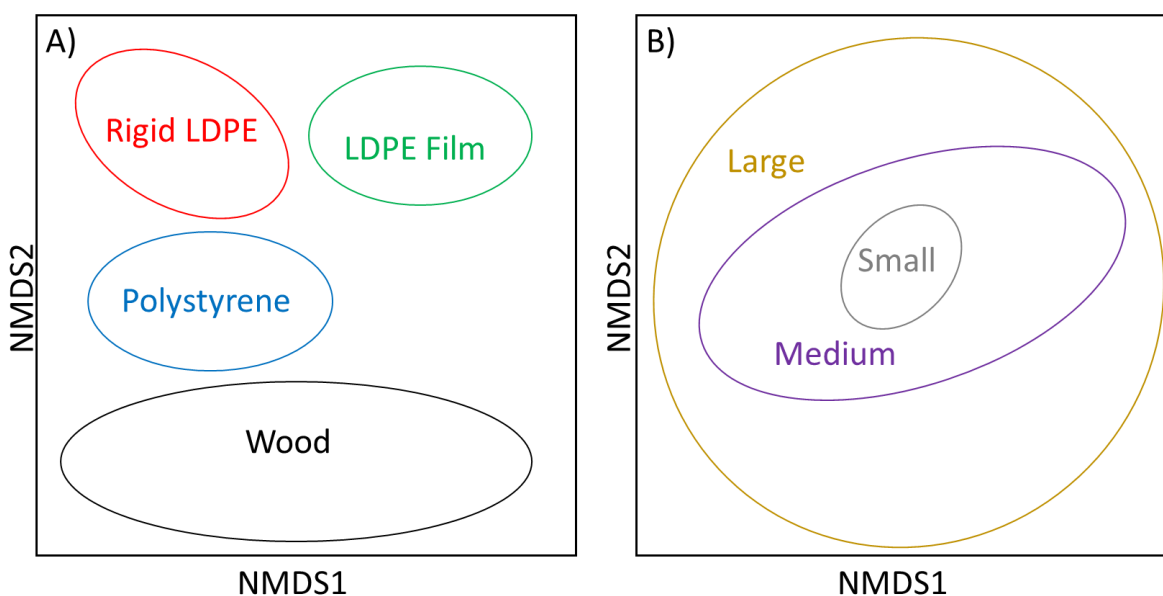


Figure 1. Our predictions for biofilm community composition for: A) substrate type and B) substrate size. LDPE = Low density polyethylene

Methods

Study Site

The North Branch Canal is a part of the Chicago Area Waterway System, in Chicago, IL, USA (Friends of the Chicago River, n.d.). The North Branch Canal is located within the North Branch of Chicago River (Friends of the Chicago River, n.d.). The canal contains a mixture of water from Lake Michigan, the urban watershed of the North Branch Chicago River, and treated wastewater from the O'Brien Water Reclamation Plant, which serves a population of approximately 1.3 million people (Metropolitan Water Reclamation District of Greater Chicago, 2019, March 3). The North Branch Chicago River is well studied for plastic litter, and the plastic substrates we selected for this study are commonly found in these habitats (Hoellein et al., 2017; McCormick et al., 2014; McCormick et al., 2016). Previous work on plastic litter and microbial biofilms have been conducted in the upstream portions in this watershed (Chaudhary et al., 2022; Hoellein et al., 2014; McCormick & Hoellein, 2016; Vincent et al., 2022; Vincent & Hoellein, 2021). Those study sites were all shallow, wadable (i.e., < 0.5 m deep) sections of the river where light reaches the benthic surface. In contrast, the study site for this project was North Branch Canal near North Ave in Chicago, IL, USA (41.91,-87.65), which is farther downstream, highly turbid, approximately 4 m deep, accessible only by boat, and close to the city center.

Study Design and Preparation

We set up an experiment to incubate plastic and natural substrates near the water surface at the study site. We selected three common types of buoyant plastic with different physical and chemical properties: foamed polystyrene which was brittle, rough, porous and hydrophobic (Density Virgin Expanded Polystyrene (EPS) Sheets, Master451, Indianapolis, IN, USA;

thickness = 6.5 mm), low-density polyethylene film which was flexible, smooth, and hydrophobic (Plastic Drop Cloth, VicMore, Zhengzhou, China; thickness = 0.0254 mm), and rigid low-density polyethylene which was hard, smooth, and hydrophobic (opaque off-white LDPE sheet, Small Parts, Logansport, IN, USA; thickness = 1.7 mm). We used untreated oak veneer, which was porous, rough, organic, and hydrophilic (Oak White Flat Sawn Veneer Pack, Woodworkers, Scottsdale, AZ, USA; thickness = 0.6 mm) as the control surface. Oak veneer was used as a control surface because it is analogous to the floating woody debris found at the site. We compared the foamed polystyrene and polyethylene plastic substrates to wood because all represent a buoyant and persistent microbial habitat in the river and are subject to similar environmental drivers of biofilm growth (i.e., light, temperature, and movement) at the water surface.

The experiment consisted of different sizes for each substrate. We cut pieces of each material type in three sizes: 1 cm², 7.5 cm², and 15 cm² (N=54 pieces/ material type/ size) (Table 1). One replicate of each material type and size (N=3 individual substrates) was arranged on a mesh wire rectangle (dimensions = 13 cm x 6 cm with 0.64 cm mesh; 308247B Hardware Cloth, YARDGARD, Long Grove, IL, USA) that was folded over into a square so that the substrates were trapped in a wire mesh 'sandwich'. Plastic zip ties (HS2515007, HUASU International, Zhenjiang, China) were then used to attach the folded mesh, with zip ties situated between individual substrates to prevent contact with one another (Fig 2). We constructed a raft (size = 1.52 x 0.76 m) made of 1.27 cm polyvinylchloride (PVC) pipe (Charlotte Pipe and Foundry, Charlotte, NC, USA) to hold the substrates for incubation near the water surface, as occurs *in situ*. Twelve wires (24 Gauge- 30.5 m Steel Galvanized Wire, OOK, Pompano Beach, FL, USA)

were wrapped around the PVC to run across the length of the raft. On every two wires, 36 substrate 'sandwiches' (N=9 of each size and material type combination) were attached to a wire in randomized order (Fig 3). Two floats (i.e., pool noodles; Deluxe Party Noodle, CONNELLY, Lynnwood, WA, USA) were attached by zip ties (46-315, Gardner Bender, Milwaukee, WI, USA) to two sides of the raft. The substrate sandwiches sunk just below the surface of the water (depth = approximately 2-10 cm). One exception was sandwiches that contained foamed polystyrene, which floated. Thus, we attached a 9.53 mm diameter metal nut using a zip tie to those experimental units, which kept them submerged at the same depth and orientation as all other substrates. The raft was attached to the seawall using metal chains and monitored regularly to ensure it remained in place and undisturbed (Fig 4). We acknowledge the use of plastic in the experiment construction (i.e., PVC, zip ties, and floats), however, we limited the experimental substrates contact to only metal surfaces, and any impact of the plastic used in the raft structure was uniform across all substrate types.

The experiment took place from June 14 to July 26, 2021, which is summer in the study area. We attached data loggers (Model UA-002-08, Onset HOBO, Bourne, MA, USA) to track temperature and light every hour throughout the experiment. We collected a subset of substrates weekly, each time removing 9 replicates of each size for each substrate type. The mesh 'sandwiches' were placed individually in clean, wide mouth, glass mason jars (0.95 L, Ball Corporation, Broomfield, CO, USA), which was partially filled with river water to submerge the substrates. Mason jars were placed in coolers with ice packs and transported to the laboratory within 1 hour. Each week we collected three 20 L carboys of water from the river for use in the respiration and nitrogen gas (N₂) flux incubations. Three of the nine replicates were used to

measure biofilm community composition and chlorophyll concentration, 3 replicates were used to measure respiration and biofilm biomass, and 3 replicates were used to measure N_2 flux.

We measured several environmental conditions on the deployment date and on each collection date (Table 2). We collected triplicate water samples by filtering river water (C2225-NN, Thermo Fisher Scientific, Waltham, MA, USA) into 20 mL scintillation vials. The water samples were kept cold and dark during transit to the lab, where they were frozen until analyses. On each collection date we measured Secchi depth as an estimate of light penetration. We measured dissolved oxygen, water temperature, and percent saturation (HQ40d portable meter, Hach, Loveland, CO, USA), as well as conductivity (30-10FT, YSI, Yellow Spring, OH, USA).

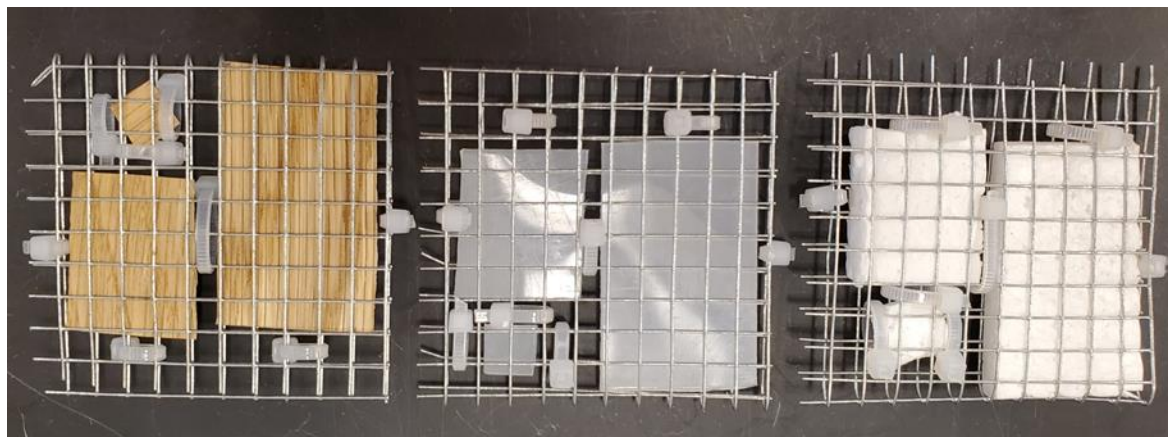


Figure 2. Wood, rigid low-density polyethylene (LDPE), and foamed polystyrene (left to right) substrates of each size within mesh ‘sandwiches’ secured by zip ties.



Figure 3. Assembled raft showing randomized placements of substrates, the PVC pipe frame, and yellow floats. Scale: the PVC frame is 152.4 x 76.2 cm.



Figure 4. Deployed raft showing substrates submerged near the water surface, attached to the seawall. The HOBO data logger is in the foreground.

Table 1. Dimensions of each substrate of each size (Foam = foamed polystyrene, Film = low-density polyethylene film, Rigid = rigid low-density polyethylene, Wood = untreated oak veneer; Large = 5 x 3 cm, Medium = 3 x 2.5 cm, Small = 1 x 1 cm).

| Material | Size | Volume cm ⁻³ | Surface Area cm ⁻² | Surface Area:Volume |
|----------|--------|-------------------------|-------------------------------|---------------------|
| Foam | Large | 9.8 | 40.4 | 4.1 |
| | Medium | 4.9 | 22.2 | 4.5 |
| | Small | 0.7 | 4.6 | 7.1 |
| Film | Large | 3.8E-02 | 30.0 | 788.5 |
| | Medium | 1.9E-02 | 15.0 | 788.9 |
| | Small | 2.54E-03 | 2.0 | 791.4 |
| Rigid | Large | 2.6 | 32.7 | 12.8 |
| | Medium | 1.3 | 16.9 | 13.2 |
| | Small | 0.2 | 2.7 | 15.8 |
| Wood | Large | 0.9 | 31.0 | 34.4 |
| | Medium | 0.5 | 15.7 | 34.8 |
| | Small | 0.1 | 2.2 | 37.3 |

Table 2. Summary of physical and chemical measurements on the deployment date and each collection date. Abbreviations: Temp = temperature, DO = dissolved oxygen.

| Date | Time | Conductivity (μS cm ⁻¹) | Temp. (°C) | DO (mg O ₂ L ⁻¹) | DO (O ₂ %) | Secchi Depth (m) | Nitrate (μg NO ₃ -N L ⁻¹) |
|------------|-------|-------------------------------------|------------|---|-----------------------|------------------|--|
| 2021-06-14 | 10:15 | 833 | 22.2 | 6.11 | 73.2 | 0.75 | 4860 |
| 2021-06-21 | 9:57 | 833 | 21.5 | 6.61 | 77.0 | 0.50 | 4287 |
| 2021-06-28 | 8:40 | 860 | 22.0 | 5.44 | 63.2 | 0.50 | 2109 |
| 2021-07-06 | 10:17 | 995 | 24.2 | 6.62 | 82.7 | 0.67 | 5658 |
| 2021-07-12 | 8:56 | 818 | 21.0 | 4.95 | 56.6 | 0.67 | 5915 |
| 2021-07-19 | 8:47 | 782 | 22.6 | 6.37 | 75.0 | 0.67 | 3906 |
| 2021-07-26 | 8:52 | 865 | 24.8 | 5.68 | 69.6 | 0.60 | 6198 |

Sequence of measurements

On each collection date, substrates were collected from the river in the morning and brought back to the laboratory within 1 hour. We placed mason jars holding substrates for N₂ flux in a refrigerator (4°C) until processing the next day. Substrates for respiration were removed from their mesh enclosure and gently rinsed with deionized (DI) water to remove any loose debris and invertebrates. Respiration measurements then began immediately. At the same time, a separate team removed the substrates designated for chlorophyll and DNA extraction from their mesh enclosure and gently rinsed them with DI water, then sample processing for chlorophyll and DNA extraction began.

Respiration and biomass

We poured about 15 L of river water into a clean bucket and measured the dissolved oxygen (DO) concentration and saturation (%DO), as well as temperature (HQ40d portable meter, Hach, Loveland, CO, USA.). After rinsing the substrates, each sample was placed in a 160 mL specimen container and then gently submerged in the bucket and capped underwater making sure no air bubbles were present. Three cups with only river water were also incubated to account for respiration in the water and abiotic changes in DO. Cups were then placed in a dark container to prohibit photosynthesis. After 3 hours at room temperature, we recorded DO concentration and saturation, temperature, and time elapsed for each sample (Hoellein et al., 2014; Vincent & Hoellein, 2021). Biofilm respiration was calculated as the change in DO between the final and initial DO concentration plus the correction for changes in DO of the river water alone (units: mg O₂ cm⁻² h⁻¹). Last, each substrate was individually wrapped in aluminum foil and frozen (-20 °C) until later measurement of biofilm biomass.

Biofilm biomass was quantified by staining substrates with 1% aqueous crystal violet (hexamethyl pararosaniline chloride; $C_{25}N_3H_{30}Cl$) and measuring absorbance at 595 nm on a spectrophotometer (Spectronic 20 Genyses Spectrophotometer, Thermo Fisher Scientific, Waltham MA) (Burton et al., 2007). Prior to quantifying biomass, substrates were thawed overnight at 4 °C. Large, medium, and small substrates were placed in 150 mL aluminum pans and stained with 1 mL, 0.5 mL, and 0.25 mL of 1% crystal violet respectively. Crystal violet stained the entire surface area of substrates for 45 minutes, substrates were then rinsed with DI water three times to remove excess stain. Water was added to submerge substrates for one hour to remove any remaining crystal violet unadhered to biofilm. A sterile metal nut was placed atop foam substrates to keep them submerged. Substrates were then left to dry for 24 hours at room temperature. We then transferred substrates to plastic weight boats, added 15 mL of 95% ethanol, and swirled for 30 seconds to elute crystal violet adhered to biofilm. The elution continued for 10 minutes with occasional swirling. This solution was poured into 5 mL test tubes, and 3 mL was measured on a spectrophotometer at 595 nm in a 10 mm quartz cuvette. A 1:5 dilution was applied if the optical density was above the spectrophotometer's detection limit. Each time the crystal violet assay was performed (N=6) we included one of each substrate and size that was uncolonized and non-experimental to account for background absorbance. Background absorbance was corrected for by subtracting the average absorbance of all controls by material type and size. Optical density for each substrate was calculated according to substrate surface area and expressed as absorbance per unit area (cm^{-2}) (Vincent et al., 2022).

Biofilm community composition and chlorophyll-a

Biofilm DNA was extracted from substrates from weeks 1, 3, and 6 for bacterial and algal community composition as indicators of the early, intermediate, and late stages of incubation. After carefully rinsing each substrate, they were placed on a 150 mL aluminum pan and cut in half with a sterile razor blade or scissors. Each half was placed in an individual 15 mL centrifuge tube for either extracting DNA or measuring chlorophyll concentration. Tubes were frozen (-20 °C) until each assay was performed. For DNA extraction, we first removed frozen substrates from the 15 mL centrifuge tubes using sterile forceps. For film substrates, the entire substrate was added directly to Powerbead tubes (i.e., no cutting), because their flexible nature allowed the entire substrate to fit in the tube and still receive sufficient bead beating to extract DNA. The same was true for the small substrates for wood, foam, and rigid polyethylene. However, we cut the medium and large wood, foam, and rigid substrates with a razor blade into small fragments and added a random portion to the Powerbead tubes to fill approximately 25% of the tube volume (tube volume = 0.5 mL). This was necessary given their thickness and lack of flexibility which inhibited bead beating.

DNA extractions were performed using the Qiagen Power Soil DNA extraction kit (Qiagen, Hilden, Germany) following the manufacturer's instructions. Two 'kit' controls were also included with DNA extractions to control for contamination. After DNA was extracted, PCR was performed using the CS1_515F and CS2_806R primers to amplify the V4 hypervariable region of the 16S rRNA gene (Caporaso et al., 2012) for bacterial taxonomic identification. PCR was also performed using the CS1_p23SrV_f1 and CS2_p23SrV_r1 primers to amplify the plastid 23S rRNA gene in eukaryotic algae and cyanobacteria (Sherwood &

Presting, 2007). PCR was confirmed by agarose gel electrophoresis. PCR products were sequenced by the Rush University Medical Center Genomics and Microbiome Core Facility in Chicago, IL on an Illumina MiniSeq 2x150 paired-end platform for 16S PCR products and on an Illumina MiSeq 2x250 paired-end platform for 23S PCR products.

Paired end reads were cleaned, assembled, and analyzed in DADA2 (Callahan et al., 2016) after demultiplexing. Raw bacterial 16S reads were 154bp and algal 23S reads were 251bp. Forward and reverse reads were trimmed to remove primer sequences with $trimLeft = c(19,20)$ for 16S reads and $trimLeft = c(20,20)$ for 23S reads. Algal 23S reads were also trimmed with $trimRight = c(20,20)$ to remove low-quality bases at the ends of reads. We also trimmed 16S reads at the first occurrence of Q = 13 with $TruncQ = 13$ and 23S reads at the first occurrence of Q = 11 with $TruncQ = 11$. Filtering was done with $maxEE = c(1,1)$ for 16S reads and with $maxEE = c(2,2)$ for 23S reads. Any 16S and 23S reads with ambiguous bases were also removed. A minimum read length filter $minLen = c(135,134)$ was applied to 16S reads and a minimum read length filter $minLen = 210$ was applied to 23S reads to keep reads long enough for proper merging. For both 16S and 23S reads, the DADA2 error learning model was run with $nbases = 10^{10}$. Bacterial ASVs were assigned and merged if they overlapped by 13 or more bases ($minoverlap = 13$). Algal ASVs were assigned and merged if they overlapped by 48 or more bases ($minoverlap = 48$). Bacterial reads that merged outside the range of the V4 region (250-256bp) and algal reads that merged outside 365-374bp were discarded. Lastly, for both 16S and 23S reads chimeras were removed with the default parameters. Bacterial 16S reads were aligned against the SILVA SSU 138.1 database (Quast et al., 2013) and were assigned taxonomy using the IDtaxa algorithm with DECIPHER (Murali et al., 2018). Algal 23S reads were aligned

against a custom algal database based off the SILVA LSU 132 database (Quast et al., 2013) using the AssignTaxonomy algorithm. Any 16S reads unclassified at the domain level or classified as chloroplast, archaea, or mitochondria were removed. Any 23S reads unclassified at the kingdom level were removed. For both 16S and 23S reads contaminant sequences were identified and removed with the Decontam R package (Davis et al., 2018) with a threshold of 0.5. Before downstream analysis we rarefied 16S reads to 11502 reads per sample and 23S reads to 7289 reads per sample without replacement with Phyloseq (McMurdie & Holmes, 2013).

Chlorophyll-a was measured using the hot ethanol method (Sartory & Grobbelaar, 1984). A day prior to measuring chlorophyll, tubes with frozen substrates were moved from the freezer into a refrigerator (4°C) to thaw overnight. Ethanol (95%) was added to each tube to fully submerge the substrate, and the volume of ethanol added to each tube was recorded. A sterile glass weight was added to tubes containing foam substrates to keep them submerged. Tubes were placed in a rack and submerged in a 75°C hot water bath for 15 minutes. After 15 minutes the rack was removed from the hot water bath and placed in the dark for two hours. Then, each tube was inverted and placed back in the rack for 15 minutes to allow any loose particles to settle. Once the extraction was complete the chlorophyll concentration of the extract was measured on a Turner Designs Trilogy Laboratory Fluorometer (Trilogy Laboratory Fluorometer, Turner Designs, San Jose, CA, USA) using the chlorophyll-a acidification module. The fluorometer was calibrated at five known concentrations of pure chlorophyll (Chlorophyll a analytical standard, MilliporeSigma, Burlington, MA, USA) in 95% ethanol the same week chlorophyll concentration was measured (Vincent et al., 2022). Calibrations and chlorophyll measurements were performed following the manufacturer's instructions.

Nitrogen flux

Flux of N_2 was measured the day after substrates were removed from the river. Substrates were removed from the refrigerator, separated from the mesh enclosure, and gently rinsed with DI water to remove any loose debris. River water was also removed from the refrigerator and allowed to come to room temperature. The river water was enriched with sodium nitrate (final concentration added = 3 mg N L^{-1}) and dextrose (final concentration added = 15 mg C L^{-1}) with the objective of measuring denitrification potential (Hoellein & Zarnoch, 2014). Individual substrates were placed in 160 mL specimen containers, submerged in enriched river water, and placed in the dark at room temperature for about 3 hours as described for respiration above. Three controls were also incubated to measure fluxes in river water alone. To collect dissolved gas samples, we used a 60 mL syringe with attached rubber tubing to slowly draw water from the specimen container (using care not to introduce turbulent flow or bubbles). We filled a 12 mL exetainer with the water, by placing the tube at the bottom and allowing to overflow for several volumes. We then sterilized samples with 200 μL of 50% zinc chloride and stored the exetainers under water in a refrigerator until analysis of dissolved gas. Triplicate samples of starting conditions in the enriched water were also taken using the same approach. Ratio of N_2 : argon (Ar) was measured on a Membrane Inlet Mass Spectrometer (MIMS Bay Instruments, Easton, MD, USA) with ultra-pure water as the standard (18 M Ω resistance; E-Pure, Barnstead International, Dubuque, IA, USA). The standard temperature was set to 21.0°C using a circulating water bath (VWR International, Radnor, PA, USA) equilibrated to the atmosphere with low-speed stirring for 24 hours (Lab Egg RW11 Basic, IKA Works, Inc., Wilmington, NC, USA) (Kana et al., 1998). During each run we analyzed a standard every 3-9 samples to account

for instrument drift. Concentrations of dissolved N₂ gas in each sample was calculated by multiplying the N₂:Ar ratio by the equilibrium concentration of Ar, which is more accurate than the N₂ concentration reported from the MIMS directly (Kana et al., 1994). Flux in N₂ was then calculated by subtracting initial N₂ from the final concentration in each sample and correcting for the flux observed in water alone.

Data Analysis

We used a non-parametric, aligned rank transformation (ART) test (Wobbrock et al., 2011) to compare differences in respiration, biomass, chlorophyll, and flux of N₂ by two factors: material type and week. We conducted the 2 factor ART tests for each substrate size separately. We used the ART approach as the data were not normally distributed and could not be transformed to meet assumptions of parametric (i.e., ANOVA) analyses. In cases where there was a significant interaction between material type and week, we performed a multifactor contrast test (ART-C) (Elkin et al., 2021) to compare combinations of factors' levels with Tukey's method for correcting p-values following multiple comparisons. All pairwise comparisons were generated but only comparisons where week was the same are presented to show differences among material types within individual weeks. All statistics were performed in R (R version 4.1.1, R Core Team 2021).

Biofilm 16S and 23S α -diversity was quantified by ASV richness and ASV Shannon diversity through Phyloseq (McMurdie & Holmes, 2013). We tested the assumptions of normality and equal variance with the Shapiro-Wilk test and Levene's test, respectively, and excluded outliers that we identified as any points more than 1.5 IQR below Q1 or more than 1.5 IQR above Q3 when they generated different results or caused a violation of the assumptions of

equal variance or normality. We compared 16S and 23S ASV richness and Shannon diversity for each size separately with material type and week as our two factors by 2-way ANOVA for all es except 16S small richness, 23S small richness, 23S large Shannon diversity, and 23S small Shannon diversity for which we used an ART test because ANOVA assumptions were not met. ART tests were followed up with multiple comparison tests if necessary, using ART-C while adjusting for multiple comparisons with Tukey's method and 2-way ANOVA was followed up with Tukey's post-hoc test when necessary. We also compared 16S and 23S ASV richness and Shannon diversity for each material type separately with size and week as our two factors with 2-way ANOVA, which we followed up with Tukey's post-hoc test when necessary. β -diversity was visualized by non-metric multidimensional scaling (NMDS) with Bray-Curtis dissimilarity index through the R package Vegan (Oksanen et al., 2020). We used Bray-Curtis distances and PERMANOVA (Oksanen et al., 2020) to compare biofilm community composition by material type, size, and week. This was followed up with pairwise PERMANOVA where we compared the effects of material type alone, week alone and size within each material type, while adjusting for multiple comparisons by the false discovery rate (FDR) method. We next calculated the mean relative abundance at the family level, grouping by material and week. We did not include size as an additional variable because PERMANOVA results revealed there were no differences among size for each material type. We visualized mean relative abundance by a stacked bar plot where we pooled any families that had a maximum relative abundance $<2.85\%$ for bacteria and $<2.70\%$ for algae across our grouping variables and grouped these as 'Other'. Pooling was done at 2.85% and 2.70% because this separated the top 20 most abundant families. We performed differential abundance analysis at the family level comparing plastic substrates to wood for each week.

Plastic substrates were pooled because our interest was primarily in comparing the taxa between wood and plastic rather than comparing the taxa on different kinds of plastic. Also, our NMDS showed differences among plastic types were not as great as their difference to wood. We tested differential abundance within each week because our NMDS also showed separation by week, and we were interested in testing which families were differentially abundant each week. Differential abundance analyses were done with a Wilcoxon rank-sum test and FDR approach for multiple comparisons. Wilcoxon effect size was also calculated for each differentially abundant family.

Results

Physical and chemical conditions

The chemical and physical conditions were typical of urban, eutrophic conditions (Table 2). Conductivity was 782-995 $\mu\text{S cm}^{-2}$, DO concentration was 4.95-6.37 $\text{mg O}_2 \text{L}^{-1}$, and DO saturation was 56.6-82.7%. Secchi depth measurements of 0.5-0.75 m and nitrate concentrations of 2109-6198 $\mu\text{g NO}_3^- \text{-N L}^{-1}$ showed relatively low light penetration and relative high inorganic N concentrations. Water temperature and illuminance at the water surface throughout the entire range of the study was 19.95-30.26 $^{\circ}\text{C}$ and 0-187378.15 lux (Fig 5), following a diel pattern (Fig 5).

Respiration

Biofilm respiration showed a significant interaction between material type and week for the large (ART $F_{15}=2.96$, $P=0.002$), medium (ART $F_{15}= 2.31$, $P=0.015$), and small (ART $F_{15}=6.40$, $P<0.001$) substrates (Table 3). So, we used a multifactor contrast test (ART-C) with Tukey's method for correcting p-values following multiple comparisons to compare substrates

within each week. The study was conducted for 6 weeks, and we compared among substrates separately for each size (large, medium, and small) for each week. Thus, there are a total of 18 comparisons where the response variables were compared among the 4 substrate material types for each week of the study (N=6 each for large, medium, and small). For 9 of the comparisons done among substrates for each week (hereafter: 'weekly comparisons'), respiration on wood was significantly higher (i.e., more negative) than all plastic substrates (e.g., weeks 1, 2, 3, and 4 for large and medium substrates, and week 1 for small substrates; Fig 6). For the remaining 9 of the weekly comparisons, wood was not significantly different from one or more of the 3 plastic substrates (e.g., week 5 and 6 for large and medium substrates, and week 2, 3, 4, 5, and 6 for small substrates; Fig 6). For 16 of the weekly comparisons, respiration on the three plastic substrates showed no differences among one another (e.g., weeks 1, 2, 4, 5, and 6 for large and medium substrates, and all 6 weeks for small substrates; Fig 6).

Biomass

Biofilm biomass showed a significant interaction between material type and week for all three substrate sizes (ART, large $F_{15}=5.40$, $P<0.001$, medium ART $F_{15}=5.25$, $P<0.001$, small ART $F_{15}=2.17$, $P=0.022$; Table 3). For each size, biomass increased in a linear fashion from weeks 1-3, with no differences among substrate types (Fig 7). On week 4, film had significantly less biomass than either wood (large; Fig 7A) or foam (medium and small; Fig 7B,C). On week 5, biomass showed no difference among substrate types. On week 6, biomass was significantly lower on large wood than all other large substrates (Fig 7A), and for the medium sized substrates, wood had significantly less biomass than foam and rigid plastic (Fig 7B).

Chlorophyll-a

Patterns for chlorophyll resembled biomass, with a significant interaction between week and material type for the large (ART, $F_{15}=1.97$, $P=0.039$) and medium (ART, $F_{15}=2.18$, $P=0.021$) substrates, although there was no interaction for small substrates (ART, $F_{15}=1.41$, $P=0.182$) (Table 3). For large substrates, there was no difference among substrate types for weeks 1-5, (Fig 8A) but on week 6, wood had significantly less chlorophyll than rigid polyethylene (Fig 8A). On medium and small substrates, chlorophyll concentration increased over time with no differences among substrates within individual weeks (Fig 8B,C).

Nitrogen (N_2) flux

Flux of N_2 was highly variable across sizes and weeks, with a significant interaction between week and material type for large (ART $F_{15}=3.57$ $P<0.001$) and medium (ART $F_{15}=2.97$ $P=0.002$) substrates, while small substrates showed only a significant effect of week (ART $F_{15}=3.32$ $P=0.012$; Table 3). For large substrates, ART-C pairwise comparisons showed N_2 flux on rigid plastic was significantly higher than foam on week 4, with the opposite pattern on week 5 (Fig 9A). For medium substrates, film had significantly higher N_2 flux than rigid substrates on week 5 (Fig 9B). Small substrates showed no significant differences within individual weeks (Fig 9C).

Biofilm Community Composition

Bacterial ASV richness showed a significant interaction between week and material type on large (2-way ANOVA, $F_6=2.87$, $P=0.030$) and small (ART, $F_6=7.13$, $P<0.001$; Table 4) substrates. On large substrates, weeks 1 and 6 showed no differences among substrate types, while on week 3, richness was higher on foam than on film and rigid substrates and richness on

wood was higher than on film substrates (Fig 10A). On small substrates, wood had higher richness than film on week 1 (Fig 10C). On week 3, foam and wood had higher richness than other small substrates, and on week 6, richness was higher on foam than rigid substrates (Fig 10C). On medium substrates, week (2-way ANOVA, $F_2=10.46$, $P<0.001$) and material (2-way ANOVA, $F_3=5.46$, $P=0.006$; Table 4) had significant effects without an interaction where week 6 was different from weeks 1 and 3 (Fig 10B), and rigid substrates were different than foam (Tukey's post-hoc test, $P=0.022$) and wood (Tukey's post-hoc test, $P=0.009$) substrates.

Bacterial ASV Shannon diversity patterns were similar to richness, with an interaction between material type and week on large (2-way ANOVA, $F_6=4.42$, $P=0.004$) and small substrates (2-way ANOVA, $F_6=5.15$, $P=0.002$; Table 4). For large substrates, there were no differences among substrates week 1, but on week 3 diversity was greater on foam compared to large film and rigid substrates, and on week 6 diversity was greater on wood than rigid substrates (Fig 11A). For small substrates, there were no differences on week 1, in week 3 foam was significantly more diverse than all other substrates, and by week 6, diversity on foam was greater than rigid substrates (Fig 11C). ASV Shannon diversity on medium substrates was different by material type (2-way ANOVA, $F_3=5.22$, $P=0.006$) and week (2-way ANOVA, $F_2=6.26$, $P=0.006$; Table 4) without an interaction. Foam and rigid substrates were different from each other (Tukey's post-hoc test, $P=0.004$) and diversity on week 6 was different than weeks 1 and 3 (Fig 11B).

Bacterial ASV richness for each material type, with size and week as our two factors, showed a significant difference among weeks for film (2-way ANOVA, $F_2=17.37$, $P<0.001$), foam (2-way ANOVA, $F_2=9.07$, $P=0.002$), rigid (2-way ANOVA, $F_2=11.55$, $P<0.001$) and wood

(2-way ANOVA, $F_2=7.82$, $P=0.004$; Table 5) substrates with no effect of size. On film substrates, each week was unique (Fig 12A). Weeks 1 and 6 were different from each other on foam substrates (Fig 12B) and on wood and rigid substrates week 6 was unique (Fig 12C,D).

Bacterial ASV Shannon diversity for each material type, with size and week as our two factors, showed a significant difference among weeks for film (2-way ANOVA, $F_2=20.43$, $P<0.001$) and foam (2-way ANOVA, $F_2=4.64$, $P=0.024$; Table 5) substrates. Week 3 was distinct on film (Fig 13A) and week 1 was distinct on foam (Fig 13B). There was also a size effect for film (2-way ANOVA, $F_2=4.93$, $P=0.020$; Table 5) where small and medium substrates were different from each other (Tukey's post-hoc test, $P=0.016$). There were no significant differences by size or among weeks for rigid polyethylene. On wood substrates there was a significant interaction between size and week (2-way ANOVA, $F_4=3.46$, $P=0.029$; Table 5), where on week 3 small and large substrates were different from each other (Fig 13D).

Non-metric multidimensional scaling (NMDS) by Bray-Curtis dissimilarity distances showed bacterial communities on wood differed more than communities across plastic types (Fig 14). Bacterial communities also grouped separately according to week, with no grouping by substrate size (Fig 14). Pairwise PERMANOVA comparing substrate types showed that communities on wood were different from all 3 plastic types, and that communities on foam were different from rigid substrates. (Table 6). For each material type, there was no difference based on substrate size (Table 6). Bacterial communities also differed between each week (Table 6).

We recorded 396 unique bacterial families, 113 of which were differentially abundant between plastic and wood, although patterns varied across the sample dates. All families

represented in Figure 15 were differentially abundant between plastic and wood substrates in one or more weeks. Week 1 had 58 differentially abundant families (Table 7), week 3 had 63 differentially abundant families (Table 8), and week 6 had 67 (Table 9). On all plastic types *Comamonadaceae* was the most abundant family on week 1 (Fig 15) which was significantly more abundant on plastic than wood (Table 7). On wood, the most abundant family week 1 was *Sphingomonadaceae* (Fig 15) which was significantly more abundant than on plastic (Table 7). Week 3, *Methylomonadaceae* was the most abundant family on all plastic (Fig 15) and was significantly more abundant than on wood (Table 8). On wood, *Sphingomonadaceae* was the most abundant family week 3 (Fig 15) and significantly more abundant than plastic (Table 8). By week 6, the most abundant family on rigid substrates was *Comamonadaceae*, on film it was *Methylomonadaceae*, and on foam it was *Chitinophagaceae* (Fig 15). Of these families only *Methylomonadaceae* was significantly more abundant on plastic week 6 (Table 9). On wood the most abundant family week 6 was *Methylophilaceae* (Fig 15) and was significantly more abundant on wood than plastic (Table 9).

Algal ASV richness was significantly different by material type on large (2-way ANOVA, $F_3=24.75$, $P<0.001$), medium (2-way ANOVA $F_3=17.33$, $P<0.001$), and small (ART, $F_3=26.31$, $P<0.001$; Table 10) substrates. Across all sizes, ASV richness on film and rigid substrates were the same, and lower than ASV richness on wood and foam, which were also not significantly different from each other (Fig 16).

Algal ASV Shannon diversity was different with an interaction between material type and week on large (ART, $F_6=6.97$, $P<0.001$), medium (2-way ANOVA, $F_6=3.79$, $P=0.009$), and small (ART, $F_6=4.10$, $P=0.006$; Table 10) substrates. For all sizes, there were no differences

among substrates in week 1 (Fig 17). On large substrates, wood and foam were significantly different than film and rigid on weeks 3 and 6 (Fig 17A). For medium and small substrates in week 3, diversity on foam was significantly higher compared to film and rigid substrates while diversity on wood was significantly higher than film substrates (Fig 17B,C). For medium substrates on week 6, diversity on foam significantly higher than on film and rigid substrates while diversity on wood was significantly higher than on rigid substrates (Fig 17B). For small substrates on week 6, diversity on foam was significantly higher than on film and rigid substrates (Fig 17C).

Algal ASV richness for each material type, with size and week as our 2 factors, showed a significant week effect for film (2-way ANOVA, $F_2=10.45$, $P<0.001$) and rigid substrates (2-way ANOVA, $F_2=5.11$, $P=0.018$; Table 11). On film, week 3 was distinct (Fig 18A), and on rigid substrates, weeks 1 and 3 were different from each other (Fig 18C). No week effect was present for foam or wood substrates and no material type had a significant effect by size.

Algal ASV Shannon diversity for each material type, with size and week as our 2 factors, showed a significant difference among weeks for film (2-way ANOVA, $F_2=27.19$, $P<0.001$), foam (2-way ANOVA, $F_2=7.74$, $P=0.004$), rigid (2-way ANOVA, $F_2=21.53$, $P<0.001$) and wood (2-way ANOVA, $F_2=4.74$, $P=0.022$; Table 11) substrates. Week 3 was distinct on film (Fig 19A) and week 6 on foam (Fig 19B). On wood substrates, weeks 3 and 6 were different from each other (Fig 19D), while on rigid substrates, each week was unique (Fig 19C). Size had no significant effect on algal diversity for any material type.

Non-metric multidimensional scaling (NMDS) by Bray-Curtis dissimilarity distances showed algal communities on wood differed more than communities across plastic types (Fig

20). Algal communities also grouped separately according to week, but there was no grouping by substrate size (Fig 20). Analysis by PERMANOVA showed algal communities were different with a material and week interaction (PERMANOVA $F_6=7.62$, $P<0.001$; Table 12). Pairwise PERMANOVA comparing substrate types showed that communities on wood and foam differed from each other and were different than film and rigid substrates (Table 12). Communities on film and rigid substrates did not differ from each other (Table 12). For each material type there was no difference based on substrate size (Table 12). Algal communities also differed between each week (Table 12).

We recorded 114 unique algal families, 53 of which were differentially abundant between plastic and wood, although patterns varied across the sample dates. Week 1 had 36 differentially abundant families (Table 13), week 3 had 31 (Table 14), and week 6 had 18 (Table 15). On film and rigid plastic types, Unclassified *Bacillariophyta* was the most abundant family week 1, on foam it was Unclassified *Chlamydomonadales* and on wood it was *Chlamydomonadaceae* (Fig 21). After pooling plastic together and testing for differentially abundant algal families, neither Unclassified *Bacillariophyta* nor Unclassified *Chlamydomonadales* were differentially abundant; however, *Chlamydomonadaceae* was significantly more abundant on wood in week 1 (Table 13). On week 3, Unclassified *Bacillariophyta* was the most abundant family on all plastic (Fig 21) and was significantly more abundant than on wood (Table 14). On wood *Chlamydomonadaceae* remained the most abundant family on week 3 (Fig 21) and was significantly more abundant than on plastic (Table 14). By week 6, the most abundant family on film and rigid substrates was Unclassified *Bacillariophyta*, on foam it was *Eustigmataceae*, and on wood it was *Chlamydomonadaceae* (Fig 21). Unclassified *Bacillariophyta* was also significantly more

abundant at a moderate effect size on plastic in week 6 and *Chlamydomonadaceae* was significantly more abundant on wood (Table 15).

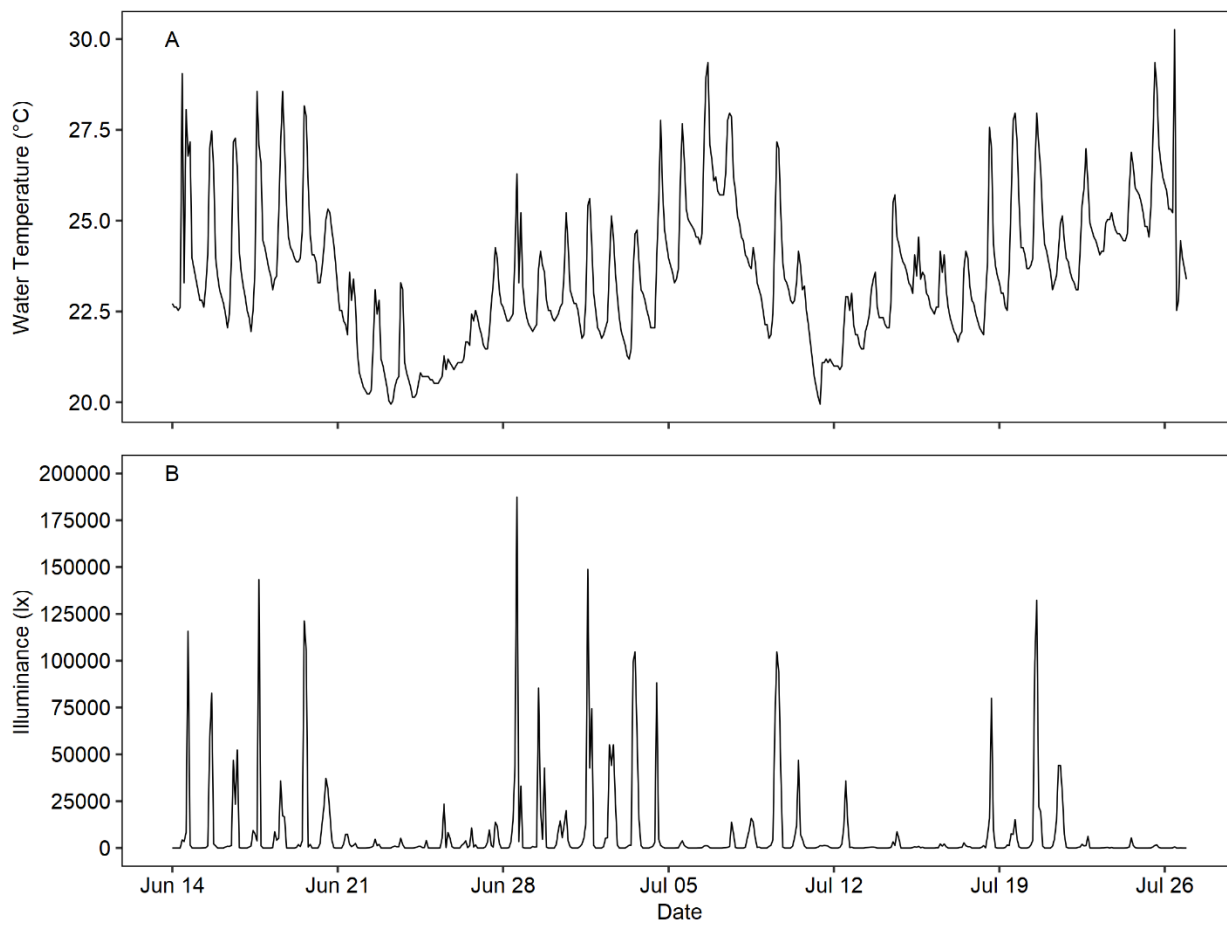


Figure 5. Timeseries of A) water temperature ($^{\circ}\text{C}$) and B) illuminance (lx) measured by the HOBO logger attached to the raft for the entire range of the study.

Table 3. Aligned-rank-transform comparisons for each measurement type for each size. Non-significant p-values are in bold.

| Size | Term | Df | F value | Pr(>F) | Size | Term | Df | F value | Pr(>F) |
|--------------------|-------------|----|---------|--------|---------------------------|-------------|----|---------|--------------|
| <i>Respiration</i> | | | | | <i>N₂ Flux</i> | | | | |
| Large | Material | 3 | 43.25 | <0.001 | Large | Material | 3 | 3.27 | 0.029 |
| | Week | 5 | 31.22 | <0.001 | | Week | 5 | 1.87 | 0.117 |
| | Interaction | 15 | 2.96 | 0.002 | | Interaction | 15 | 3.57 | <0.001 |
| Medium | Material | 3 | 36.20 | <0.001 | Medium | Material | 3 | 0.30 | 0.828 |
| | Week | 5 | 19.98 | <0.001 | | Week | 5 | 5.80 | <0.001 |
| | Interaction | 15 | 2.31 | 0.015 | | Interaction | 15 | 2.97 | 0.002 |
| Small | Substrate | 3 | 38.35 | <0.001 | Small | Material | 3 | 1.77 | 0.166 |
| | Week | 5 | 36.22 | <0.001 | | Week | 5 | 3.32 | 0.012 |
| | Interaction | 15 | 6.40 | <0.001 | | Interaction | 15 | 1.55 | 0.124 |
| <i>Biomass</i> | | | | | <i>Chlorophyll</i> | | | | |
| Large | Material | 3 | 8.57 | <0.001 | Large | Material | 3 | 9.40 | <0.001 |
| | Week | 5 | 55.32 | <0.001 | | Week | 5 | 32.55 | <0.001 |
| | Interaction | 15 | 5.40 | <0.001 | | Interaction | 15 | 1.97 | 0.039 |
| Medium | Material | 3 | 16.65 | <0.001 | Medium | Material | 3 | 8.96 | <0.001 |
| | Week | 5 | 65.05 | <0.001 | | Week | 5 | 40.46 | <0.001 |
| | Interaction | 15 | 5.25 | <0.001 | | Interaction | 15 | 2.18 | 0.021 |
| Small | Material | 3 | 6.99 | <0.001 | Small | Material | 3 | 9.28 | <0.001 |
| | Week | 5 | 38.74 | <0.001 | | Week | 5 | 21.85 | <0.001 |
| | Interaction | 15 | 2.17 | 0.022 | | Interaction | 15 | 1.41 | 0.182 |

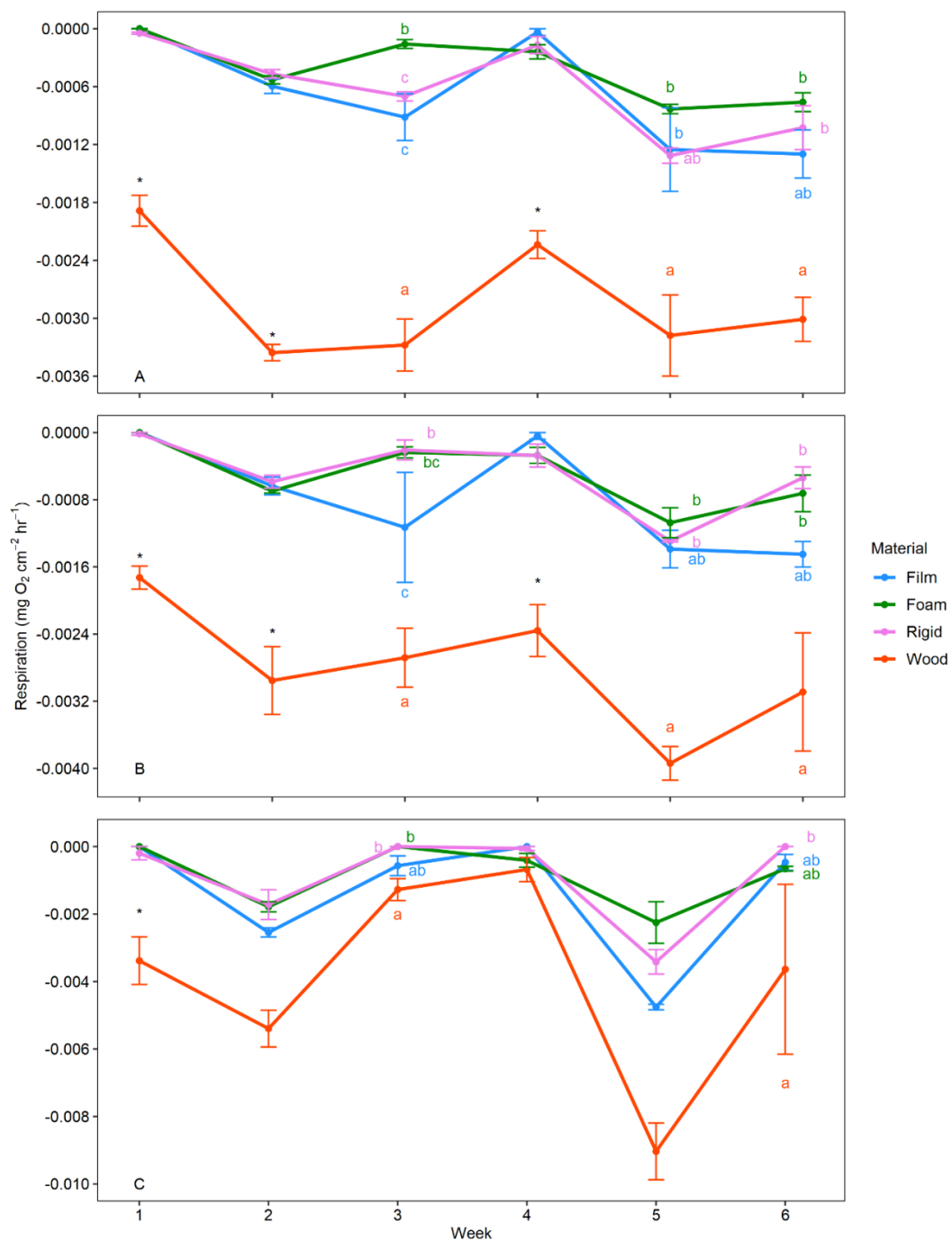


Figure 6. Mean (\pm SE) respiration rates ($\text{mg O}_2 \text{ cm}^{-2} \text{ h}^{-1}$) over six-week period on A) large, B) medium and C) small substrates. Small letters correspond to ART-C pairwise comparison results after a significant substrate \times week interaction; ‘*’ is used when wood was significantly different than all other substrate types. More negative values indicate higher rates of respiration.

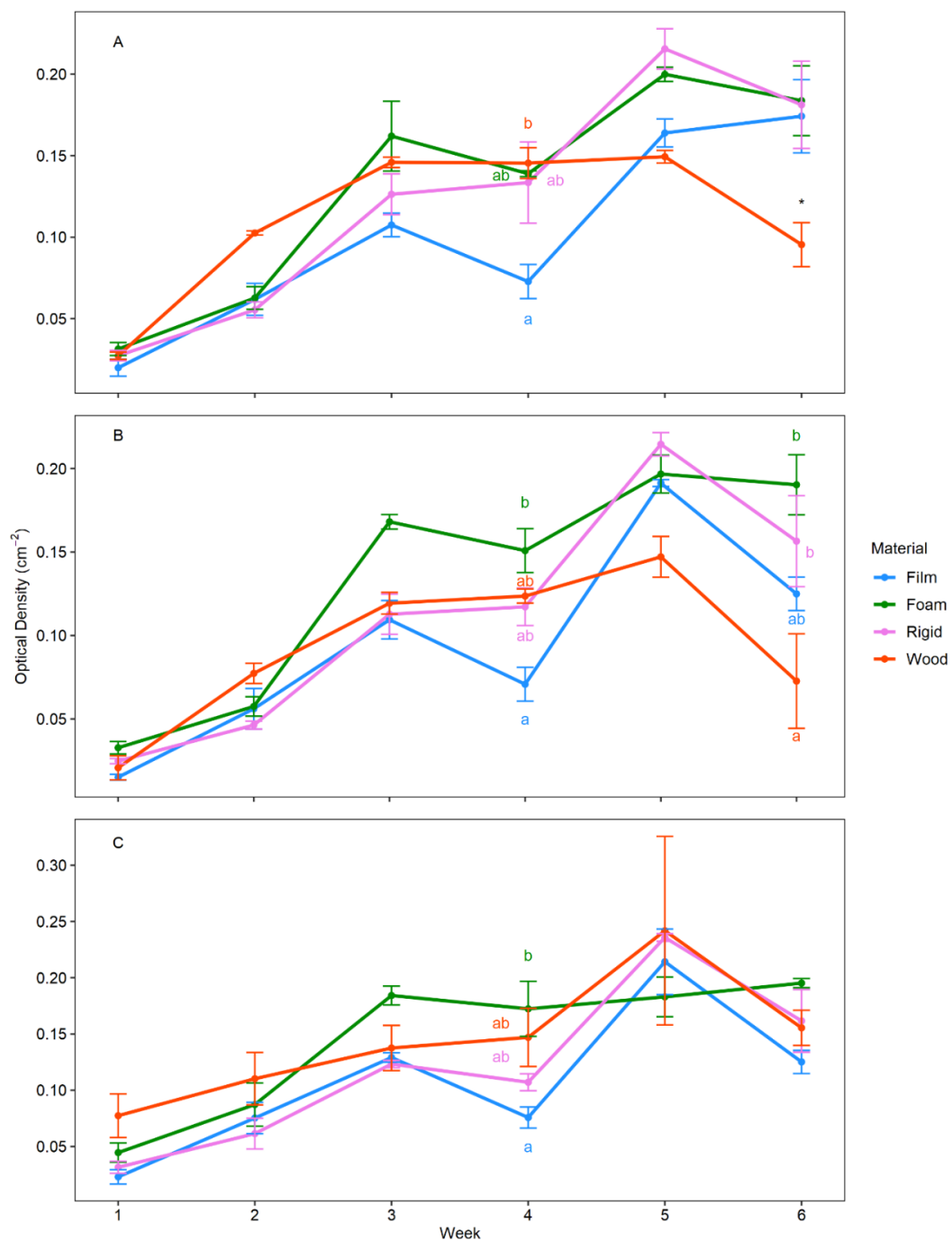


Figure 7. Mean (\pm SE) optical density (cm⁻²) of crystal violet (biomass) over six-week period on A) large, B) medium and C) small substrates. Small letters correspond to ART-C pairwise comparison results after a significant substrate x week interaction; ‘*’ is used when wood was significantly different than all other substrate types.

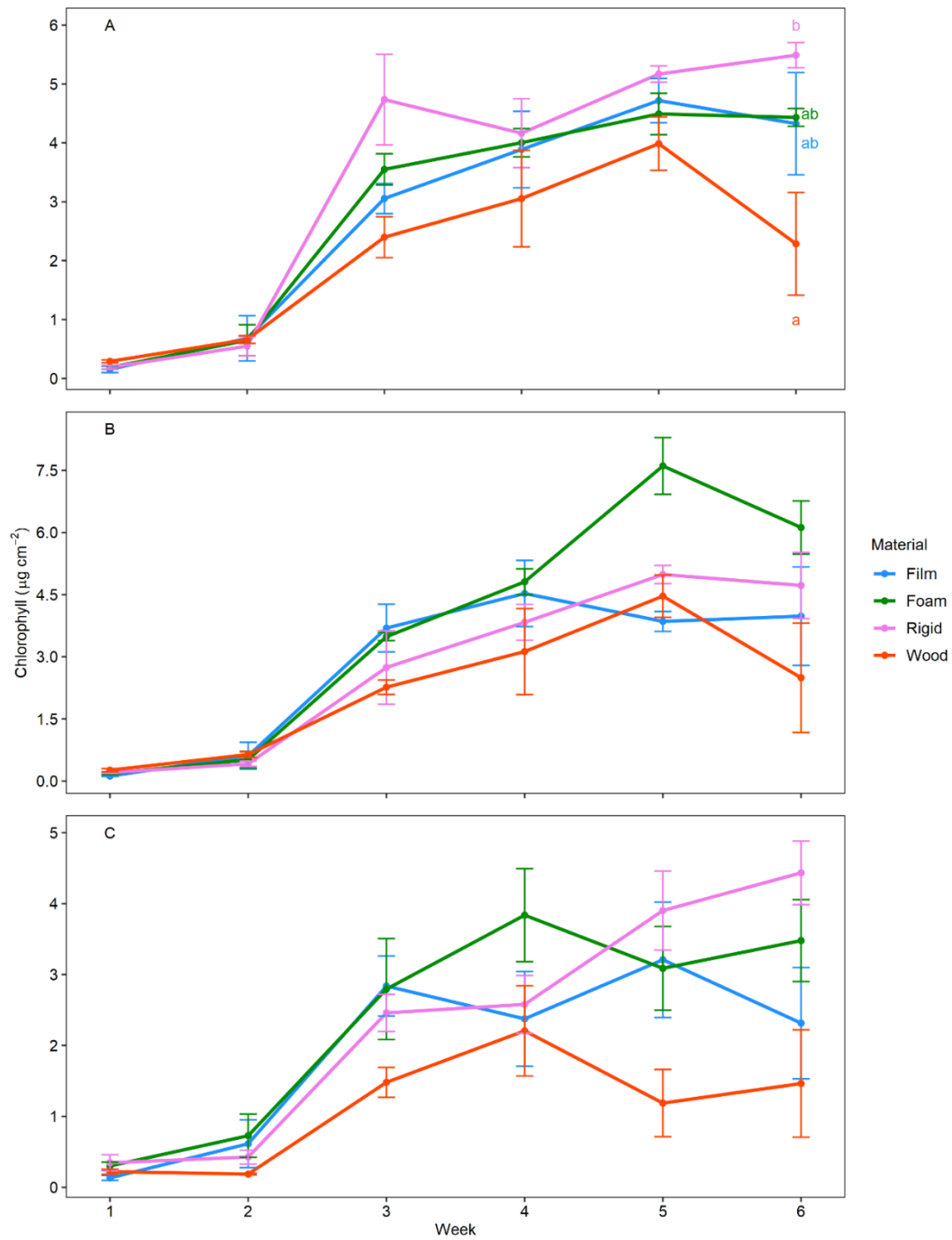


Figure 8. Mean (\pm SE) chlorophyll concentration ($\mu\text{g cm}^{-2}$) over six-week period on A) large, B) medium and C) small substrates. Small letters correspond to ART-C pairwise comparison results after a significant substrate \times week interaction; ‘*’ is used when wood was significantly different than all other substrate types.

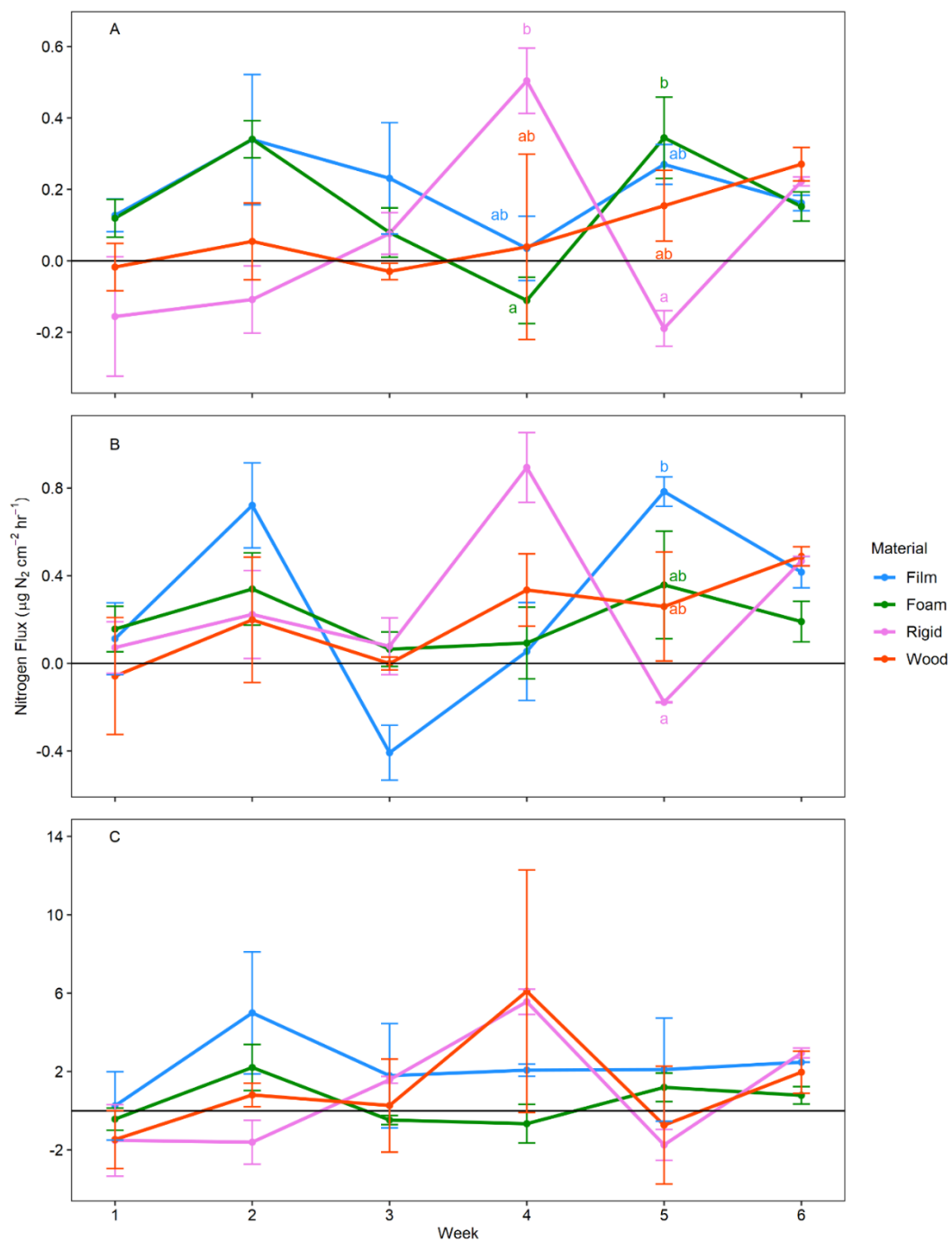


Figure 9. Mean (\pm SE) Nitrogen flux ($\mu\text{g N}_2 \text{ cm}^{-2} \text{ hr}^{-1}$) over six-week period on A) large, B) medium and C) small substrates. Small letters correspond to ART-C pairwise comparison results after a significant substrate \times week interaction; ‘*’ is used when wood was significantly different than all other substrate types.

Table 4. Results from 2-way ANOVA for bacterial ASV richness and ASV Shannon diversity and from ART for small ASV richness among material type and week for each size. Values in bold indicate significant p-values.

| Size | Term | Df | F value | Pr(>F) |
|------------------------------|-------------|----|---------|------------------|
| <i>ASV Richness</i> | | | | |
| Large | Material | 3 | 10.32 | <0.001 |
| | Week | 2 | 7.46 | 0.003 |
| | Interaction | 6 | 2.87 | 0.030 |
| Medium | Material | 3 | 5.46 | 0.006 |
| | Week | 2 | 10.46 | <0.001 |
| | Interaction | 6 | 0.49 | 0.807 |
| Small | Material | 3 | 31.06 | <0.001 |
| | Week | 2 | 17.38 | <0.001 |
| | Interaction | 6 | 7.13 | <0.001 |
| <i>ASV Shannon Diversity</i> | | | | |
| Large | Material | 3 | 10.55 | <0.001 |
| | Week | 2 | 3.83 | 0.037 |
| | Interaction | 6 | 4.42 | 0.004 |
| Medium | Material | 3 | 5.22 | 0.006 |
| | Week | 2 | 6.26 | 0.006 |
| | Interaction | 6 | 1.40 | 0.255 |
| Small | Material | 3 | 26.26 | <0.001 |
| | Week | 2 | 14.05 | <0.001 |
| | Interaction | 6 | 5.15 | 0.002 |

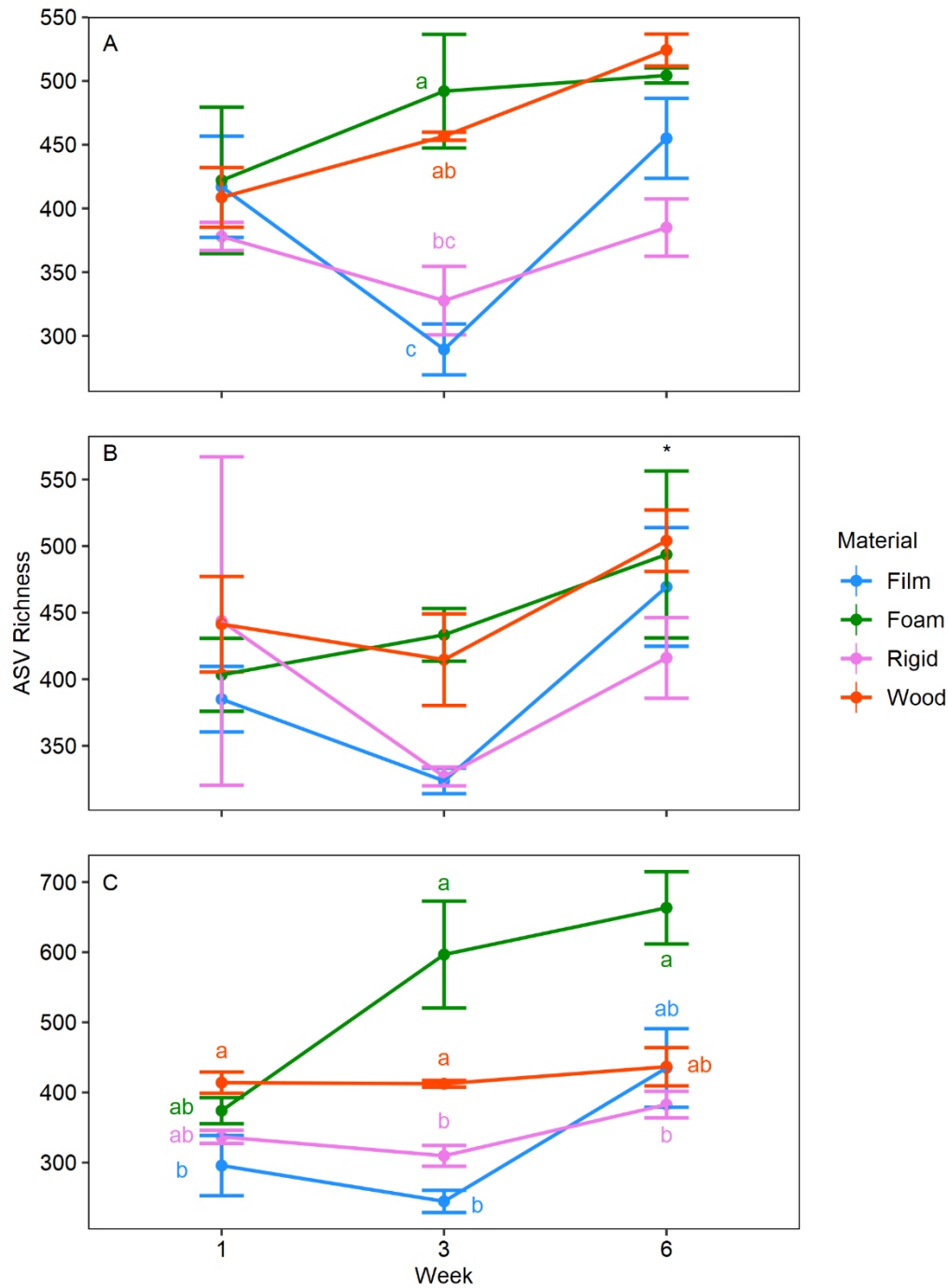


Figure 10. Mean (\pm SE) bacterial ASV Richness on each material type for weeks 1, 3 and 6 on A) large, B) medium, and C) small substrates. The small letters correspond to results from ART-C pairwise comparisons with Tukey's adjustment for multiple comparisons and Tukey's post-hoc test. The '*' in panel B indicates week 6 is different from weeks 1 and 3.

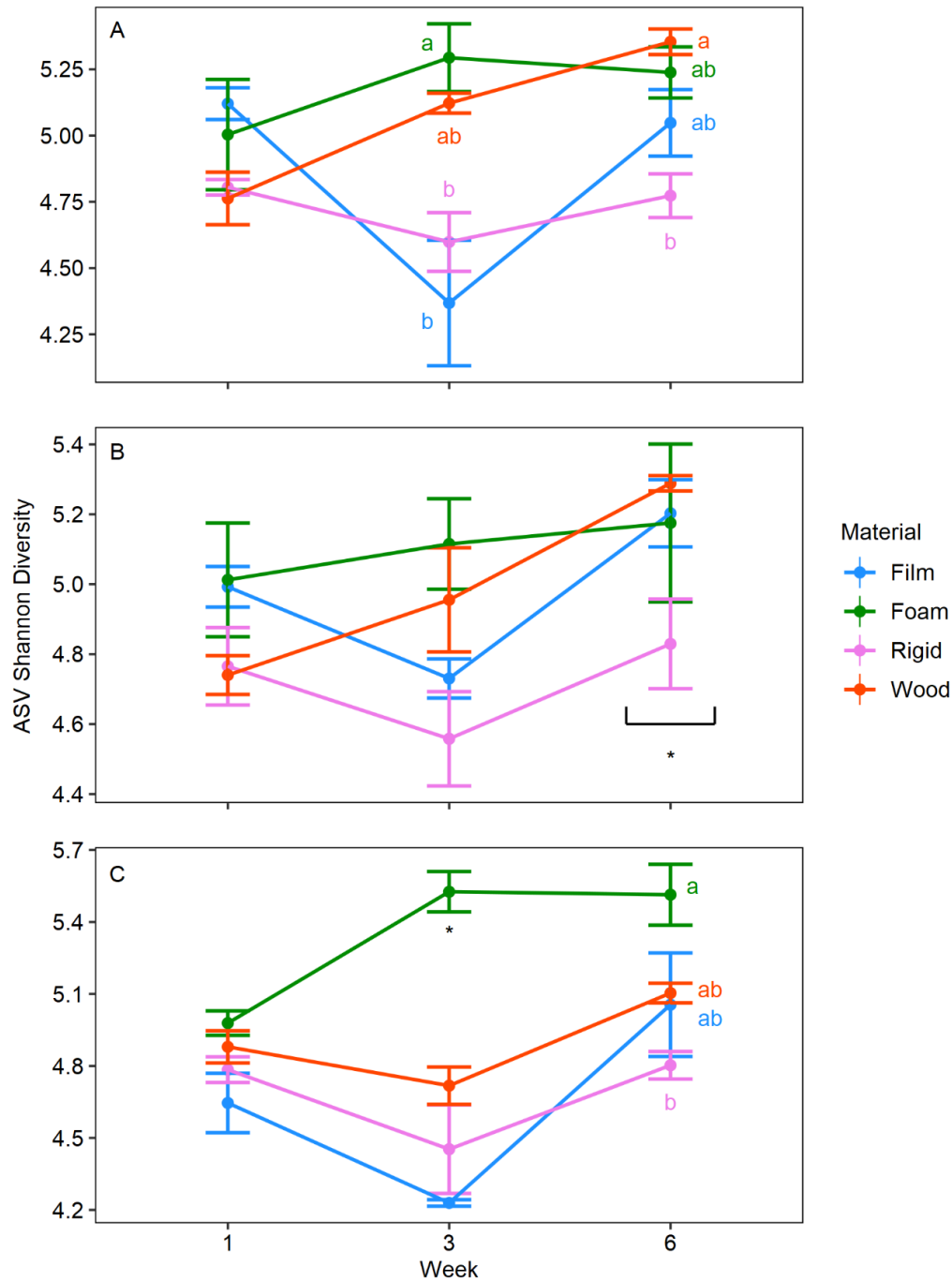


Figure 11. Mean (\pm SE) bacterial ASV Shannon diversity on each material type for weeks 1, 3 and 6 on A) large, B) medium, and C) small substrates. The small letters correspond to results from Tukey's post-hoc test. The line with '*' in panel B indicates weeks 6 is different than weeks 1 and 3. The singular '*' in panel C indicates foam is different than all other material types.

Table 5. Results from 2-way ANOVA for bacterial ASV richness and Shannon diversity among size and week for each material type. Values in bold indicate significant p-values.

| Material | Term | Df | F value | Pr(>F) |
|------------------------------|-------------|----|---------|------------------|
| <i>ASV Richness</i> | | | | |
| Film | Size | 2 | 3.49 | 0.052 |
| | Week | 2 | 17.37 | <0.001 |
| | Interaction | 4 | 0.66 | 0.626 |
| Foam | Size | 2 | 0.89 | 0.429 |
| | Week | 2 | 9.07 | 0.002 |
| | Interaction | 4 | 1.41 | 0.276 |
| Rigid | Size | 2 | 0.97 | 0.398 |
| | Week | 2 | 11.55 | <0.001 |
| | Interaction | 4 | 1.24 | 0.331 |
| Wood | Size | 2 | 2.79 | 0.088 |
| | Week | 2 | 7.82 | 0.004 |
| | Interaction | 4 | 1.50 | 0.244 |
| <i>ASV Shannon Diversity</i> | | | | |
| Film | Size | 2 | 4.93 | 0.020 |
| | Week | 2 | 20.43 | <0.001 |
| | Interaction | 4 | 1.50 | 0.244 |
| Foam | Size | 2 | 2.12 | 0.150 |
| | Week | 2 | 4.64 | 0.024 |
| | Interaction | 4 | 0.73 | 0.581 |
| Rigid | Size | 2 | 0.19 | 0.826 |
| | Week | 2 | 1.59 | 0.239 |
| | Interaction | 4 | 0.26 | 0.900 |
| Wood | Size | 2 | 4.21 | 0.032 |
| | Week | 2 | 28.44 | <0.001 |
| | Interaction | 4 | 3.46 | 0.029 |

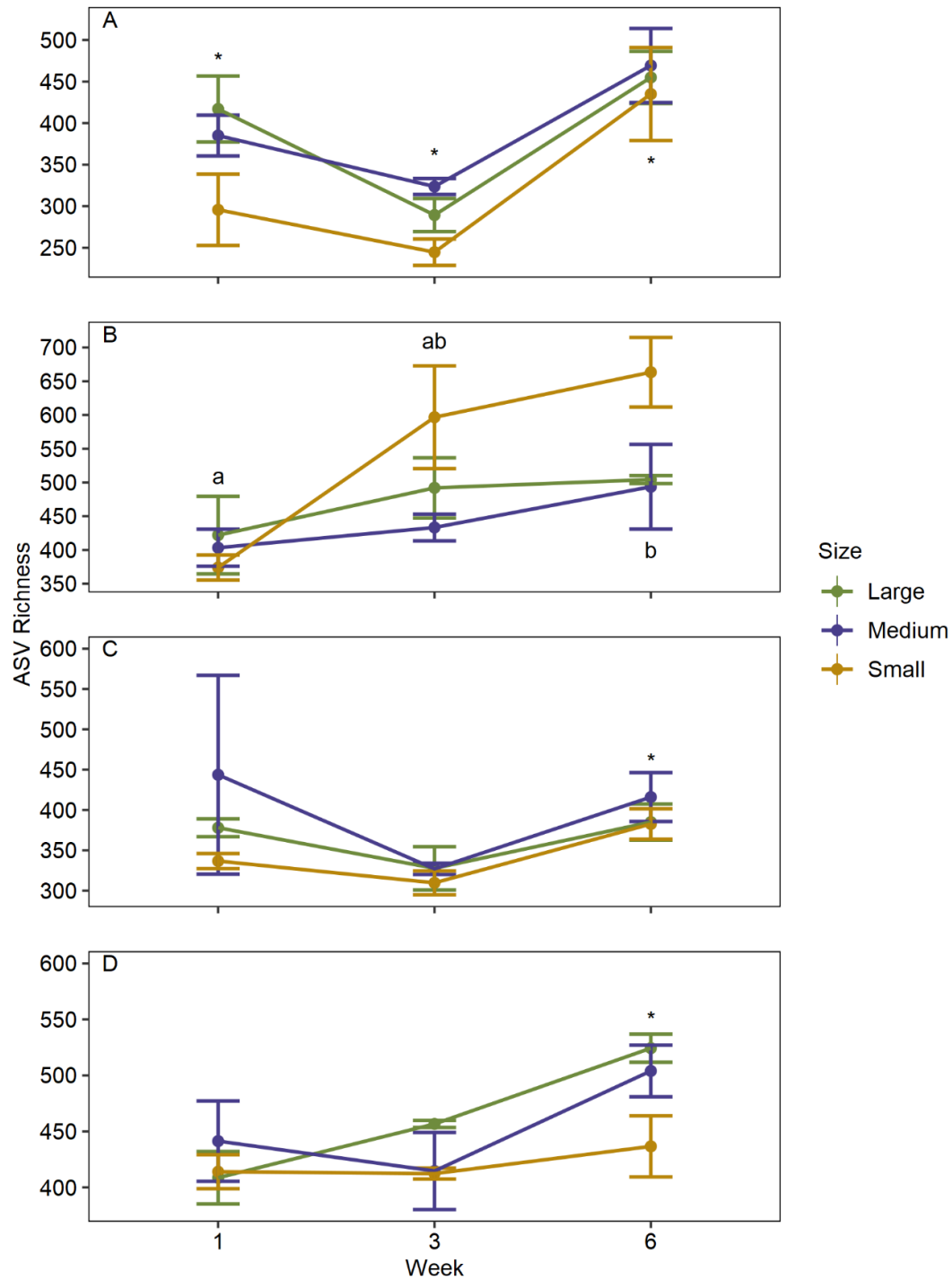


Figure 12. Mean (\pm SE) bacterial ASV Richness on each material type for weeks 1, 3 and 6 on A) film, B) foam, C) rigid, and D) wood substrates. The small letters correspond to results from Tukey's post-hoc test. The '*' indicate that week is different from the rest.

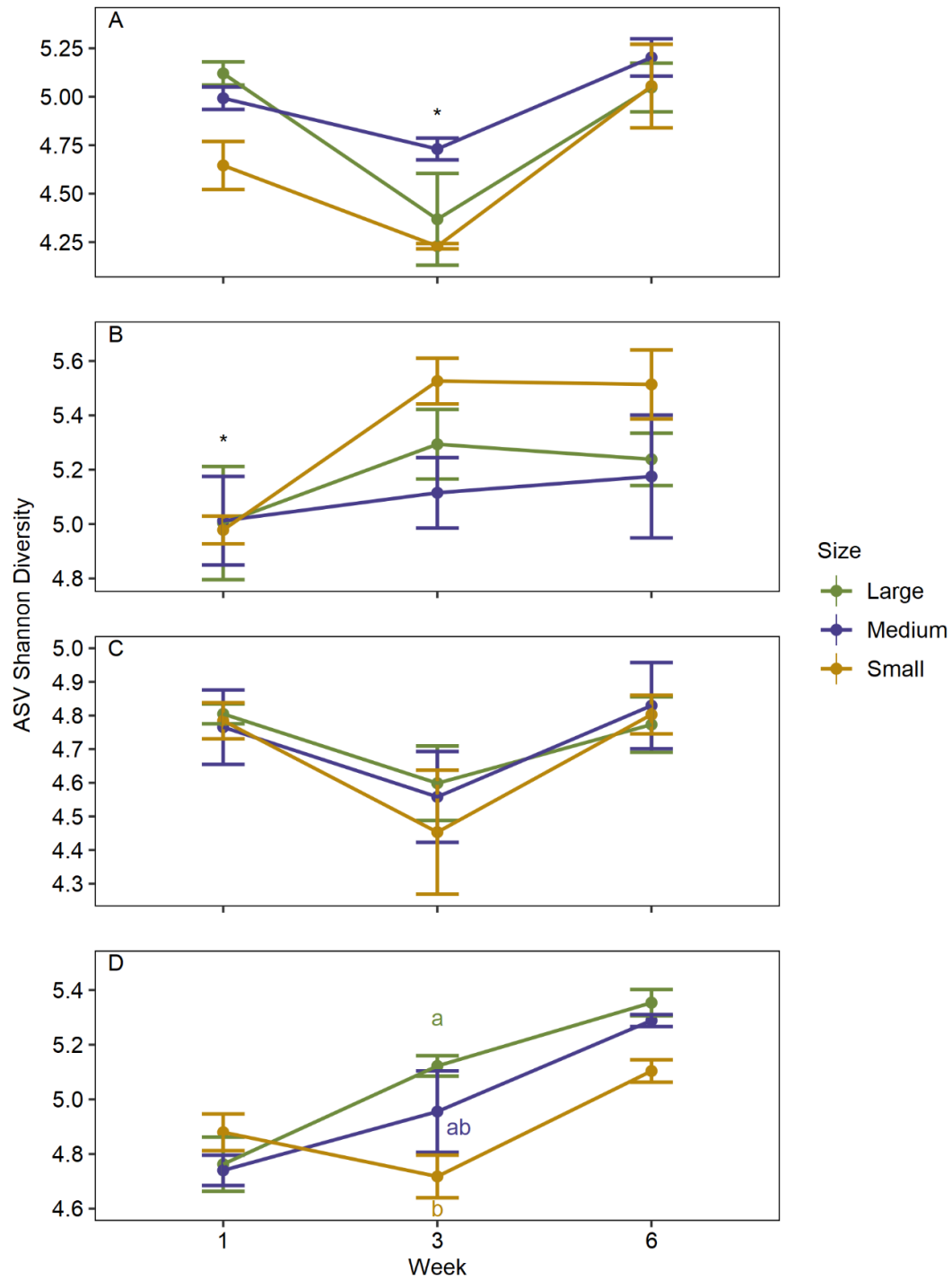


Figure 13. Mean (\pm SE) bacterial ASV Shannon diversity on each material type for weeks 1, 3 and 6 on A) film, B) foam, C) rigid, and D) wood substrates. The small letters correspond to results from Tukey's post-hoc test. The '*' indicate that week is different from the rest.

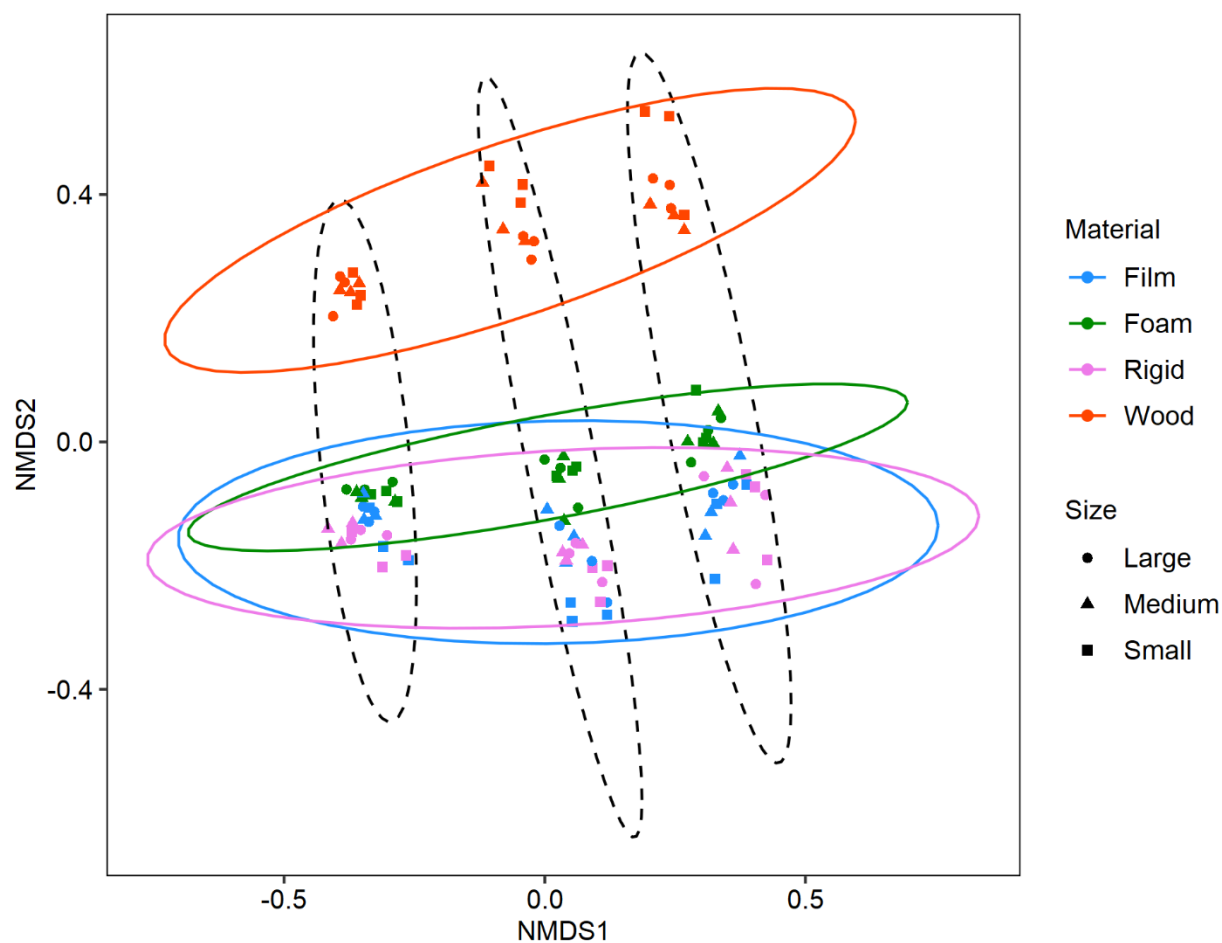


Figure 14. Nonmetric multidimensional scaling (NMDS) ordination of bacterial communities (Bray-Curtis dissimilarity) from substrates of four different material types and three different sizes in weeks 1, 3 and 6. Ellipses represent 95% CI. Solid ellipses correspond to material colors in the legend. Dashed line ellipses correspond from left to right to weeks 1, 3 and 6. Stress = 0.0927. Ordination created using 100 iterations.

Table 6. Results from full PERMANOVA on bacterial communities as well as pairwise PERMANOVA on weeks, size within each material type, and all material types. Values in bold indicate a significant p-value. All PERMANOVA performed with 1000 permutations.

| | Term | Df | F value | R2 | Pr(>F) |
|--------------|---------------|----|---------|--------------|------------------|
| Main factors | Material | 3 | 32.00 | 0.244 | <0.001 |
| | Week | 2 | 73.96 | 0.376 | <0.001 |
| | Size | 2 | 3.58 | 0.018 | <0.001 |
| | Material:Week | 6 | 7.62 | 0.116 | <0.001 |

| | | | | | |
|----------|--------------------|----|-------|--------------|--------------|
| | Material: Size | 6 | 1.20 | 0.018 | 0.179 |
| | Week:Size | 4 | 1.62 | 0.016 | 0.030 |
| | Material:Week:Size | 12 | 0.95 | 0.029 | 0.586 |
| Week | 1:3 | 1 | 29.88 | 0.299 | 0.002 |
| | 3:6 | 1 | 16.16 | 0.188 | 0.002 |
| | 1:6 | 1 | 50.70 | 0.420 | 0.002 |
| Material | Film: Foam | 1 | 3.49 | 0.063 | 0.191 |
| | Film:Rigid | 1 | 1.27 | 0.024 | 1.000 |
| | Film:Wood | 1 | 19.40 | 0.270 | 0.002 |
| | Foam: Rigid | 1 | 4.80 | 0.085 | 0.027 |
| | Foam: Wood | 1 | 19.29 | 0.271 | 0.002 |
| | Rigid: Wood | 1 | 20.79 | 0.286 | 0.002 |
| Film | Large:Medium | 1 | 0.30 | 0.018 | 1.000 |
| | Large:Small | 1 | 0.83 | 0.049 | 1.000 |
| | Medium:Small | 1 | 0.72 | 0.043 | 1.000 |
| Foam | Large:Medium | 1 | 0.32 | 0.019 | 1.000 |
| | Large:Small | 1 | 1.01 | 0.059 | 1.000 |
| | Medium:Small | 1 | 1.24 | 0.072 | 1.000 |
| Rigid | Large:Medium | 1 | 0.32 | 0.019 | 1.000 |
| | Large:Small | 1 | 0.47 | 0.028 | 1.000 |
| | Medium:Small | 1 | 0.77 | 0.046 | 1.000 |
| Wood | Large:Medium | 1 | 0.25 | 0.015 | 1.000 |
| | Large:Small | 1 | 0.48 | 0.029 | 1.000 |
| | Medium:Small | 1 | 0.60 | 0.036 | 1.000 |

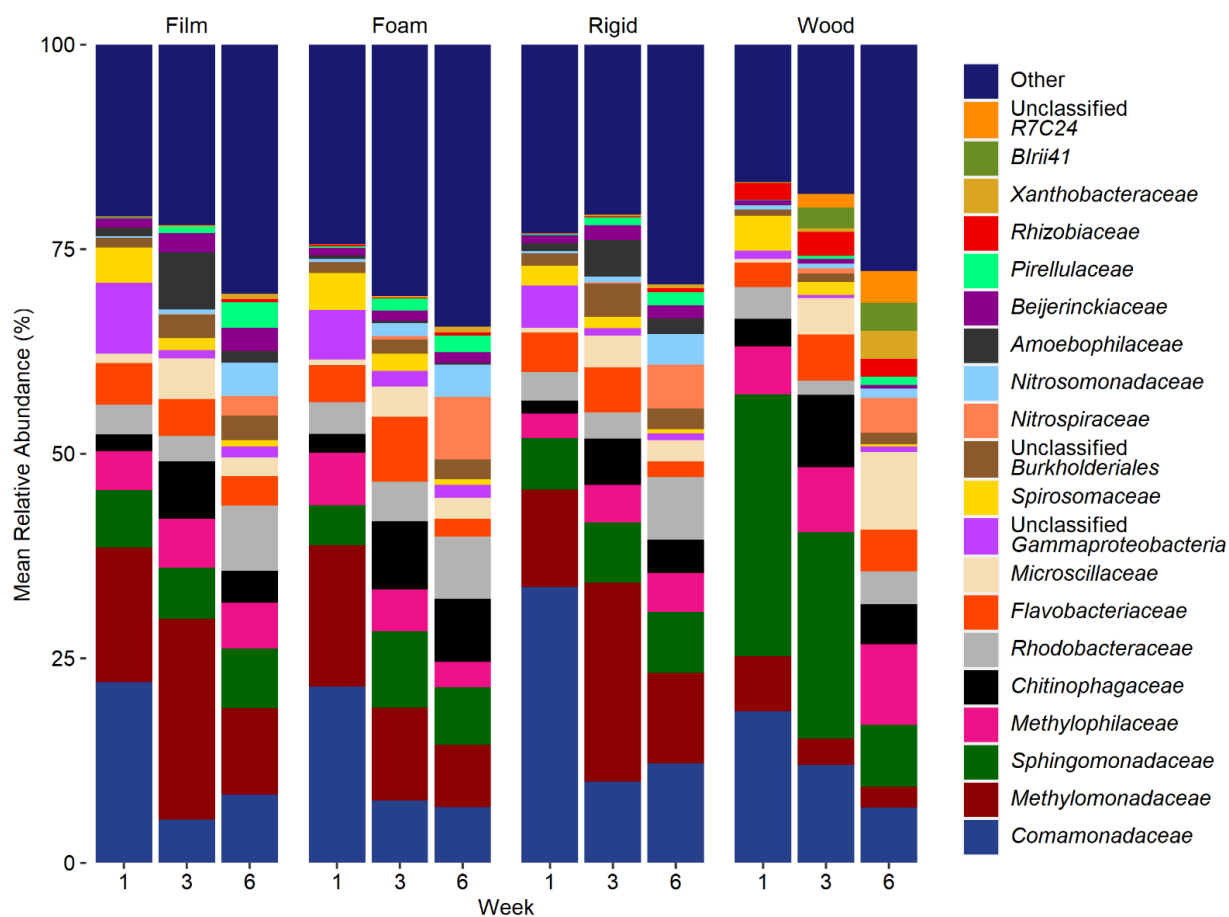


Figure 15. Mean relative abundance (%) of the top 20 bacterial families on each material type for weeks 1, 3 and 6. Families are organized from bottom to top in order of greatest overall mean relative abundance and the legend follows the same order. The ‘Other’ category includes all taxa where the maximum mean relative abundance was $<2.85\%$.

Table 7. Differentially abundant bacterial families between plastic and wood substrates in week 1 and the mean relative abundance (%). Families are organized in descending order by effect size.

| Family | Plastic Mean Relative Abundance (%) | Wood Mean Relative Abundance (%) | Effect Size | Magnitude | P |
|------------------------------------|---|--|----------------|-----------|----------|
| Unclassified <i>211ds20</i> | 0.00 | 0.65 | 0.973 | large | 2.03E-06 |
| <i>Azospirillaceae</i> | 0.00 | 0.21 | 0.907 | large | 9.88E-06 |
| <i>Blrii41</i> | 0.00 | 0.07 | 0.874 | large | 1.97E-05 |
| Unclassified <i>Blfdi19</i> | 0.00 | 0.05 | 0.784 | large | 2.36E-04 |
| Unclassified <i>Polyangiales</i> | 0.00 | 0.03 | 0.76 | large | 2.70E-04 |
| <i>Devosiaceae</i> | 0.05 | 0.28 | 0.755 | large | 2.70E-04 |
| <i>Rhizobiaceae</i> | 0.12 | 2.00 | 0.744 | large | 2.70E-04 |
| <i>Cellvibrionaceae</i> | 0.07 | 1.13 | 0.742 | large | 2.70E-04 |
| <i>Amoebophilaceae</i> | 0.79 | 0.02 | 0.741 | large | 2.70E-04 |
| <i>Cyclobacteriaceae</i> | 0.11 | 0.58 | 0.741 | large | 2.70E-04 |
| Unclassified | | | | | |
| <i>Gammaproteobacteria</i> | 6.60 | 1.03 | 0.74 | large | 2.70E-04 |
| <i>Sphingomonadaceae</i> | 6.06 | 32.03 | 0.74 | large | 2.70E-04 |
| <i>Oxalobacteraceae</i> | 2.40 | 1.04 | 0.731 | large | 3.20E-04 |
| <i>Legionellaceae</i> | 0.01 | 0.05 | 0.725 | large | 3.51E-04 |
| <i>Methylomonadaceae</i> | 15.21 | 6.72 | 0.709 | large | 4.96E-04 |
| <i>Clostridiaceae</i> | 0.29 | 0.12 | 0.682 | large | 9.44E-04 |
| <i>Peptostreptococcaceae</i> | 0.49 | 0.18 | 0.679 | large | 9.66E-04 |
| <i>Bacillaceae</i> | 0.25 | 0.02 | 0.675 | large | 1.02E-03 |
| Unclassified <i>PeM15</i> | 0.48 | 0.20 | 0.664 | large | 1.27E-03 |
| <i>Caedibacteraceae</i> | 0.00 | 0.04 | 0.657 | large | 1.50E-03 |
| <i>Chitinophagaceae</i> | 1.99 | 3.42 | 0.649 | large | 1.68E-03 |
| <i>Erysipelotrichaceae</i> | 0.11 | 0.05 | 0.647 | large | 1.68E-03 |
| Unclassified <i>Bacteria</i> | 1.11 | 0.54 | 0.621 | large | 2.99E-03 |
| <i>Porticoccaceae</i> | 0.00 | 0.03 | 0.614 | large | 3.40E-03 |
| <i>Caulobacteraceae</i> | 1.04 | 0.59 | 0.612 | large | 3.40E-03 |
| <i>Gemmatimonadaceae</i> | 0.14 | 0.03 | 0.607 | large | 3.60E-03 |
| Unclassified <i>KD4-96</i> | 0.36 | 0.13 | 0.606 | large | 3.60E-03 |
| Unclassified <i>Actinobacteria</i> | 0.35 | 0.16 | 0.6 | large | 4.01E-03 |
| <i>Xanthomonadaceae</i> | 0.44 | 0.22 | 0.597 | large | 4.01E-03 |
| <i>Moraxellaceae</i> | 0.49 | 0.07 | 0.597 | large | 4.01E-03 |
| Unknown <i>Family_4</i> | 0.02 | 0.06 | 0.579 | large | 5.93E-03 |
| <i>67-14</i> | 0.10 | 0.04 | 0.577 | large | 5.97E-03 |

| | | | | | |
|-----------------------------------|-------|-------|-------|----------|----------|
| <i>Sphingobacteriaceae</i> | 0.03 | 0.11 | 0.575 | large | 6.05E-03 |
| Unclassified <i>OPB41</i> | 0.13 | 0.06 | 0.571 | large | 6.34E-03 |
| <i>Pirellulaceae</i> | 0.16 | 0.05 | 0.57 | large | 6.34E-03 |
| <i>Mycobacteriaceae</i> | 0.28 | 0.16 | 0.567 | large | 6.59E-03 |
| <i>Alteromonadaceae</i> | 0.97 | 0.38 | 0.563 | large | 6.89E-03 |
| Unclassified <i>Subgroup 17</i> | 0.13 | 0.06 | 0.553 | large | 8.44E-03 |
| <i>Hyphomonadaceae</i> | 0.27 | 0.11 | 0.548 | large | 9.02E-03 |
| <i>Rickettsiaceae</i> | 0.06 | 0.21 | 0.542 | large | 1.01E-02 |
| <i>Flavobacteriaceae</i> | 4.81 | 3.04 | 0.539 | large | 1.05E-02 |
| Unclassified <i>Clostridia</i> | 0.11 | 0.04 | 0.537 | large | 1.06E-02 |
| <i>Nitrosomonadaceae</i> | 0.30 | 0.51 | 0.521 | large | 1.45E-02 |
| <i>Microscillaceae</i> | 0.81 | 0.41 | 0.515 | large | 1.60E-02 |
| <i>DEV007</i> | 0.00 | 0.01 | 0.514 | large | 1.68E-02 |
| <i>Armatimonadaceae</i> | 0.30 | 0.19 | 0.506 | large | 1.83E-02 |
| <i>Rhizobiales Incertae Sedis</i> | 0.18 | 0.38 | 0.499 | moderate | 2.03E-02 |
| <i>Ilumatobacteraceae</i> | 0.12 | 0.04 | 0.498 | moderate | 2.05E-02 |
| <i>Beijerinckiaceae</i> | 1.02 | 0.62 | 0.496 | moderate | 2.07E-02 |
| <i>Anaerolineaceae</i> | 0.23 | 0.11 | 0.494 | moderate | 2.15E-02 |
| Unclassified <i>SJA-15</i> | 0.09 | 0.03 | 0.492 | moderate | 2.17E-02 |
| <i>Bryobacteraceae</i> | 0.01 | 0.03 | 0.485 | moderate | 2.45E-02 |
| <i>Comamonadaceae</i> | 25.80 | 18.52 | 0.478 | moderate | 2.73E-02 |
| <i>Opitutaceae</i> | 0.27 | 0.58 | 0.472 | moderate | 2.98E-02 |
| <i>Blastocatellaceae</i> | 0.05 | 0.02 | 0.464 | moderate | 3.39E-02 |
| <i>Rhodocyclaceae</i> | 1.46 | 1.08 | 0.463 | moderate | 3.42E-02 |
| <i>env.OPS 17</i> | 0.12 | 0.04 | 0.448 | moderate | 4.37E-02 |
| Unclassified | | | | | |
| <i>Burkholderiales</i> | 1.33 | 0.78 | 0.445 | moderate | 4.59E-02 |

Table 8. Differentially abundant bacterial families between plastic and wood substrates in week 3. Families are organized in descending order by effect size.

| Family | Plastic Mean Relative Abundance (%) | Wood Mean Relative Abundance (%) | Effect Size | Magnitude | P |
|-------------------------------|-------------------------------------|----------------------------------|-------------|-----------|----------|
| <i>Birii41</i> | 0.00 | 2.57 | 0.973 | large | 8.34E-07 |
| Unclassified | | | | | |
| <i>Polyangiales</i> | 0.00 | 1.68 | 0.973 | large | 8.34E-07 |
| <i>Azospirillaceae</i> | 0.00 | 0.08 | 0.907 | large | 4.06E-06 |
| Unclassified <i>211ds20</i> | 0.01 | 1.59 | 0.907 | large | 4.06E-06 |
| <i>Micromonosporaceae</i> | 0.00 | 0.30 | 0.861 | large | 1.49E-05 |
| <i>Haliangiaceae</i> | 0.01 | 0.75 | 0.842 | large | 2.20E-05 |
| <i>Rhodanobacteraceae</i> | 0.01 | 0.11 | 0.828 | large | 2.89E-05 |
| Unclassified <i>R7C24</i> | 0.02 | 1.63 | 0.782 | large | 1.01E-04 |
| <i>Legionellaceae</i> | 0.01 | 0.12 | 0.776 | large | 1.07E-04 |
| <i>Polyangiaceae</i> | 0.02 | 0.27 | 0.768 | large | 1.20E-04 |
| Unclassified <i>Polyangia</i> | 0.00 | 0.20 | 0.76 | large | 1.45E-04 |
| <i>Rhizobiaceae</i> | 0.11 | 2.88 | 0.742 | large | 1.67E-04 |
| <i>Devosiaceae</i> | 0.26 | 1.47 | 0.74 | large | 1.67E-04 |
| <i>Gemmatimonadaceae</i> | 1.39 | 0.30 | 0.74 | large | 1.67E-04 |
| <i>Methylomonadaceae</i> | 20.07 | 3.24 | 0.74 | large | 1.67E-04 |
| <i>Sphingomonadaceae</i> | 7.67 | 25.19 | 0.74 | large | 1.67E-04 |
| <i>Amoebophilaceae</i> | 3.89 | 0.03 | 0.737 | large | 1.68E-04 |
| <i>Rubinisphaeraceae</i> | 0.41 | 0.14 | 0.725 | large | 2.23E-04 |
| Unclassified | | | | | |
| <i>Gammaproteobacteria</i> | 1.26 | 0.36 | 0.722 | large | 2.32E-04 |
| <i>Beijerinckiaceae</i> | 1.84 | 0.52 | 0.691 | large | 4.50E-04 |
| <i>Rhodocyclaceae</i> | 1.43 | 0.52 | 0.691 | large | 4.50E-04 |
| <i>Comamonadaceae</i> | 7.62 | 12.00 | 0.691 | large | 4.50E-04 |
| <i>Verrucomicrobiaceae</i> | 1.33 | 0.29 | 0.688 | large | 4.66E-04 |
| <i>Rhodobacteraceae</i> | 3.72 | 1.72 | 0.673 | large | 6.61E-04 |
| <i>Bryobacteraceae</i> | 0.14 | 0.58 | 0.668 | large | 7.25E-04 |
| <i>Methylophilaceae</i> | 5.19 | 7.95 | 0.661 | large | 8.29E-04 |
| Unclassified <i>PeM15</i> | 0.27 | 0.09 | 0.655 | large | 9.21E-04 |
| <i>Bacillaceae</i> | 0.25 | 0.02 | 0.653 | large | 9.27E-04 |
| Unclassified <i>SepB-3</i> | 0.49 | 0.00 | 0.652 | large | 9.27E-04 |
| <i>Phaselicystidaceae</i> | 0.02 | 0.11 | 0.634 | large | 1.39E-03 |
| <i>Hyphomonadaceae</i> | 0.92 | 0.27 | 0.627 | large | 1.58E-03 |

| | | | | | |
|-----------------------------|------|------|-------|----------|----------|
| Unclassified | | | | | |
| <i>Cyanobacteriia</i> | 0.63 | 0.04 | 0.622 | large | 1.70E-03 |
| <i>NS9 marine group</i> | 0.39 | 0.14 | 0.621 | large | 1.70E-03 |
| <i>Isosphaeraceae</i> | 0.03 | 0.17 | 0.619 | large | 1.77E-03 |
| <i>Opitutaceae</i> | 0.82 | 0.13 | 0.606 | large | 2.30E-03 |
| <i>Xanthobacteraceae</i> | 0.14 | 0.48 | 0.601 | large | 2.53E-03 |
| <i>Chamaesiphonaceae</i> | 0.13 | 0.00 | 0.597 | large | 2.66E-03 |
| Unclassified | | | | | |
| <i>Burkholderiales</i> | 2.88 | 1.02 | 0.585 | large | 3.45E-03 |
| <i>Rhizobiales Incertae</i> | | | | | |
| <i>Sedis</i> | 0.14 | 0.39 | 0.583 | large | 3.48E-03 |
| <i>Cytophagaceae</i> | 0.25 | 0.03 | 0.568 | large | 4.76E-03 |
| <i>Nitrospiraceae</i> | 0.24 | 0.60 | 0.554 | large | 6.22E-03 |
| <i>Armatimonadaceae</i> | 0.69 | 0.22 | 0.551 | large | 6.50E-03 |
| <i>Kineosporiaceae</i> | 0.03 | 0.13 | 0.544 | large | 7.41E-03 |
| <i>Pirellulaceae</i> | 1.04 | 0.43 | 0.542 | large | 7.53E-03 |
| <i>Raineyaceae</i> | 0.36 | 0.09 | 0.539 | large | 7.65E-03 |
| <i>PHOS-HE36</i> | 0.06 | 0.02 | 0.539 | large | 7.65E-03 |
| Unclassified <i>KD4-96</i> | 0.16 | 0.05 | 0.522 | large | 1.07E-02 |
| <i>AEGEAN-169 marine</i> | | | | | |
| <i>group</i> | 0.00 | 0.00 | 0.514 | large | 1.27E-02 |
| <i>Nannocystaceae</i> | 0.00 | 0.02 | 0.514 | large | 1.27E-02 |
| <i>Moraxellaceae</i> | 0.13 | 0.02 | 0.509 | large | 1.31E-02 |
| <i>NS11-12 marine group</i> | 1.04 | 0.35 | 0.502 | large | 1.45E-02 |
| Unclassified <i>Bfidi19</i> | 0.00 | 0.01 | 0.496 | moderate | 1.64E-02 |
| <i>Leptolyngbyaceae</i> | 0.25 | 0.01 | 0.496 | moderate | 1.62E-02 |
| <i>Crocinitomicaceae</i> | 0.85 | 0.28 | 0.493 | moderate | 1.64E-02 |
| <i>Parachlamydiaceae</i> | 0.00 | 0.03 | 0.49 | moderate | 1.77E-02 |
| <i>TRA3-20</i> | 0.10 | 0.01 | 0.485 | moderate | 1.84E-02 |
| <i>Alcaligenaceae</i> | 0.10 | 0.03 | 0.476 | moderate | 2.15E-02 |
| <i>Haliaceae</i> | 0.13 | 0.04 | 0.458 | moderate | 2.95E-02 |
| <i>Herpetosiphonaceae</i> | 0.00 | 0.04 | 0.455 | moderate | 3.12E-02 |
| <i>Sporichthyaceae</i> | 0.08 | 0.04 | 0.455 | moderate | 3.08E-02 |
| <i>Phycisphaeraceae</i> | 0.01 | 0.00 | 0.438 | moderate | 4.07E-02 |
| <i>Bdellovibrionaceae</i> | 0.08 | 0.02 | 0.435 | moderate | 4.20E-02 |
| <i>Blastocatellaceae</i> | 0.03 | 0.08 | 0.427 | moderate | 4.74E-02 |

Table 9. Differentially abundant bacterial families between plastic and wood substrates in week 6. Families are organized in descending order by effect size.

| Family | Plastic Mean Relative Abundance (%) | Wood Mean Relative Abundance (%) | Effect Size | Magnitude | P |
|-----------------------------|---|--|-------------|-----------|----------|
| Unclassified <i>211ds20</i> | 0.00 | 1.81 | 0.973 | large | 1.76E-06 |
| <i>Birii41</i> | 0.00 | 3.45 | 0.907 | large | 8.53E-06 |
| Unclassified | | | | | |
| <i>Polyangiales</i> | 0.01 | 2.56 | 0.86 | large | 2.50E-05 |
| <i>Micromonosporaceae</i> | 0.01 | 0.64 | 0.853 | large | 2.50E-05 |
| <i>Steroidobacteraceae</i> | 0.00 | 0.07 | 0.833 | large | 3.51E-05 |
| Nannocystaceae | 0.00 | 0.16 | 0.829 | large | 3.51E-05 |
| Unclassified <i>R7C24</i> | 0.01 | 3.84 | 0.813 | large | 4.89E-05 |
| <i>Ferrovibrionaceae</i> | 0.00 | 0.02 | 0.76 | large | 2.01E-04 |
| Unclassified | | | | | |
| <i>Cytophagales</i> | 0.01 | 0.14 | 0.743 | large | 2.01E-04 |
| <i>Rhizobiaceae</i> | 0.40 | 2.20 | 0.74 | large | 2.01E-04 |
| <i>Haliangiaceae</i> | 0.16 | 2.23 | 0.74 | large | 2.01E-04 |
| <i>Microscillaceae</i> | 2.49 | 9.52 | 0.74 | large | 2.01E-04 |
| <i>Xanthobacteraceae</i> | 0.59 | 3.41 | 0.74 | large | 2.01E-04 |
| <i>Rhodocyclaceae</i> | 1.64 | 0.27 | 0.74 | large | 2.01E-04 |
| <i>Amoebophilaceae</i> | 1.15 | 0.01 | 0.729 | large | 2.50E-04 |
| <i>Methylomonadaceae</i> | 9.78 | 2.55 | 0.722 | large | 2.65E-04 |
| <i>Methylophilaceae</i> | 4.51 | 9.87 | 0.722 | large | 2.65E-04 |
| Unclassified | | | | | |
| <i>Alphaproteobacteria</i> | 0.11 | 0.43 | 0.719 | large | 2.65E-04 |
| <i>Beijerinckiaceae</i> | 1.95 | 0.46 | 0.719 | large | 2.65E-04 |
| <i>Nitrosomonadaceae</i> | 3.93 | 1.14 | 0.715 | large | 2.65E-04 |
| Unclassified | | | | | |
| <i>vadinHA49</i> | 1.67 | 0.00 | 0.715 | large | 2.65E-04 |
| <i>Dongiaceae</i> | 0.01 | 0.07 | 0.696 | large | 4.11E-04 |
| <i>Azospirillaceae</i> | 0.00 | 0.04 | 0.696 | large | 4.11E-04 |
| <i>Raineyaceae</i> | 0.17 | 0.01 | 0.686 | large | 4.93E-04 |
| <i>Caulobacteraceae</i> | 0.29 | 0.76 | 0.682 | large | 5.28E-04 |
| <i>TRA3-20</i> | 0.44 | 0.07 | 0.673 | large | 6.19E-04 |
| <i>Pirellulaceae</i> | 2.26 | 1.00 | 0.673 | large | 6.19E-04 |
| <i>Gemmatimonadaceae</i> | 1.15 | 0.34 | 0.67 | large | 6.21E-04 |
| <i>Xanthomonadaceae</i> | 0.77 | 0.20 | 0.67 | large | 6.21E-04 |

| | | | | | |
|--------------------------------|------|------|-------|----------|----------|
| Unclassified <i>Bacteria</i> | 2.04 | 0.96 | 0.664 | large | 7.02E-04 |
| <i>Hyphomonadaceae</i> | 0.83 | 0.35 | 0.649 | large | 9.86E-04 |
| Unclassified <i>SepB-3</i> | 0.39 | 0.00 | 0.646 | large | 1.04E-03 |
| Unclassified | | | | | |
| <i>Verrucomicrobiae</i> | 0.10 | 0.34 | 0.634 | large | 1.34E-03 |
| Unclassified | | | | | |
| <i>Burkholderiales</i> | 2.66 | 1.43 | 0.624 | large | 1.63E-03 |
| <i>Leptolyngbyaceae</i> | 0.40 | 0.03 | 0.619 | large | 1.81E-03 |
| Unclassified | | | | | |
| <i>Bacteroidia</i> | 0.87 | 0.28 | 0.609 | large | 2.14E-03 |
| <i>Devosiaceae</i> | 0.77 | 1.70 | 0.609 | large | 2.14E-03 |
| <i>NS9 marine group</i> | 0.21 | 0.06 | 0.606 | large | 2.21E-03 |
| <i>Cytophagaceae</i> | 0.07 | 0.28 | 0.605 | large | 2.24E-03 |
| <i>Ancalomicrobiaceae</i> | 0.00 | 0.02 | 0.603 | large | 2.44E-03 |
| <i>Rhodobacteraceae</i> | 7.76 | 3.98 | 0.588 | large | 3.16E-03 |
| Unclassified | | | | | |
| <i>Blastocatellia</i> | 0.04 | 0.14 | 0.578 | large | 3.78E-03 |
| <i>Haliaceae</i> | 0.17 | 0.02 | 0.578 | large | 3.78E-03 |
| Unclassified <i>CCD24</i> | 0.00 | 0.02 | 0.569 | large | 4.55E-03 |
| Unclassified | | | | | |
| <i>Ga0077536</i> | 0.11 | 0.03 | 0.565 | large | 4.72E-03 |
| <i>Bacillaceae</i> | 0.17 | 0.03 | 0.555 | large | 5.78E-03 |
| <i>Sporichthyaceae</i> | 0.08 | 0.02 | 0.542 | large | 7.42E-03 |
| <i>Alcaligenaceae</i> | 0.05 | 0.00 | 0.54 | large | 7.54E-03 |
| <i>env.OPS 17</i> | 0.36 | 1.01 | 0.539 | large | 7.58E-03 |
| Unclassified | | | | | |
| <i>Oligoflexales</i> | 0.32 | 0.02 | 0.537 | large | 7.73E-03 |
| Unclassified | | | | | |
| <i>Planctomycetes</i> | 0.01 | 0.04 | 0.516 | large | 1.21E-02 |
| <i>AEGEAN-169 marine group</i> | 0.00 | 0.01 | 0.514 | large | 1.27E-02 |
| <i>PHOS-HE36</i> | 0.03 | 0.00 | 0.504 | large | 1.42E-02 |
| Unclassified | | | | | |
| <i>Cyanobacteria</i> | 0.45 | 0.14 | 0.497 | moderate | 1.62E-02 |
| <i>Ilumatobacteraceae</i> | 0.17 | 0.05 | 0.494 | moderate | 1.67E-02 |
| <i>Moraxellaceae</i> | 0.10 | 0.00 | 0.482 | moderate | 2.09E-02 |
| <i>Vicinamibacteraceae</i> | 0.00 | 0.04 | 0.477 | moderate | 2.29E-02 |
| Unclassified | | | | | |
| <i>Gammaproteobacteria</i> | 1.26 | 0.69 | 0.472 | moderate | 2.42E-02 |
| <i>Rickettsiaceae</i> | 0.07 | 0.01 | 0.459 | moderate | 2.98E-02 |
| Unclassified <i>mle1-27</i> | 0.07 | 0.02 | 0.459 | moderate | 2.98E-02 |

| <i>Unclassified</i> | | | | | | |
|----------------------------|------|------|-------|----------|----------|--|
| <i>Bacteroidetes VC2.1</i> | | | | | | |
| <i>Bac22</i> | 0.00 | 0.01 | 0.451 | moderate | 3.50E-02 | |
| <i>Flavobacteriaceae</i> | 2.54 | 5.06 | 0.441 | moderate | 3.93E-02 | |
| <i>Verrucomicrobiaceae</i> | 0.53 | 0.20 | 0.439 | moderate | 4.07E-02 | |
| <i>Spirosomaceae</i> | 0.64 | 0.23 | 0.432 | moderate | 4.47E-02 | |
| <i>Mycobacteriaceae</i> | 0.09 | 0.04 | 0.428 | moderate | 4.72E-02 | |
| <i>Xenococcaceae</i> | 0.67 | 0.07 | 0.427 | moderate | 4.72E-02 | |
| <i>SM2D12</i> | 0.22 | 0.10 | 0.426 | moderate | 4.72E-02 | |

Table 10. Results from 2-way ANOVA on algal large and medium ASV richness and medium ASV Shannon diversity and ART on algal small ASV richness and large and small ASV Shannon diversity among material type and week for each size. Values in bold indicate significant p-values.

| Size | Term | Df | F value | Pr(>F) |
|------------------------------|-------------|----|---------|------------------|
| <i>ASV Richness</i> | | | | |
| Large | Material | 3 | 25.75 | <0.001 |
| | Week | 2 | 1.95 | 0.164 |
| | Interaction | 6 | 2.16 | 0.083 |
| Medium | Material | 3 | 17.33 | <0.001 |
| | Week | 2 | 0.98 | 0.391 |
| | Interaction | 6 | 0.79 | 0.590 |
| Small | Material | 3 | 26.31 | <0.001 |
| | Week | 2 | 1.08 | 0.357 |
| | Interaction | 6 | 2.12 | 0.088 |
| <i>ASV Shannon Diversity</i> | | | | |
| Large | Material | 3 | 27.96 | <0.001 |
| | Week | 2 | 18.02 | <0.001 |
| | Interaction | 6 | 6.97 | <0.001 |
| Medium | Material | 3 | 27.29 | <0.001 |
| | Week | 2 | 11.77 | <0.001 |
| | Interaction | 6 | 3.79 | 0.009 |
| Small | Material | 3 | 25.42 | <0.001 |
| | Week | 2 | 15.32 | <0.001 |
| | Interaction | 6 | 4.10 | 0.006 |

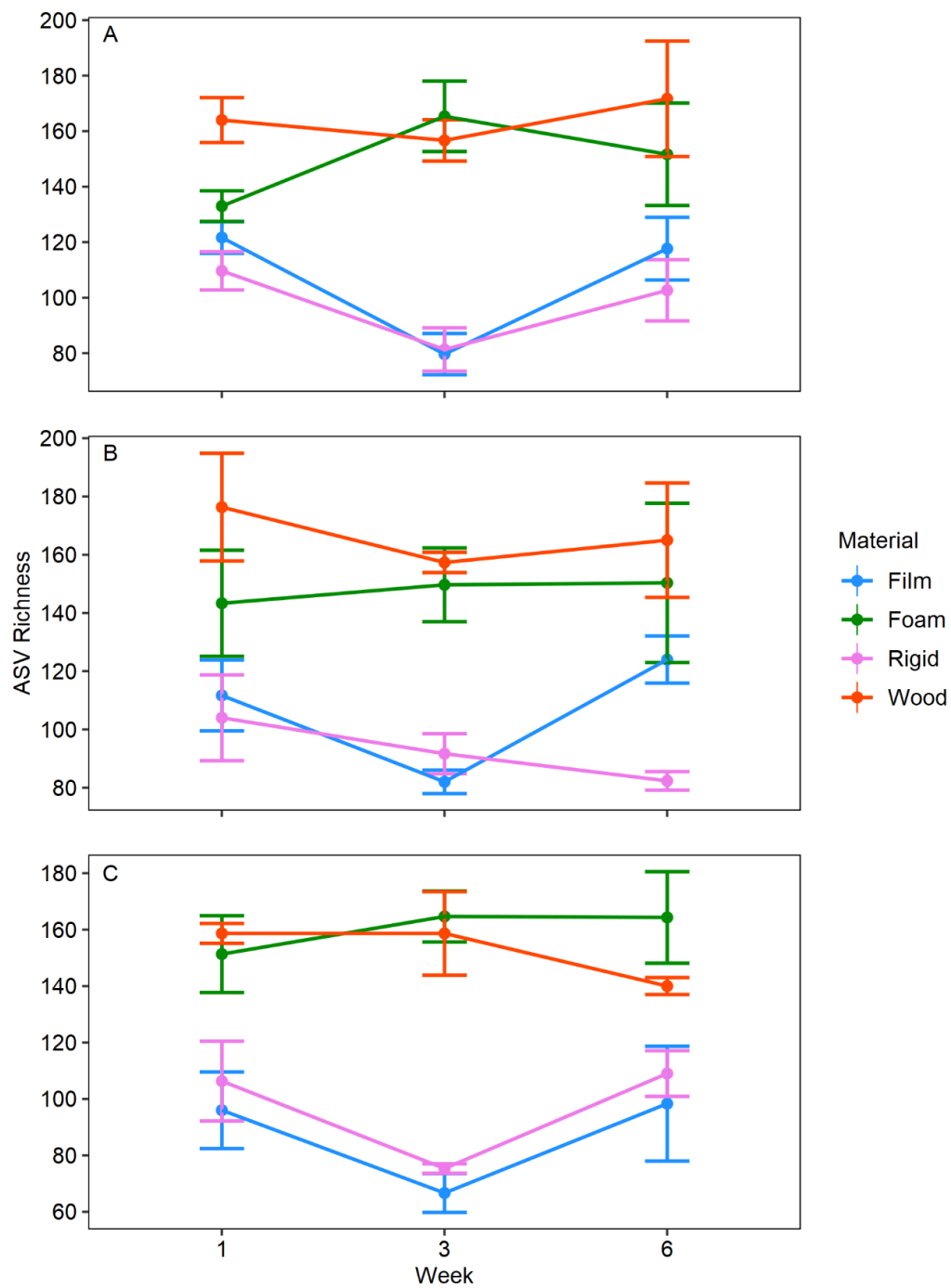


Figure 16. Mean (\pm SE) algal ASV Richness on each material type for weeks 1, 3 and 6 on A) large, B) medium, and C) small substrates.

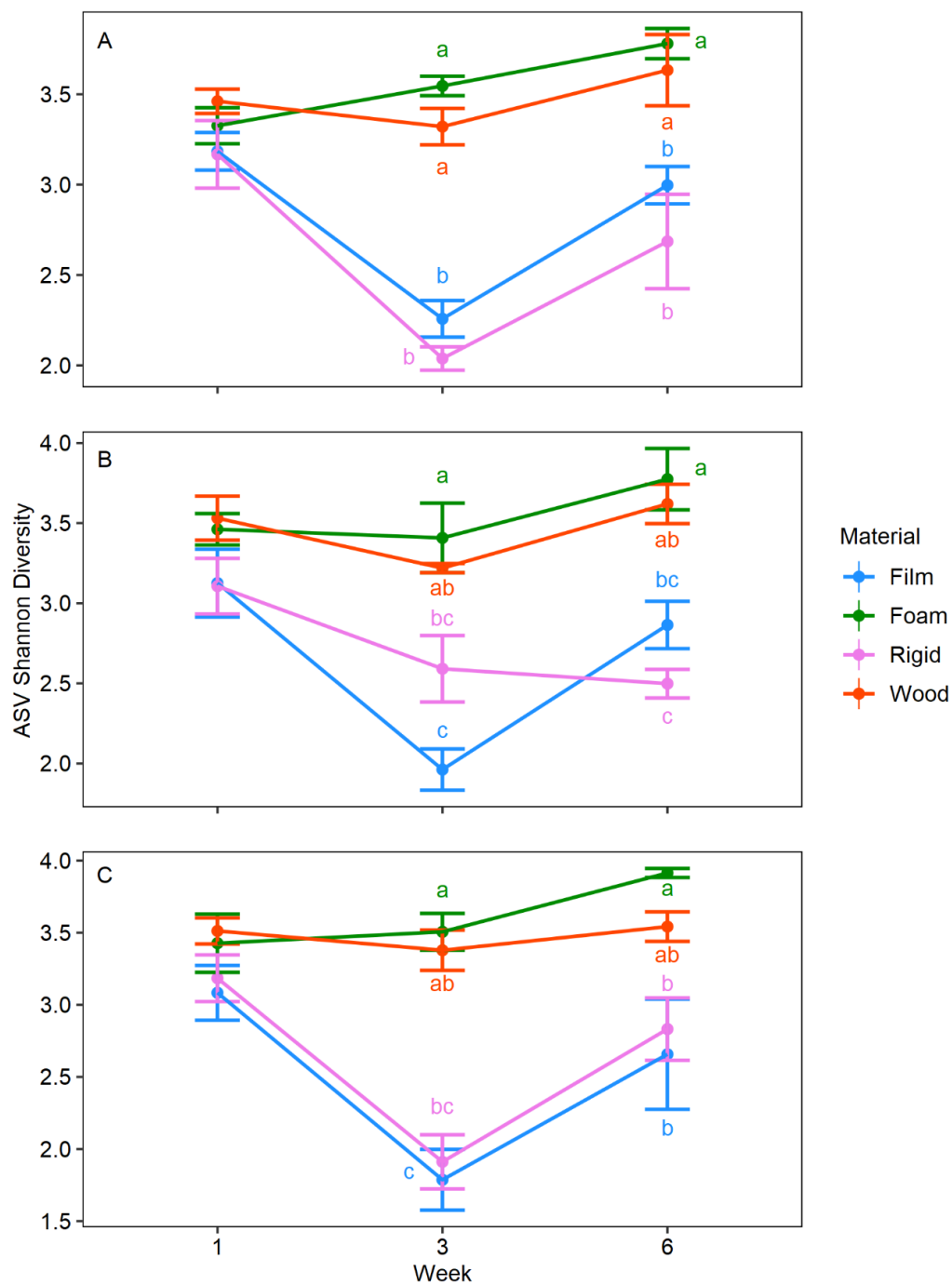


Figure 17. Mean (\pm SE) algal ASV Shannon diversity on each material type for weeks 1, 3 and 6 on A) large, B) medium, and C) small substrates. The small letters correspond to results from ART-C pairwise comparisons with Tukey's adjustment for multiple comparisons and Tukey's post-hoc test.

Table 11. Results from ART on algal ASV Richness and ASV Shannon Diversity among size and week for each material type. Values in bold indicate significant p-values.

| Size | Term | Df | F value | Pr(>F) |
|------------------------------|-------------|----|---------|------------------|
| <i>ASV Richness</i> | | | | |
| Film | Size | 2 | 3.02 | 0.074 |
| | Week | 2 | 10.45 | <0.001 |
| | Interaction | 4 | 0.20 | 0.934 |
| Foam | Size | 2 | 0.51 | 0.611 |
| | Week | 2 | 0.95 | 0.405 |
| | Interaction | 4 | 0.18 | 0.945 |
| Rigid | Size | 2 | 0.27 | 0.768 |
| | Week | 2 | 5.11 | 0.018 |
| | Interaction | 4 | 1.44 | 0.261 |
| Wood | Size | 2 | 0.33 | 0.725 |
| | Week | 2 | 2.50 | 0.115 |
| | Interaction | 4 | 0.15 | 0.959 |
| <i>ASV Shannon Diversity</i> | | | | |
| Film | Size | 2 | 1.83 | 0.189 |
| | Week | 2 | 27.19 | <0.001 |
| | Interaction | 4 | 0.25 | 0.904 |
| Foam | Size | 2 | 0.23 | 0.794 |
| | Week | 2 | 7.74 | 0.004 |
| | Interaction | 4 | 0.31 | 0.867 |
| Rigid | Size | 2 | 0.28 | 0.758 |
| | Week | 2 | 21.53 | <0.001 |
| | Interaction | 4 | 2.29 | 0.099 |
| Wood | Size | 2 | 0.03 | 0.976 |
| | Week | 2 | 4.74 | 0.022 |
| | Interaction | 4 | 0.35 | 0.840 |

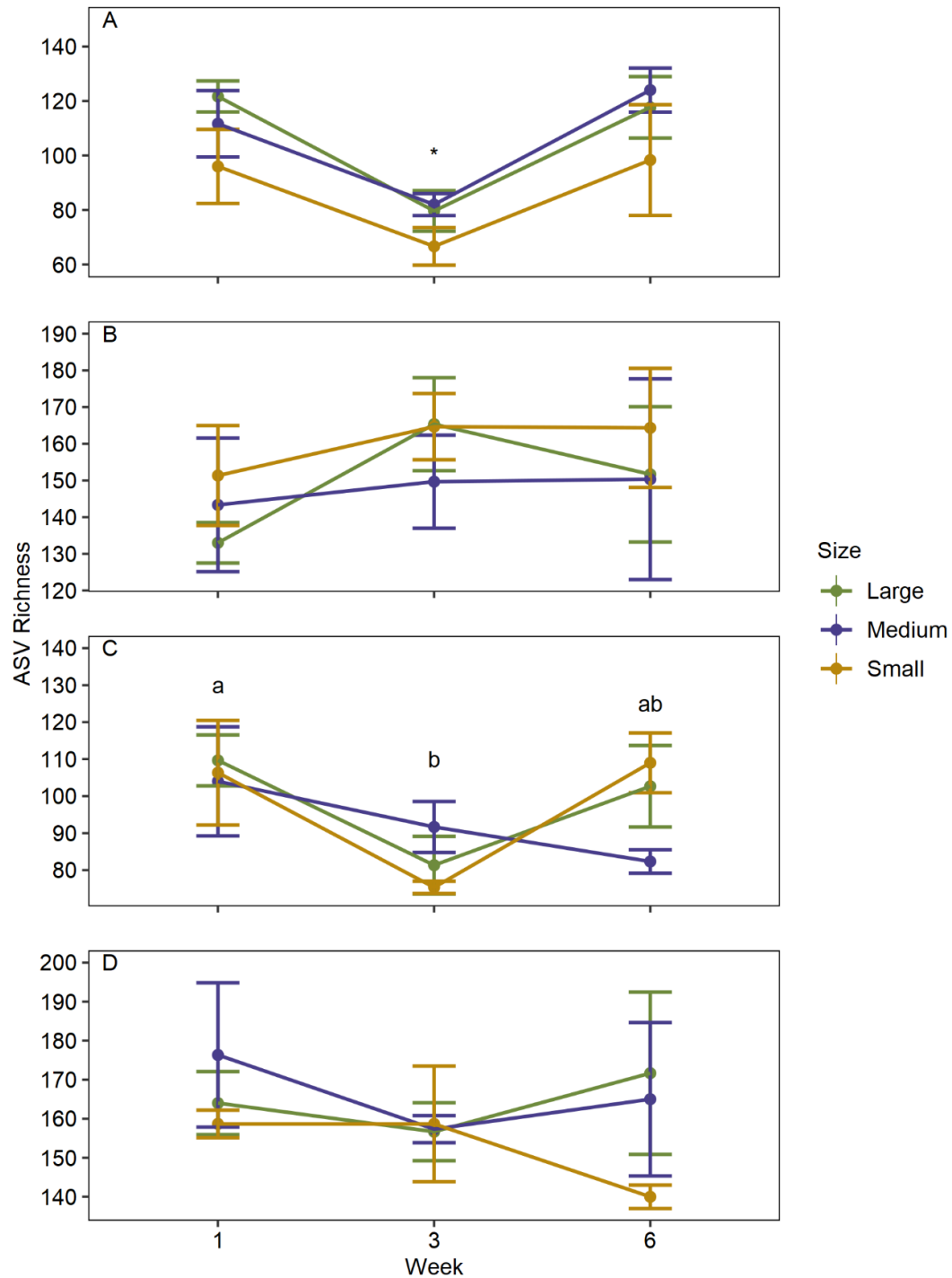


Figure 18. Mean (\pm SE) algal ASV Richness on each material type for weeks 1, 3 and 6 on A) film, B) foam, C) rigid, and D) wood substrates. The small letters correspond to results from Tukey's post-hoc test. The '*' indicate that week is different from the rest.

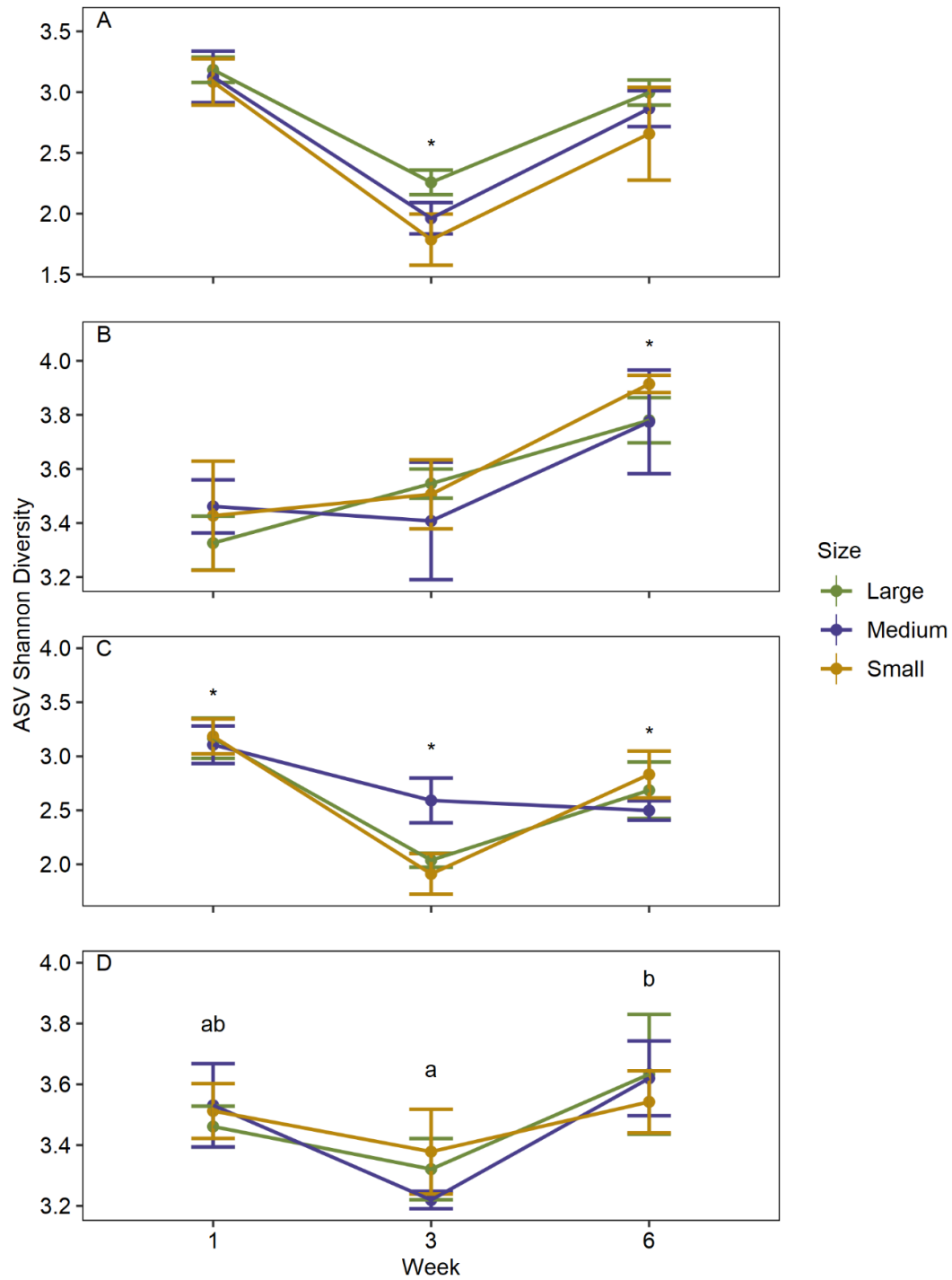


Figure 19. Mean (\pm SE) algal ASV Richness on each material type for weeks 1, 3 and 6 on A) film, B) foam, C) rigid, and D) wood substrates. The small letters correspond to results from Tukey's post-hoc test. The '*' indicate that week is different from the rest.

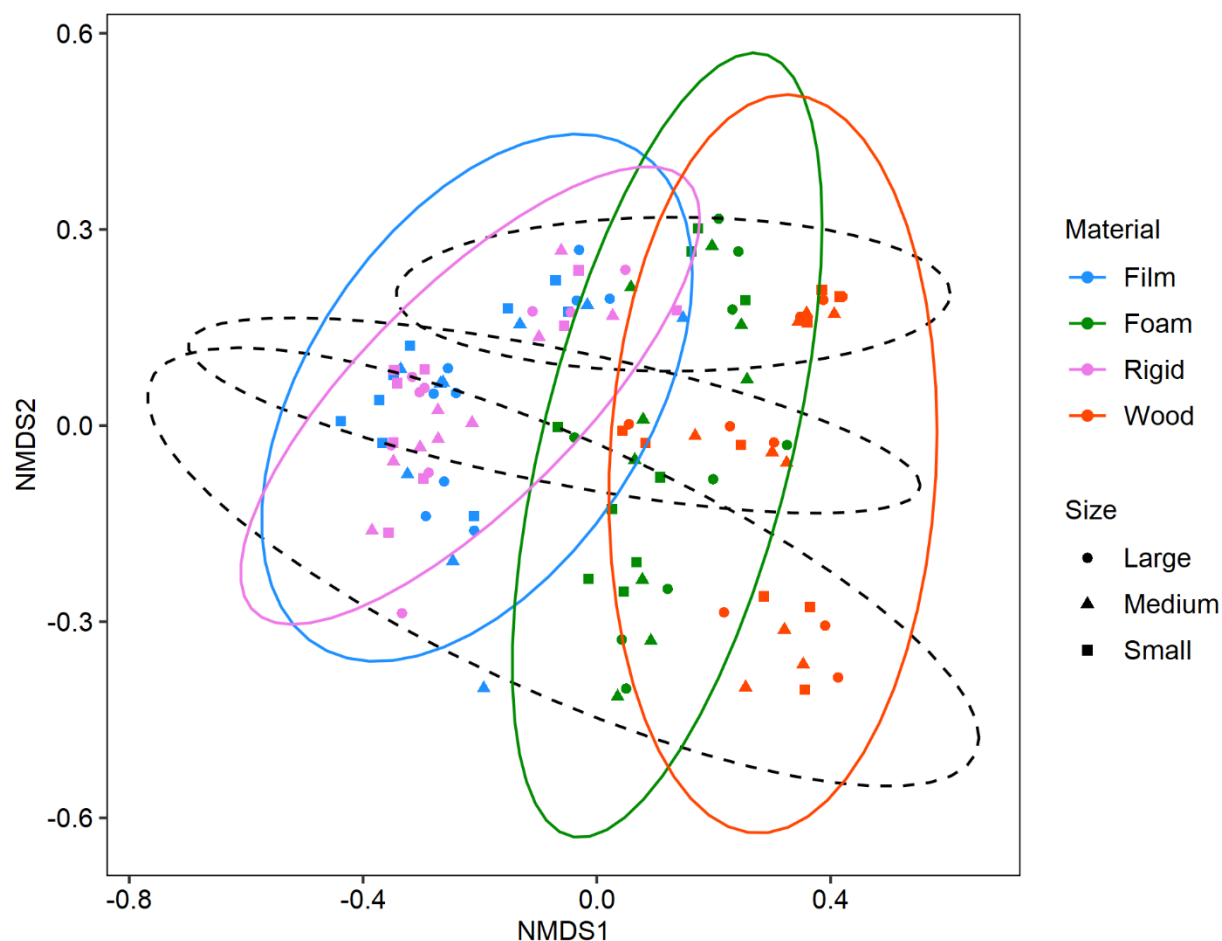


Figure 20. Nonmetric multidimensional scaling (NMDS) ordination of algal communities (Bray-Curtis dissimilarity) from substrates of four different material types and three different sizes in weeks 1, 3 and 6. Ellipses represent 95% CI. Solid ellipses correspond to material colors in the legend. Dashed line ellipses correspond from top right to bottom left to weeks 1, 3 and 6. Stress = 0.158. Ordination created using 100 iterations.

Table 12. Results from full PERMANOVA on algal communities as well as pairwise PERMANOVA on weeks, size within each material type, and all material types. Values in bold indicate a significant p-value. All PERMANOVA performed with 1000 permutations.

| Main Factors | Term | Df | F value | R2 | Pr(>F) |
|--------------|---------------|----|---------|--------------|------------------|
| | Material | 3 | 39.06 | 0.334 | <0.001 |
| | Week | 2 | 42.29 | 0.241 | <0.001 |
| | Size | 2 | 3.00 | 0.017 | <0.001 |
| | Material:Week | 6 | 7.62 | 0.131 | <0.001 |

| | | | | | |
|----------|--------------------|----|-------|--------------|--------------|
| | Material:Size | 6 | 1.27 | 0.022 | 0.128 |
| | Week:Size | 4 | 1.41 | 0.016 | 0.092 |
| | Material:Week:Size | 12 | 0.97 | 0.033 | 0.554 |
| Week | 1:3 | 1 | 19.26 | 0.216 | 0.002 |
| | 3:6 | 1 | 7.39 | 0.095 | 0.004 |
| | 1:6 | 1 | 24.86 | 0.262 | 0.002 |
| Material | Film:Foam | 1 | 17.36 | 0.250 | 0.002 |
| | Film:Rigid | 1 | 0.63 | 0.012 | 0.675 |
| | Film:Wood | 1 | 25.31 | 0.327 | 0.002 |
| | Foam:Rigid | 1 | 19.62 | 0.274 | 0.002 |
| | Foam:Wood | 1 | 13.63 | 0.208 | 0.002 |
| | Rigid:Wood | 1 | 27.32 | 0.344 | 0.002 |
| Film | Large:Medium | 1 | 0.26 | 0.016 | 0.944 |
| | Large:Small | 1 | 0.94 | 0.055 | 1.000 |
| | Medium:Small | 1 | 0.86 | 0.051 | 1.000 |
| Foam | Large:Medium | 1 | 0.45 | 0.027 | 0.854 |
| | Large:Small | 1 | 1.52 | 0.087 | 1.000 |
| | Medium:Small | 1 | 1.18 | 0.069 | 1.000 |
| Rigid | Large:Medium | 1 | 0.33 | 0.020 | 0.927 |
| | Large:Small | 1 | 0.61 | 0.036 | 1.000 |
| | Medium:Small | 1 | 1.35 | 0.078 | 1.000 |
| Wood | Large:Medium | 1 | 0.21 | 0.013 | 0.966 |
| | Large:Small | 1 | 0.52 | 0.031 | 0.763 |
| | Medium:Small | 1 | 0.73 | 0.043 | 1.000 |

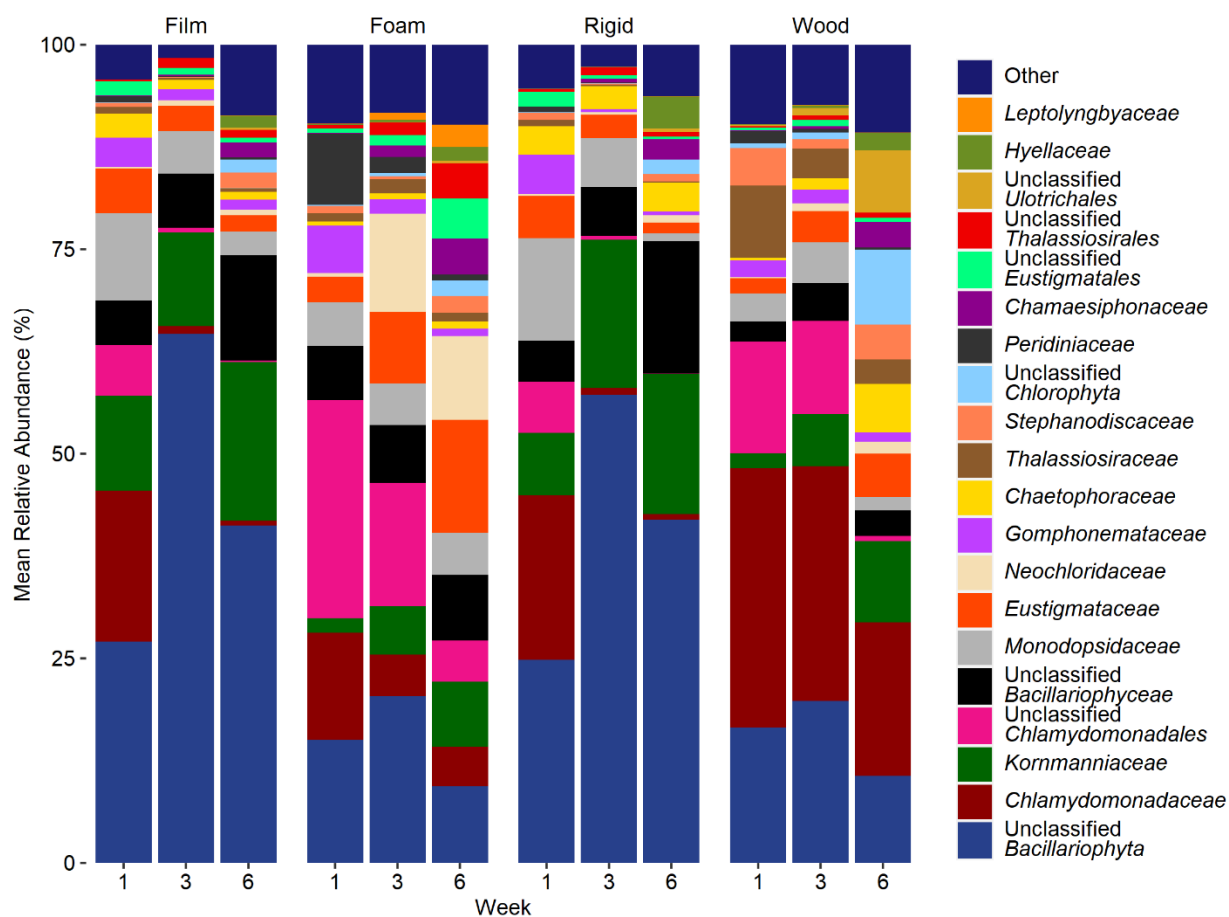


Figure 21. Mean relative abundance (%) of the top 20 algal families on each material type for weeks 1, 3 and 6. Families are organized from bottom to top in order of greatest overall mean relative abundance and the legend follows the same order. The ‘Other’ category includes all taxa where the maximum mean relative abundance was <2.70%.

Table 13. Differentially abundant algal families between plastic and wood substrates in week 1 and the mean relative abundance (%). Families are organized in descending order by effect size.

| Family | Plastic Mean Relative Abundance (%) | Wood Mean Relative Abundance (%) | Effect Size | Magnitude | P |
|-----------------------------------|---|--|-------------|-----------|----------|
| <i>Chromulinaceae</i> | 0.03 | 0.28 | 0.749 | large | 2.09E-04 |
| <i>Thalassiosiraceae</i> | 0.89 | 8.87 | 0.740 | large | 2.09E-04 |
| <i>Stephanodiscaceae</i> | 0.73 | 4.55 | 0.740 | large | 2.09E-04 |
| Unclassified <i>Chlorophyta</i> | 0.10 | 0.57 | 0.735 | large | 2.09E-04 |
| <i>Chlorellaceae</i> | 0.17 | 0.91 | 0.734 | large | 2.09E-04 |
| Unclassified | | | | | |
| <i>Chlorophyceae</i> | 0.10 | 0.54 | 0.724 | large | 2.28E-04 |
| <i>Chlamydomonadaceae</i> | 17.22 | 31.70 | 0.715 | large | 2.41E-04 |
| <i>Euglenaceae</i> | 0.04 | 0.26 | 0.712 | large | 2.41E-04 |
| Unclassified <i>Ulotrichales</i> | 0.04 | 0.18 | 0.697 | large | 3.14E-04 |
| Unclassified <i>Viridiplantae</i> | 0.03 | 0.27 | 0.687 | large | 3.66E-04 |
| <i>Scenedesmaceae</i> | 0.05 | 0.31 | 0.678 | large | 4.10E-04 |
| <i>Eustigmataceae</i> | 4.59 | 1.86 | 0.676 | large | 4.10E-04 |
| <i>Selenastraceae</i> | 0.05 | 0.27 | 0.672 | large | 4.24E-04 |
| <i>Monodopsidaceae</i> | 9.49 | 3.42 | 0.667 | large | 4.44E-04 |
| <i>Chaetophoraceae</i> | 2.29 | 0.27 | 0.642 | large | 7.58E-04 |
| Unclassified <i>Chlorellales</i> | 0.00 | 0.05 | 0.614 | large | 1.38E-03 |
| Unclassified | | | | | |
| <i>Bacillariophyceae</i> | 5.68 | 2.52 | 0.612 | large | 1.38E-03 |
| <i>Fragilariaceae</i> | 0.30 | 1.03 | 0.610 | large | 1.38E-03 |
| <i>Phacaceae</i> | 0.01 | 0.14 | 0.605 | large | 1.46E-03 |
| <i>Desmidiaceae</i> | 0.14 | 0.75 | 0.602 | large | 1.47E-03 |
| <i>Oedogoniaceae</i> | 0.02 | 0.14 | 0.601 | large | 1.47E-03 |
| Unclassified | | | | | |
| <i>Eustigmatales</i> | 1.35 | 0.31 | 0.594 | large | 1.63E-03 |
| Unclassified | | | | | |
| <i>Stramenopiles</i> | 0.01 | 0.11 | 0.582 | large | 2.07E-03 |
| <i>Bacillariaceae</i> | 0.60 | 1.30 | 0.570 | large | 2.56E-03 |
| <i>Compsopogonaceae</i> | 0.00 | 0.07 | 0.546 | large | 4.17E-03 |
| Unclassified | | | | | |
| <i>Cyanobacteria</i> | 0.22 | 0.03 | 0.529 | large | 5.60E-03 |
| <i>Neochloridaceae</i> | 0.31 | 0.09 | 0.518 | large | 6.69E-03 |
| <i>Vaucheriaceae</i> | 0.01 | 0.07 | 0.516 | large | 6.69E-03 |

| | | | | | |
|-------------------------|------|------|-------|----------|----------|
| <i>Synechococcaceae</i> | 0.01 | 0.07 | 0.516 | large | 6.69E-03 |
| Unclassified | | | | | |
| <i>Trebouxiophyceae</i> | 0.00 | 0.01 | 0.514 | large | 6.97E-03 |
| <i>Kornmanniaceae</i> | 6.99 | 1.84 | 0.484 | moderate | 1.14E-02 |
| Unclassified | | | | | |
| <i>Synechococcales</i> | 0.15 | 0.02 | 0.476 | moderate | 1.29E-02 |
| <i>Gomphonemataceae</i> | 4.72 | 2.07 | 0.472 | moderate | 1.35E-02 |
| <i>Naviculaceae</i> | 1.52 | 0.26 | 0.469 | moderate | 1.38E-02 |
| <i>Schizomeridaceae</i> | 0.11 | 0.27 | 0.449 | moderate | 1.95E-02 |
| <i>Trebouxiophyceae</i> | 0.01 | 0.05 | 0.408 | moderate | 3.85E-02 |

Table 14. Differentially abundant algal families between plastic and wood substrates in week 3 and the mean relative abundance (%). Families are organized in descending order by effect size.

| Family | Plastic Mean Relative Abundance (%) | Wood Mean Relative Abundance (%) | Effect Size | Magnitude | P |
|---------------------------|---|--|-------------|-----------|----------|
| Unclassified | | | | | |
| <i>Ulotrichales</i> | 0.02 | 0.93 | 0.769 | large | 4.19E-04 |
| <i>Chlamydomonadaceae</i> | 2.27 | 28.72 | 0.740 | large | 4.72E-04 |
| <i>Trebouxiophyceae</i> | 0.04 | 0.21 | 0.697 | large | 8.60E-04 |
| <i>Chlorellaceae</i> | 0.03 | 0.23 | 0.692 | large | 8.60E-04 |
| Unclassified | | | | | |
| <i>Chlorophyta</i> | 0.16 | 0.85 | 0.668 | large | 1.26E-03 |
| <i>Scenedesmaceae</i> | 0.02 | 0.19 | 0.639 | large | 2.01E-03 |
| <i>Thalassiosiraceae</i> | 0.74 | 3.58 | 0.631 | large | 2.01E-03 |
| <i>Hazeniacea</i> | 0.05 | 0.28 | 0.625 | large | 2.01E-03 |
| <i>Stephanodiscaceae</i> | 0.21 | 1.16 | 0.624 | large | 2.01E-03 |
| Unclassified | | | | | |
| <i>Chlorophyceae</i> | 0.06 | 0.33 | 0.621 | large | 2.01E-03 |
| Unclassified | | | | | |
| <i>Cyanobacteria</i> | 0.46 | 0.05 | 0.604 | large | 2.74E-03 |
| Unclassified | | | | | |
| <i>Sphaeropleales</i> | 0.01 | 0.05 | 0.581 | large | 3.92E-03 |
| <i>Bacillariaceae</i> | 0.15 | 0.78 | 0.581 | large | 3.92E-03 |
| <i>Schizomeridaceae</i> | 0.03 | 0.11 | 0.554 | large | 6.49E-03 |
| <i>Selenastraceae</i> | 0.05 | 0.14 | 0.514 | large | 1.38E-02 |
| <i>Naviculaceae</i> | 0.16 | 0.54 | 0.510 | large | 1.41E-02 |
| <i>Synechococcaceae</i> | 0.04 | 0.16 | 0.494 | moderate | 1.84E-02 |

| | | | | | |
|--------------------------|-------|-------|-------|----------|----------|
| Unclassified | | | | | |
| <i>Bacillariophyta</i> | 47.41 | 19.80 | 0.484 | moderate | 2.08E-02 |
| <i>Rhizosoleniaceae</i> | 0.07 | 0.35 | 0.478 | moderate | 2.25E-02 |
| Unclassified | | | | | |
| <i>Synechococcales</i> | 0.89 | 0.25 | 0.463 | moderate | 2.69E-02 |
| <i>Fragilariaceae</i> | 0.12 | 0.17 | 0.462 | moderate | 2.69E-02 |
| <i>Peronosporaceae</i> | 0.00 | 0.02 | 0.432 | moderate | 4.40E-02 |
| Unclassified | | | | | |
| <i>Chlamydomonadales</i> | 5.37 | 11.40 | 0.429 | moderate | 4.40E-02 |
| Unclassified | | | | | |
| <i>Viridiplantae</i> | 0.01 | 0.04 | 0.426 | moderate | 4.51E-02 |
| <i>Eunotiaceae</i> | 0.39 | 0.50 | 0.421 | moderate | 4.71E-02 |
| <i>Chromulinaceae</i> | 0.00 | 0.02 | 0.418 | moderate | 4.80E-02 |
| Unclassified | | | | | |
| <i>Chlorellales</i> | 0.00 | 0.01 | 0.414 | moderate | 4.80E-02 |
| <i>Oocystaceae</i> | 0.00 | 0.03 | 0.414 | moderate | 4.80E-02 |
| <i>Vitrellaceae</i> | 0.00 | 0.01 | 0.414 | moderate | 4.80E-02 |
| <i>Hemiaulaceae</i> | 0.23 | 0.97 | 0.409 | moderate | 4.80E-02 |
| <i>Compsopogonaceae</i> | 0.00 | 0.02 | 0.407 | moderate | 4.94E-02 |

Table 15. Differentially abundant algal families between plastic and wood substrates in week 6 and the mean relative abundance (%). Families are organized in descending order by effect size.

| Family | Plastic Mean Relative Abundance (%) | Wood Mean Relative Abundance (%) | Effect Size | Magnitude | P |
|---------------------------|---|--|-------------|-----------|----------|
| <i>Hazeniacea</i> | 0.00 | 0.36 | 0.937 | large | 2.23E-06 |
| Unclassified | | | | | |
| <i>Ulotrichales</i> | 0.35 | 7.62 | 0.740 | large | 4.19E-04 |
| <i>Chlamydomonadaceae</i> | 2.03 | 18.77 | 0.728 | large | 4.19E-04 |
| Unclassified | | | | | |
| <i>Chlorophyta</i> | 1.76 | 9.10 | 0.722 | large | 4.19E-04 |
| Unclassified | | | | | |
| <i>Ectocarpales</i> | 0.00 | 0.07 | 0.701 | large | 6.06E-04 |
| <i>Thalassiosiraceae</i> | 0.57 | 2.96 | 0.650 | large | 1.78E-03 |
| Unclassified | | | | | |
| <i>Viridiplantae</i> | 0.19 | 1.06 | 0.613 | large | 3.73E-03 |
| Unclassified | | | | | |
| <i>Bacillariophyceae</i> | 12.33 | 3.14 | 0.606 | large | 3.84E-03 |

| | | | | | |
|---------------------------------|-------|-------|-------|----------|----------|
| <i>Chaetophoraceae</i> | 1.80 | 5.96 | 0.588 | large | 5.17E-03 |
| Unclassified | | | | | |
| <i>Pleurocapsales</i> | 0.21 | 0.74 | 0.578 | large | 5.73E-03 |
| <i>Batrachospermaceae</i> | 0.03 | 0.22 | 0.557 | large | 8.27E-03 |
| <i>Chlorocystidaceae</i> | 0.00 | 0.01 | 0.514 | large | 1.98E-02 |
| <i>Oscillatoriaceae</i> | 0.02 | 0.23 | 0.496 | moderate | 2.49E-02 |
| Unclassified | | | | | |
| <i>Stramenopiles</i> | 0.01 | 0.26 | 0.486 | moderate | 2.77E-02 |
| <i>Pseudanabaenaceae</i> | 0.33 | 0.56 | 0.471 | moderate | 3.44E-02 |
| Unclassified <i>Naviculales</i> | 1.06 | 0.20 | 0.466 | moderate | 3.51E-02 |
| Unclassified | | | | | |
| <i>Bacillariophyta</i> | 30.85 | 10.64 | 0.454 | moderate | 4.16E-02 |
| <i>Stephanodiscaceae</i> | 1.59 | 4.29 | 0.448 | moderate | 4.38E-02 |

Discussion

Our objective was to determine if plastic selected for a distinct biofilm community relative to wood, by considering biofilm abundance, activity, and community composition. Because the experimental design also incorporated time and substrate size as factors, a variety of patterns emerged across the response variables and dates. Our hypothesis that wood would show distinct patterns from all three plastic types was supported by data for several metrics including respiration, chlorophyll, and bacterial assemblage, but not for others such as biofilm biomass and algal assemblage. In addition, our hypothesis that the three plastic types would show distinct biofilms from one another was not supported, as biofilms on foamed polystyrene were distinct from the two polyethylene types, which were similar to each other. Finally, our prediction that larger substrates would have increased taxonomic richness and diversity relative to smaller ones was not supported. The rich dataset generated by this experiment demonstrated that substrate type and time-controlled biofilm composition and activity on biofilms colonizing wood, foamed polystyrene, and polythene in an urban river.

Biofilm Activity: Respiration and N₂ flux

The clearest trend in rates for ecosystem processes in this experiment was that wood had higher rates of respiration compared to all 3 plastic types, which showed low and similar respiration rates for all sizes of substrates (Fig 6). The likely explanation is wood is both a growth surface and energy source for colonizing microbes, while plastic served as a growth surface but not a carbon source during the 6-week incubation (Oberbeckmann et al., 2021). Anecdotally, wood degradation was visible over the course of the incubation. From an ecological perspective, wood and buoyant plastic provide a similar habitat for biofilm growth and move in a comparable way in large rivers. However, the durability of wood as habitat is short-lived relative to plastic, suggesting the microbial downstream transport will be much longer on plastic (Hoellein et al., 2019; Webster et al., 1999).

Other studies have found mixed results when comparing respiration on natural surfaces and plastic, although the 'natural' surface varies across publications. Chaudhary et al., (2022) found rates of respiration were higher on tile (i.e., a surrogate for periphyton on rocks) than on rigid and soft polyethylene and polyvinylchloride (PVC), although the authors found foamed polystyrene had higher rates of respiration. Higher rates of respiration were also recorded on tile compared to plastic by Hoellein et al., (2014). In contrast, Vincent et al., (2022) measured biofilm respiration at six sites across the United States and found no differences in respiration between biofilms on tile compared to PVC and polystyrene at 4 of the locations. Comparing studies is complicated by variation in the choice of plastic types used, and the habitats where the incubations took place. As this field of study matures, aligning comparisons that have similar

duration, substrate types, habitats, and response variables is needed to generate insights into the influence of plastic substrates on ecosystem processes such as respiration.

Unlike respiration, there were no significant trends among substrates for N_2 flux. We added nitrate and dextrose to the incubation assays with the objective of measuring *potential* denitrification (i.e., the amount of N_2 produced by denitrification when N and C are not limiting; DNP). However, N_2 flux did not show a consistent temporal pattern or differences among substrate types, or a clear relationship to other biofilm characteristics. This suggests that the chemical and physical properties of the substrates used in the study did not affect DNP. Different approaches to DNP (e.g., acetylene block), measurements of N cycling gene abundance, or longer incubation times may offer more insight into potential impacts of plastic substrates on N_2 flux.

Relatively few studies have examined impacts of plastic litter on N_2 dynamics and have focused on microplastics. In a mesocosm setting, Chen et al., (2020) measured DNP (via acetylene inhibition) on polypropylene (PP) microplastics and water column microbes every 5 days for 25 days. Initially DNP was higher on PP microplastic than on just water but by the end of the experiment rates were similar (Chen et al., 2020). Seeley et al., (2020) observed increased denitrification in sediments amended with polylactic acid (PLA) and polyurethane foam (PUF) microplastics compared to sediment alone. Although we did not see a trend between material type and DNP, N_2 flux was dynamic on our macroplastic substrates. The collective data provide evidence that plastic litter could affect N dynamics under some circumstances, via microbial colonization or effects on sediment porosity, and merits more research attention.

Biofilm structure: Biomass and chlorophyll

In contrast to the respiration results, biofilms biomass and chlorophyll were similar on all substrates throughout the six-week incubation, suggesting that biofilms have similar structural characteristics over time. Other studies have found similar chlorophyll concentrations among biofilms across plastic polymers (Chaudhary et al., 2022), plastic polymers and tile (Vincent et al., 2022), and plastics, steel and wood (Muthukrishnan et al., 2019). In contrast to chlorophyll, however, the same studies noted different patterns for biofilm biomass across substrates. Chaudhary et al., (2022) found no differences in biomass across substrates, Vincent et al. (2022) found higher biomass on polystyrene than tile and PVC, and Muthukrishnan et al., (2019) noted significantly lower biofilm biomass on PET and polyethylene bags compared to wood and steel substrates. The emerging patterns across studies suggest that chlorophyll density is more similar across substrates while biofilm biomass shows variable dynamics, perhaps because biomass measurements are broader and may include living and dead cells as well the EPS.

Biofilm assemblage: Richness and diversity

We predicted richness and diversity of bacterial and algal taxa would be highest on wood relative to all 3 plastic types, but the results did not align clearly with our expectation. By substrate type, richness and Shannon diversity for bacteria and algae were highest on wood and foam compared to film and rigid polyethylene. By date, the ASV richness for bacteria and algae were most similar across substrates on week 1, and more variable across substrates during weeks 3 and 6. We attribute the results to the impact of physical surface properties, as foam and wood have more complex and rougher surfaces than the film and rigid polyethylene which were smoother and more homogenous.

Surface roughness promotes biofilm development because it offers greater surface area for colonization and protection from shear stress, and increased asperity reduces energy requirement for cell adhesion (Ammar et al., 2015; Cazzaniga et al., 2015; Donlan, 2016; Katsikogianni et al., 2004; Renner & Weibel, 2011). Foam and wood both offer a porous texture and thereby greater heterogeneity of conditions for biofilm organisms, which likely enhanced ASV richness and diversity. In contrast, the homogenous, smooth surface of film and rigid substrates likely limited the potential microhabitats which limited richness and diversity.

Other studies have also found increased surface roughness or textural complexity was associated with increased metrics of alpha diversity for biofilms on wood compared to plastic. Muthukrishnan et al., (2019) found bacterial richness on wood was significantly higher than on PE and PET at one of two sites. Keszy et al., (2019) incubated high density polyethylene (HDPE) and hard PS microplastic and wood pellets in tanks along the shore of the Baltic Sea. Bacterial richness on HDPE and hard PS was significantly lower than on wood at all sites. Oberbeckmann et al., (2021) found bacterial alpha diversity was higher on wood compared to HDPE and hard PS. In a laboratory incubation Miao et al., 2019 found bacterial communities on wood and cobblestone were significantly richer and more diverse than those on both LPE and PP microplastics. Finally, in a lake incubation study, wood biofilms had greater bacterial richness and diversity than biofilms on PET and polymethyl methacrylate (PMMA) (Shen et al., 2021). The consistent pattern across studies clearly shows greater richness and diversity of bacterial taxa on wood than plastic, which is a logical consequence of its biodegradable nature and the long evolutionary history of the wood-degrading microorganisms.

Increased surface roughness and textural heterogeneity also explain the patterns of diversity and richness on our foamed PS substrates. Published studies have shown mixed results when addressing the same question, although considering the variety of physical and chemical characteristics within the category of ‘foamed PS’ is important. On one of two collections of floating PE, foamed PS, and PP microplastic in the coastal bay of Brest (Brittany, France) bacterial diversity on PS was significantly higher compared to PE (Frère et al., 2018). In an incubation study, foamed PS microplastic had significantly higher bacterial diversity than hard polyamide and PP film microplastics following (Chen et al., 2021). In contrast to our results, an *in situ* incubation in the Haihe Estuary (Bohai Bay, China) with foamed PS, PVC, PP, PE, and polyurethane (PU) showed no differences in bacterial Chao1 index across polymers (Li et al., 2019). Vincent et al., (2022) found differences in bacterial richness and diversity at 2 of 6 stream incubation sites, and at those sites foamed PS was the least rich and diverse compared to PVC and tile. In addition, Vincent et al., (2022) also found no differences in algal richness and diversity by polymer type at any site. Not all studies report the specific type of PS used which limits our comparisons. Physical and chemical differences within foamed PS varieties may explain why patterns of richness and diversity differ across studies. However, our results are attributable to the conditions (e.g., surface roughness, heterogeneity) that promote biofilm adhesion and development (McGivney et al., 2020; Nauendorf et al., 2016).

Biofilm assemblage: Bacterial communities among substrates

We predicted bacterial community composition would be different across the four substrate types, but the NMDS and PERMANOVA results offered mixed support for this hypothesis. The bacterial community on wood was unique compared to bacterial communities on

plastic, but the communities on plastic showed more nuanced differences: no difference between film polyethylene and foamed polystyrene, and no difference between film and rigid polyethylene. Our results were also consistent with studies elsewhere that have demonstrated differences in bacterial biofilm assemblage on wood relative to plastic (Debroas et al., 2017; Kesy et al., 2019; Miao et al., 2019; Muthukrishnan et al., 2019; Oberbeckmann et al., 2018, 2021; Shen et al., 2021). The collective body of work offers a consistent statement that distinct bacterial communities evolved between plastic and wood, across a wide variety of ecosystem types and conditions.

Several of bacterial families that were dominant members of the overall community showed differences between plastic and wood. Those most abundant on wood may suggest selection for organisms that metabolize it. For example, *Rhizobiaceae* were an abundant overall and significantly more common on wood than plastic on weeks 1, 3, and 6. *Rhizobiaceae* are mostly aerobic, chemoorganotrophs that metabolize carbohydrates and organic acids (Carrareto Alves et al., 2014), including wood (Pettersen, 1984). Hoellein et al. (2014) found *Rhizobiaceae* was significantly more abundant on leaves than on cardboard, aluminum, tile, and plastic debris substrates in an artificial stream study. *Brii41* was also significantly more abundant on wood than plastic throughout the study, and it decomposes organic matter (Cai et al., 2018; Dai et al., 2021). Finally, both *Methylophilaceae* was significantly more abundant on wood than plastic in weeks 3 and 6. Release of methanol from the degradation of the pectin and lignin in wood substrates (Galbally & Kirstine, 2002) could stimulate the growth of *Methylophilaceae*, which oxidize single-carbon compounds (Doronina et al., 2014; Kalyuhznaya et al., 2009). Our phylogenetic approach does not identify the metabolic potential of bacterial families, however,

their patterns among substrates, combined with other metrics (e.g., respiration) suggests substrate-mediated selection is occurring.

Several families of bacteria were common overall and showed preferential abundance on plastic relative to wood, including the bacterial families *Methylomonadaceae*, *Beijerinckiaceae* and Unclassified *Gammaproteobacteria*. Previous studies have also found Unclassified *Gammaproteobacteria* on plastic biofilms (Hoellein et al., 2014; McCormick et al., 2016; Vincent et al., 2022). Each contain methane oxidizing bacteria (MOB) (Cabrol et al., 2020), which could be connected to the oxidation of plastic polymers into CH₄ when exposed to solar radiation and water (Royer et al., 2018). *Amoebophilaceae* was also significantly more abundant on plastic throughout the study. Elsewhere, this taxon increased in the gut of a soil oligochaete *Enchytraeus crypticus*, which was fed nanoplastics (Zhu et al., 2018). Finally, the families *Alteromonadaceae*, *Xanthomonadaceae* and *Spirosomaceae* were differentially abundant on plastic in one or more weeks. These families were among those identified by a recent review (Wright et al., 2021) as potential hydrocarbon degrading bacteria that are consistently more abundant on plastic relative to other substrate types.

Biofilm assemblage: Algal communities among substrates

The differentially abundant algal families on plastic vs. wood offers some insight into substrate-based selection of biofilm composition. Overall, green algae were abundant on all substrates, so patterns between wood and plastic were relegated to other algal groups. The algal taxa with greater abundance on wood than plastic included two families of red algae (*Compsopogonaceae* on weeks 1 and 3 and *Batrachospermaceae* on week 6), one golden algae family (*Chromulinaceae* on weeks 1 and 3), one yellow-green algal family (*Vaucheriaceae* on

week 1), and one brown algal family (Unclassified *Ectocarpales* on week 6). In contrast, there were few taxa that were more abundant on plastic than wood. Of the 85 entries of differentially abundant algae (Tables 13, 14, and 15) in only 17 cases was the algal family significantly more abundant on plastic than on wood, and those were not taxa that were abundant overall. The relative abundance of taxa on plastic vs. wood could be attributed to the substrate characteristics or community dynamics (Kettner et al., 2019). Our data cannot determine a definitive mechanism but offers some support for the preferential colonization of wood, which is a component of the evolutionary history of algae, rather than the novel surface properties of plastic.

Although we did not perform differential abundance analysis across the 3 plastic substrates, the mean relative abundance results show clear differences between the two LDPE substrates and the foamed polystyrene. We note that the diatom community structure was more similar between wood and foam than foam compared to the polyethylene substrates, which had greater abundance of diatoms. A possible mechanism for this might be stronger adherence by diatoms to hydrophobic surfaces (Finlay et al., 2002; R. Holland et al., 2004) since polyethylene was more hydrophobic than foamed polystyrene (Min et al., 2020). However, we did not measure hydrophobicity of our substrates directly (e.g., by measuring contact angles) and we note that biofilm colonization decreases surface hydrophobicity (Lobelle & Cunliffe, 2011; Wright et al., 2020). To our knowledge, there are no published studies that compare algal community composition on plastic and wood substrates, which limits our ability to make comparisons to previous work. However, previous assessments of overall eukaryote community composition (which includes most algae), show that found that the eukaryote community on

wood was distinct from the communities on HDPE and hard PS (Kettner et al., 2019). Distinct eukaryote communities were also identified between wood and plastic debris in the north Atlantic (Debroas et al., 2017). Overall, the unique properties of plastic surfaces can select for distinct algal communities relative to natural habitats, but this merits greater investigation to quantify the mechanisms of action and the ecological implications.

Biofilm assemblage: No impact of substrate size

We predicted a positive relationship between size and richness and diversity for all substrate types, but our analyses provided conclusive evidence that this hypothesis was not supported. Neither bacterial nor algal community composition differed according to substrate size, the bacterial NMDS (Fig 1.11) and algal NMDS (Fig 1.16) did not show any grouping by size, and there was no difference among substrate sizes for algal richness or diversity. Bacterial Shannon diversity showed only 2 instances of differences by substrate size (between small and medium film polyethylene and small and large wood substrates week 3) with high temporal variation overall. Finally, our PERMANOVA analysis further confirmed that there was no difference in community structure based on size for any material type (Table 6, 12). At least within the range of particle sizes we selected, there was no difference in community composition depending on size.

Previous work has found similar patterns when examining the relationship between plastic particle size and biofilm communities, although the size ranges of previous studies vary widely. Frère et al., (2018) collected floating foamed PS, PE, and PP microplastics, pooled them into sizes (5-2 mm, 2-1 mm, and 1-0.3 mm) and found no difference in bacterial community composition among sizes classes for any polymer type. In another study, there was no difference

in bacterial community structure between 125–250 μm and 250–500 μm sized PE, and between PS beads with diameters of 106–125 μm and 355–425 μm (Parrish & Fahrenfeld, 2019). In contrast, Debroas et al., (2017) noted differences in bacterial and eukaryote community composition when comparing macroplastics (5 mm-20 cm PE) and microplastics (300 μm -5mm; 90% of which were PE), with lower bacterial and eukaryote richness and diversity on microplastic. Based on our findings and those of others, for a particular polymer type, it is less likely that size will have little effect on biofilm richness and diversity, unless compared across large size ranges (macro- and microplastics). In addition, we note that biofilms impact fate of particles by size, and particles with larger surface area to volume ratios will sink faster (Amaral-Zettler et al., 2021; Chen et al., 2019; Fazey & Ryan, 2016; Liu et al., 2022). This implies that smaller plastic litter may be more likely to be retained by rivers rather than being transported downstream, even where the relative richness, diversity, and community composition of biofilms on smaller particles is the same as larger particles.

Long-term ecological implications of biofilm growth on plastic relative to wood surfaces

The degradation of wood relative to the recalcitrance of plastic, combined with the robust biofilm growth on both surfaces, has implications for the fate of plastic and its impacts in rivers. The persistence of plastic surfaces allows more generations of biofilms to grow on the same surface relative to wood. In addition, the relatively new (i.e., 75 years) and accelerating input of plastic litter to aquatic ecosystems provides more surface area for biofilms to colonize than would be available otherwise. Plastic retention in rivers can also be enhanced by biofilm growth which adds mass and ‘stickiness’ to plastics resulting in retention rather than transport (Chen et al., 2019; Fazey & Ryan, 2016; Hoellein et al., 2019; Kaiser et al., 2017; Lobelle & Cunliffe,

2011). At larger spatial scales, the implications of plastic-associated biofilms may have an impact on biogeochemistry (e.g., respiration, production, and N cycling). Future studies can improve our understanding of the biofilm communities on plastic litter by focusing on higher temporal resolution, including fungi and protozoa in the analysis of the biofilm community, and measuring the effect of plastic-associated biofilms on biogeochemical processes. In addition, 'omics' approaches including metagenomics, metatranscriptomics, metaproteomics as well as machine learning will help answer questions regarding the ongoing genetic and physiological processes of plastic on biofilm communities and biofilm-mediated ecosystem processes.

CHAPTER III

THE EFFECTS OF MICROPLASTIC ON ECOSYSTEM PROCESSES

Introduction

Plastic litter in ecosystems worldwide has become a focus of research and public attention. Plastic pollution encompasses a wide array of material types and particle sizes, including macroplastic, microplastic (plastic between 1 μm and 5 mm (Frias & Nash, 2019), and nanoplastic (plastic particles between 1 nm to 1 μm (Gigault et al., 2018). Impacts of plastic litter include entanglement and ingestion by animals, which also ingest associated chemicals (i.e., additives and adsorbed contaminants), and its use as a habitat for a range of taxa, including animals, algae, and bacteria (Choy & Drazen, 2013; Gregory, 2009; Jepsen & de Bruyn, 2019; Rochman et al., 2013; Schuyler et al., 2014).

The buoyancy and persistence of microplastics create a novel habitat for colonization by microbes (McCormick et al., 2016; Wright et al., 2020) which are key drivers of carbon and nutrient cycling (Battin et al., 2003; X. Chen et al., 2020). Microbes colonize hard surfaces as biofilms (Zobell & Allen, 1935), which are aggregates of bacterial, fungal, algal, and protozoan cells in an extracellular polymeric matrix (Battin et al., 2016). The unique properties and abundance of microplastics suggest that they may influence microbially-mediated processes in aquatic ecosystems. For example, microplastic-associated biofilms can increase rates of N_2 respiration pathways (e.g., denitrification potential) in sediments (Chen et al., 2020). In addition, biofilm communities on plastic litter showed similar rates of photosynthesis

and respiration relative to other hard surfaces in urban streams (e.g., glass and rock) (Hoellein et al. 2014, Vincent et al., 2022). Since plastic litter is highly durable and retained in urban streams (McCormick & Hoellein, 2016), high levels of plastic pollution may impact microbially-mediated processes at larger spatial scales, although this has not yet been quantified. Studies on the influence of plastic litter on ecosystem processes are newly emerging (e.g., leaf decomposition, nitrogen cycling, ecosystem metabolism), and are most commonly laboratory studies rather than in situ experiments (Lopez-Rojo et al., 2020, Seeley et al., 2020).

Ecosystem metabolism includes production of organic matter through photosynthesis (i.e., gross primary production; GPP) and oxidation of organic matter through aerobic respiration (R), where the balance between the processes is net ecosystem productivity (NEP) (Odum, 1956). Ecosystem metabolism is a highly integrative metric which aggregates multiple biological and physical dynamics (Staehr et al., 2010). Thus, metabolism can be used to assess how environmental changes affect ecosystem conditions, for both natural variation (i.e., seasonality, biomes), and anthropogenic stressors (e.g., climate change and pollution). (Jankowski et al., 2021).

Nitrogen (N) cycling metrics (e.g., nitrification, denitrification, and nitrogen fixation), also integrate the activity of many organisms and can be used to infer ecosystem response to environmental changes at large spatial scales (Loeks-Johnson & Cotner, 2020; McCarthy et al., 2007a). N-fixation is the conversion of dinitrogen gas (N_2) into biologically available forms of N, and conversely, denitrification and anaerobic ammonium oxidation (anammox) generate N_2 (Bernhard, 2010). Measuring factors that drive the balance between those processes (i.e., net N_2 flux) is important as N can be a key limiting nutrient for ecosystem production, and in eutrophic

ecosystems N_2 flux out of the environment is critical for mitigating N pollution (Hoellein & Zarnoch, 2014; McCarthy et al., 2007b; Mulholland et al., 2008; Schindler, 1974).

The objective of this study was to determine if microplastics influenced ecosystem metabolism and diel N_2 flux in large, in situ lake mesocosms. In addition, we measured ecosystem metabolism and diel N_2 flux at the whole-lake scale (in the absence of microplastic addition) to place mesocosm-based measurements in context. We predicted microplastic would serve as a novel and abundant surface for biofilm colonization, which would increase GPP and R, with the greatest impact at the highest microplastic concentrations. We also predicted that biofilm colonization of microplastics would impact N_2 flux rates, by increasing N_2 uptake (i.e., N-fixation) during the day, conducted by cyanobacteria that colonize microplastics. At the whole-lake scale, we expected relatively low rates of metabolism overall as is typical for oligotrophic lakes. In addition, we predicted that the epilimnion of the lake would show net N_2 uptake (i.e., under saturation) and the hypolimnion to show net N_2 production (super saturation) due to the relative impact of N-fixation and anaerobic respiration pathways that affect N_2 in the water column and sediment, respectively.

Methods

Study Site and Experimental Context

This experiment was carried out at Lake 378 in the International Institute for Sustainable Development's Experimental Lakes Area (IISD-ELA) in Ontario, Canada (49.83, -93.77). The IISD-ELA contains 58 lakes reserved for whole-lake ecological studies. Like the other lakes in this boreal forest biome, Lake 378 is oligotrophic and dimictic. The area of Lake 378 is 0.247

km² and the maximum depth is 16.7 m. Monitoring of phytoplankton, zooplankton, fish, hydrology, and water chemistry has been ongoing at lake 378 since summer 2019.

This study was one part the overarching 'pELAstic' project, a 10+ year collection of studies focusing on the fate and effects of microplastics in freshwater. The objectives of the overall pELAstic project were to determine: 1) the physical, chemical, and biological fate of microplastics in lakes and their watersheds; 2) how microplastic affects aquatic ecosystems at all levels of biological organization; 3) how microplastic affects ecosystem processes; 4) how ecosystems recover after microplastic exposure. The pELAstic project began in 2018 with a baseline assessment of microplastics at the IISD-ELA. The current study is part of the second phase of the pELAstic project where pelagic mesocosms were deployed and dosed with a range of microplastic concentrations.

Experimental Design

Pelagic mesocosms (N=9) (10m diameter Decagon Carp Protected Limno-Corral, CURRY INDUSTRIES LTD, Winnipeg, MB, Canada) were constructed and deployed throughout lake 378 by May 11, 2021. Mesocosms were 10 m in diameter and 2 m deep and filled with 157,000 L of water by May 14, 2021. Zooplankton seeding began May 15, 2021 and ended May 17, 2021. Mesocosms were stocked with yellow perch (Table 16) between May 17 and May 28, 2021. On June 2, 2021, mesocosms were dosed with microplastic fragments (10-500 µm) of polyethylene (PE), polystyrene (PS), and polyethylene terephthalate (PET) at a range of concentrations (Table 16). The color and additives of each polymer are described in Table 17. The mesocosms were dismantled on August 10, 2021. This was a large collaborative study, with

many simultaneous measurements including water chemistry, fish physiology, plankton dynamics, and ecosystem-scale processes.

Ecosystem Metabolism in the pelagic mesocosms

We measured ecosystem metabolism via continuous measurements of dissolved oxygen (DO) and water temperature (HOBO U26 loggers, Onset HOBO, Bourne, MA, USA). Before the loggers were placed in the mesocosms, they were deployed together for 24 hours to calibrate their measurements with one another. Afterwards, in each mesocosm a logger was deployed at 1 m depth by attaching the logger to carabiners hung on a rope attached to a cork block. The cork block was attached to a manila rope that stretched across each mesocosm. A logger was also attached to a buoy at the center of the lake at 1 m depth. At the same buoy a thermistor chain was attached with temperature loggers (Onset HOBO MX2202 Bluetooth temperature/light loggers ITM Instruments Inc., Sainte-Anne-de-Bellevue, Québec, Canada) every meter and set to record water temperature every hour. We removed the DO loggers July 13-15 to clean by lightly scrubbing the sensor head with a toothbrush and water from the lake. At that time all data were downloaded, and the loggers cleaned and redeployed. Photosynthetically active radiation (i.e., PAR; LI 192 Underwater Quantum Sensor, LI-COR Biosciences, Lincoln, NE, USA) and wind speed with an R.M. Young anemometer (CR1000, Campbell Scientific, Logan, UT, USA) were measured continuously every 15 minutes by a meteorological station about 1 km from Lake 378 at a 10 m height.

Data from the loggers and meteorological station were compiled and organized by date and time for each mesocosm as required for running LakeMetabolizer (Winslow et al., 2016). One logger (mesocosm F) recorded DO at 10-minute intervals (rather than 15 minutes). To align

the mesocosm F data with the meteorological data, the average DO, and water temperature was taken between the 10- and 20-minute intervals to estimate DO and water temperature for the quarter hour point. We did the same to the 40- and 50-minute measurements to estimate DO and water temperature at the 45-minute point. Before any other variables were derived, sensor differences were corrected for and applied to the entire DO dataset. The DO signal over the 24-hour period where loggers were deployed together was first visualized. Two loggers (F and D) were distinct from the remainder. Thus, the mean DO for all the loggers except the two obvious outliers was calculated, we generated a correction factor for each logger, and data from all loggers were corrected to that mean.

Three metabolism components, GPP, R, and NEP for each mesocosm and the whole lake were estimated for each day with the Bayesian metabolism model using uninformative priors, since it is not recommended to run the model with constraints on the signs of GPP and R (Winslow et al., 2016). All models successfully converged. We assessed the model's estimates for each day using the standard deviations of parameters and parameter coefficients. With the median of the posterior parameter coefficients, we performed a posterior predictive check on observed vs predicted values (Holtgrieve et al., 2013). Deriving the model's predictions of O₂ from the median parameter coefficients allowed us to assess whether the median was successfully able to recreate the DO signal for each day (Holtgrieve et al., 2013). We followed previous examples where two individuals independently assessed the fit of the model for each day and decided if the fit was good, questionable, or poor based on the observed vs predicted figures and model statistics (Richardson et al., 2017). Both numerical and visual data were used because model statistics and the visual model fit were not always in agreement due to the large

number of data used to calculate both (Richardson et al., 2017). Assessments by the two individuals were compared afterwards, if both agreed a day had a poor fit that day was considered a poor fit. On days where assessments disagreed a consensus was reached jointly. We acknowledge the subjectivity in assessing model fits, which is a consistent challenge in ecosystem metabolism measurements in oligotrophic lakes (Brentrup et al., 2021; Richardson et al., 2017; Rose et al., 2014). We maintain our approach was conservative by only using days where across all mesocosms a day's fit was good for further analysis. If a day had a poor fit in one of the mesocosms that day was also removed from all other mesocosms, so data were compared from the same days.

A common problem in estimating ecosystem metabolism is models can return days where GPP is negative or R is positive, which are biologically impossible (Engel et al., 2019; Winslow et al., 2016). There is not a consensus on how to treat these estimates (Pace et al., 2021; Solomon et al., 2013a). Common approaches include removing all days with impossible estimates from further analysis (Honious et al., 2021; Rabaey et al., 2021; Stefanidis & Dimitriou, 2019) or keeping all or some days with impossible estimates (Hornbach et al., 2020; Jane & Rose, 2018; Ulseth et al., 2018). In the latter case, the assumption is that data with impossible estimates are balanced out on the other extreme of estimates (Staeher et al., 2010) but this assumption may be inaccurate (Brothers et al., 2017). Considering the oligotrophic, low-productivity status of lake 378, days with impossible estimates but good observed vs predicted DO fits were treated as days where the biological signal was exceedingly low, and the estimate was therefore set as 0. Days with impossible estimates but bad fits were already removed in the previous assessment steps We

concluded that our approach introduced less bias compared to simply removing all days with impossible estimates or keeping all days, regardless of model fits or model uncertainty statistics.

Diel N₂ Gas Flux

We collected N₂ samples every hour from 9 am August 3 to 9 am August 4, 2021, from three pelagic mesocosms as well as the epilimnion and hypolimnion in the open water of lake 378. Samples were collected from mesocosms B (0 particles L⁻¹), I (1710 particles L⁻¹) and D (29240 particles L⁻¹), representing control, medium, and high microplastic concentrations. We used a Van Dorn sampler to collect water from each of the three mesocosms and for the open lake epilimnion (at 1 m depth) and hypolimnion (14 m depth). The Van Dorn was deployed to collect water, brought to the surface, and the clamp on the outlet tubing was removed, allowing for smooth filling of three 12 mL glass exetainers. We placed the tubing at the bottom of the exetainer and slowly filled the exetainer, allowing it to overflow for ~10 seconds, and drawing out the tubing while the water was flowing, leaving a meniscus on top (Hoellein & Zarnoch, 2014; Reisinger et al., 2016). The same was done for the other two exetainers immediately afterwards. We used care to avoid introducing any bubbles into the sample water during filling. Next, 200uL of 50% zinc chloride was added to the top of the exetainer to preserve the sample (McCarthy et al., 2007a). Once capped, exetainers were kept in a cooler with ice temporality, then stored in a refrigerator at 4°C until measurement of dissolved N₂.

We measured the ratio of N₂ to argon (Ar) in preserved samples on a membrane inlet mass spectrometer (MIMS) with ultra-pure water as the standard (18 M Ω resistance; E-Pure, Barnstead International, Dubuque, IA, USA). The standard temperature was set to 23.44°C (the average temperature of the epilimnion) using a circulating water bath (VWR International,

Radnor, PA, USA) equilibrated to the atmosphere with low speed stirring for 24 hours prior to measuring (Lab Egg RW11 Basic, IKA Works, Inc., Wilmington, NC, USA) the mesocosm and open water epilimnion samples (Kana et al., 1998). Hypolimnion samples were run separately with the water bath set at the hypolimnion temperature (5.24 °C). During each run we analyzed a standard every 3-9 samples to account for instrument drift. Concentrations of dissolved N₂ gas in each sample was calculated by multiplying the N₂:Ar ratio by the equilibrium concentration of Ar, which is more accurate than the N₂ concentration reported from the MIMS directly (Kana et al., 1994)

Calculations

The Bayesian metabolism model required the depth of the actively mixed layer (*z.mix*) and DO at 100% saturation, which we generated using additional measurements for the mesocosms and the whole-lake metrics. The depth of the actively mixed layer in each mesocosm was set to 2 m because that was the depth of the mesocosm. For whole-lake metabolism, the actively mixed layer was calculated using the temperature profile and the *ts.meta.depths* function in rLakeAnalyzer (Read et al., 2011). Estimates of the depth of the actively mixed layer at each hour were used for all 15-minute intervals within 1-hour increments. DO at 100% saturation (DO.Sat) was calculated based on measurements of water temperature, salinity and barometric pressure. We used the *o2.at.sat* function in LakeMetabolizer using the Garcia-Benson method with the mean salinity and barometric pressure from at the study site.

Calculation of ecosystem metabolism and N₂ flux required an estimate of gas transfer velocity (*k*), which is typically calculated for the whole-lake scale using wind speed (Cole & Caraco, 1998; Crusius & Wanninkhof, 2003; Vachon & Prairie, 2013). However, whole-lake

reaeration estimates are not well suited for use in the pelagic mesocosms due to the weaker surface wave energy and the impact of lee effects from mesocosm walls (Matthews et al., 2003; Schindler, 1988). Thus, we used the k_{600} value from Saunders et al., (2022) who directly measured the mass transfer coefficient of sulfur hexafluoride in mesocosm of similar dimensions in Lake 260 at IISD-ELA between June 18, and August 20, 2018 (Saunders et al., 2022). With this k_{600} value, we used the function $k600.2.kGAS$ function with $n=-0.5$ (Saunders et al., 2022) to convert k_{600} into a gas- and temperature-specific transfer velocity k . We converted k_{600} to k_{O_2} for our ecosystem metabolism calculation and converted to k_{N_2} for our N_2 flux calculations. For the whole lake metabolism estimates and epilimnion N_2 flux calculations, we calculated k_{600} with the Vachon method (Vachon & Prairie 2013) in LakeMetabolizer, which incorporates wind speed and lake area and then converted to k_{O_2} and k_{N_2} respectively with $k600.2.kGAS$.

We adapted the equations for estimating ecosystem metabolism to calculate N_2 flux. We attributed changes in N_2 to biological and physical processes with the following equations:

$$\frac{dN_2}{dt} = N_{2b} + F$$

$$N_{2t} = N_{2t-1} + N_{2b,t-1} + F_{t-1}$$

$$F_t = \frac{k_t}{z_t} \times (N_{2s,t} - N_{2t})$$

where $dN_2 dt^{-1}$ is the rate of change in the measured N_2 concentration, N_{2b} is the rate of change of N_2 concentration due to biological processes, F is the rate change of N_2 between the water and atmosphere, z is the depth of the actively mixed layer, k is the transfer velocity for N_2 , N_{2s} is the N_2 concentration at saturation. The depth of the actively mixed layer z was set to 2 m for the mesocosms and from the temperature profile for the epilimnion. N_2 concentration at saturation

was calculated based on salinity and temperature. We first solved F over the period of one hour to get the abiotic flux of N_2 . In the hypolimnion F is 0 since there is no interaction between atmosphere and hypolimnion waters; therefore, abiotic N_2 flux was 0. We were then able to solve for N_{2b} over each hour to get the biotic N_2 flux.

Data Analysis

The complete timeseries of DO, water temperature, transfer velocity of O_2 , and DO at saturation in each mesocosm were compared across mesocosms using 1-way ANOVA and Tukey's post-hoc test. Mesocosm estimates of GPP, R and NEP were also compared across mesocosms with 1-way ANOVA. A simple linear regression between the log microplastic concentration and each metabolism estimate was performed to test if there was a correlation between metabolism estimates and the log microplastic concentration. The log microplastic concentration was used as our explanatory variable because microplastic addition concentrations were designed based on a log scale. We visually inspected q-q plots and plots of residuals vs fitted values for the timeseries of GPP, R, NEP, DO, DO at saturation, transfer velocity of O_2 and water temperature to make sure data met the assumptions of normality and equal variance respectively. Visual inspection of these plots was used to ensure the data did not deviate seriously from the assumptions of ANOVA since ANOVA is robust against moderate departures from the assumptions of ANOVA with large sample sizes ($n=44$ for metabolism estimates in each mesocosm) and with samples with hundreds of observations parametric tests can be used regardless of the distribution ($n=6425$ for physical data in each mesocosm) (Altman & Bland, 1995; Elliot & Woodward, 2007; Ghasemi & Zahediasl, 2012). The presence of outliers in the

physical data and metabolism datasets did not change the results of our ecosystem metabolism analyses or physical data analyses.

For N_2 data, we compared data across the 3 mesocosms with microplastics, and separately compared results between the epilimnion and hypolimnion. We used a 1-way ANOVA to compare the difference between measured N_2 concentration and N_2 concentration at saturation across mesocosms. We compared biotic and abiotic N_2 flux across mesocosms using 2-way ANOVA with time (day or night) as a second factor because we expected biotic N_2 flux may be negative during the day when light is available to cyanobacteria which they can use to fix N_2 . Measured N_2 concentration and N_2 concentration at saturation were compared across mesocosms with an aligned rank transform test (Wobbrock et al., 2011) and an aligned rank contrast test for multiple comparisons (Elkin et al., 2021) since data could not be transformed to meet ANOVA assumptions. The difference in measured N_2 concentration and N_2 concentration at saturation was compared between the epilimnion and hypolimnion with a Wilcoxon rank sum test since data could not be transformed to meet t-test assumptions. Biotic N_2 flux was compared with 2-way ANOVA with daytime (i.e., light vs dark) as an additional factor. Day and night abiotic N_2 flux in the epilimnion was compared using a Wilcoxon rank sum test. Finally, we compared measured N_2 concentration and N_2 concentration at saturation between the hypolimnion and epilimnion with an aligned rank transform test (Wobbrock et al., 2011) followed by multiple comparison tests using an aligned rank contrast test (Elkin et al., 2021). For all N_2 analyses we tested the assumptions of normality and equal variance with the Shapiro-Wilk test and Levene's test respectively and excluded outliers from our N_2 analyses which we identified as any points more than 1.5 IQR below Q_1 or more than 1.5 IQR above Q_3 .

We did not perform any statistical analyses comparing whole lake and mesocosm ecosystem metabolism because we removed the same set of days from the mesocosm data before analysis to compare across the same days. The same set of dates was not removed from the whole lake dataset and the range of days for which data was available was also larger. Therefore, any comparison between the mesocosm and whole lake would not be equal to the comparison we made across mesocosms. In addition, the whole lake dataset's primary use will be in the next phase of the pELAstic project where this data will serve as the 'pre-treatment' conditions before the whole-lake microplastic addition.

Table 16. Mass (g) and number of particles of PS, PET, and PE microplastic added to each mesocosm to reach the desired microplastic concentration (particles L⁻¹) as well as the number of yellow perch (*Perca flavescens*) at the beginning and end of the study. Mesocosm A fell apart on the final sampling, so no fish were collected.

| Mesocosm ID | Concentration (particles L ⁻¹) | Dose (for 150,000 L mesocosm; (particles L ⁻¹) | Weight of PS needed to dose with (g) | Weight of PET needed to dose with (g) | Weight of PE needed to dose with (g) | Initial Yellow Perch Pop. (No.) | Final Yellow Perch Pop. (No.) |
|-------------|--|--|--------------------------------------|---------------------------------------|--------------------------------------|---------------------------------|-------------------------------|
| B | 0 | 0 | 0 | 0 | 0 | 24 | 4 |
| H | 0 | 0 | 0 | 0 | 0 | 26 | 17 |
| F | 6 | 900000 | 0.765 | 0.942 | 0.801 | 23 | 9 |
| A | 24 | 3600000 | 3.06 | 3.768 | 3.204 | 24 | NA |
| E | 100 | 15000000 | 12.75 | 15.7 | 13.35 | 23 | 12 |
| C | 414 | 62100000 | 52.785 | 64.998 | 55.269 | 25 | 10 |
| I | 1710 | 256500000 | 218.025 | 268.47 | 228.285 | 23 | 10 |
| G | 7071 | 1060650000 | 901.5525 | 1110.147 | 943.9785 | 23 | 9 |
| D | 29,240 | 4386000000 | 3728.1 | 4590.68 | 3903.54 | 23 | 9 |
| TOTAL | --- | --- | 20332.808 | 25037.26 | 5148.428 | | |

Table 17. Percent (%) chemical composition of each polymer type including additives.

| Polymer | Composition | CAS Number |
|----------------------|-------------------------------------|------------|
| Blue PET PTM515063 | 0.25% Ultramarine Blue Red Shade | 57455-37-5 |
| | 0.35% 25u Rutile white | 13463-67-7 |
| | Resin is PET – 99.40% | 25038-59-9 |
| | 0.05% Perylene Red | 3089-17-6 |
| Red PS PSM412348 | 0.15% Titanium Dioxide | 13463-67-7 |
| | 0.1% Irgafos 126 Antioxidant | 27676-62-6 |
| | 0.1% N,N Ethylene Bis-stearamide | 110-30-5 |
| | Resin is PS- 99.6% | 9003-53-6 |
| | 0.25% Bismuth Vanadate Pigment | 14059-33-7 |
| | 0.05% Chimassorb 944 HALS UV | 70624-18-9 |
| Yellow LLDPE PM27432 | 0.05% Tinuvin 622 HALS UV | 65447-77-0 |
| | 0.025% Irganox B215 Antioxidant | 6683-19-8 |
| | 0.025% Irganox 168 Antioxidant | 31570-04-4 |
| | Resin is LLDPE – 99.55% | 25087-34-7 |
| | 0.05% Benzotriazole – Acetostab 236 | 3896-11-5 |

Results

Mesocosm Physical Data, Ecosystem Metabolism, and N₂

Between June 3, and August 10, 2021 the data for wind and light showed typical diel patterns expected for summer in this geographic area. Wind speed ranged from 0 - 5.96 (m s⁻¹) with less wind at night on most days (Fig 22A). The average wind speed was 1.97 m s⁻¹ ± 0.97 SD. Across the same range of dates, PAR was 0-2128.91 μmol m⁻² s⁻¹ (Fig 22B).

We compared measured DO, DO at 100% saturation, water temperature, and O₂ transfer velocity across mesocosms (Fig 24). Measured DO was different among mesocosms (1-way ANOVA F₈=837 P<0.001) (Table 18). Tukey's post hoc test revealed measured DO in all mesocosms were significantly different from each other, except G (7071 particles L⁻¹) and C

(414 particles L⁻¹), with no pattern in the difference relative to microplastic concentrations (Fig 24A). Differences across mesocosms were also present for DO at saturation (1-way ANOVA $F_8=5.35$ $P<0.001$), O₂ transfer velocity (1-way ANOVA $F_8=5.34$ $P<0.001$), and water temperature (1-way ANOVA $F_8=5.52$ $P<0.001$) (Table 18). Tukey's post-hoc test revealed mesocosms C (414 particles L⁻¹), D (29240 particles L⁻¹), F (6 particles L⁻¹) and H (0 particles L⁻¹) were significantly different than mesocosm B (0 particles L⁻¹) in DO at saturation, O₂ transfer velocity, and water temperature (Fig 24B,C,D).

Metabolism rates showed low production with stochastic variation over time (Fig 25A, B, C). Across microplastic treatments, there was no difference in GPP (1-way ANOVA $F_8=0.87$ $P=0.543$), R (1-way ANOVA $F_8=0.55$ $P=0.818$), or NEP (1-way ANOVA $F_8=0.58$ $P=0.796$) (Table 18). Median rates of GPP remained near 0.2 mg O₂ L⁻¹ day⁻¹ across mesocosms and the variation across mesocosms was similar, although variation was highest in mesocosms I (1710 particles L⁻¹) and D (29240 particles L⁻¹) (Fig 26A). Median rates of R remained near -0.2 mg O₂ L⁻¹ day⁻¹ (Fig 2.5A,B). Median rates of NEP were near 0 mg O₂ L⁻¹ day⁻¹ for all mesocosms (Fig 26C). There were no significant relationships between microplastic concentration (log transformed) and GPP (SLR $F_1=0.03$ $P=0.866$ $R^2=-2.26\times 10^{-3}$), R (SLR $F_1=1.13$ $P=0.288$ $R^2=3.08\times 10^{-4}$), or NEP (SLR $F_1=1.83$ $P=0.177$ $R^2=1.92\times 10^{-3}$).

Results from N₂ measurements showed no effect of microplastics and suggested measured N₂ was below saturation across all microplastic treatments (Fig 27). The measured N₂ concentration and N₂ concentration at 100% saturation were the same across the 3 microplastic treatments (zero, low, and high; (ART $F_2=0.17$, $P=0.842$; Fig 28A). However, N₂ concentration

at 100% saturation was significantly higher than the measured N_2 concentration in all mesocosms (ART $F_1=377.97$ $P<0.001$; Table 19; Fig 28A).

We next compared abiotic and biotic N_2 flux according to microplastic treatment and time of day. Abiotic N_2 flux was higher during the day than at night (2-way ANOVA $F_1=6.16$ $P=0.016$) but was not affected by microplastic concentration (2-way ANOVA $F_2=0.35$ $P=0.705$; Table 2.4, Fig 28B). Biotic N_2 flux showed no difference by time of day (2-way ANOVA $F_1=0.004$ $P=0.948$) or microplastic concentration (2-way ANOVA $F_2=0.04$ $P=0.960$; Table 19). For both daytime and nighttime, median biotic N_2 flux was near 0 for all 3 microplastic treatments (Fig 2.7C). For all mesocosms, the difference between measured N_2 concentration and N_2 concentration at saturation was negative (indicating under-saturation of N_2 ; Fig 29), and there was no difference among the 3 microplastic treatments (1-way ANOVA $F_2=0.34$ $P=0.715$; Table 18).

Whole Lake Metabolism and N_2 Flux

A whole-lake temperature profile was required to calculate mixing depth and incorporated into the whole-lake metabolism calculations. The temperature profile showed that before June, water temperature was cool and uniform through the entire depth of the lake (Fig 30). Starting in early June (at the same time the mesocosm study began), water temperature increased near the surface indicating stratification (Fig 30). Stratification persisted through mid to late October when water temperature decreased and became uniform throughout (Fig 30).

We compared DO, DO at 100% saturation, O_2 transfer velocity, and water temperature (at 1 m depth) for the whole lake metabolism measurements from May through September 2021. For both DO and DO at 100% saturation, values were highest in May, lowest in July, and began

increasing again in late July through September. (Fig 31A,B). Water temperature showed the inverse pattern (Fig 31D). Last, O₂ transfer velocity exhibited a pattern similar to wind (Fig 31C). Median DO, DO at saturation, O₂ transfer velocity, and water temperature were 8.51 (mg O₂ L⁻¹), 8.39 (mg O₂ L⁻¹), 1.28 (m day⁻¹), and 21.72 (°C) respectively (Fig 32).

Whole lake metabolism data were similar in scale and stochasticity to the data from the pelagic mesocosms (Fig 33). Median GPP was near 0.07 mg O₂ L⁻¹ d⁻¹ (Fig 34A) and varied without a temporal trend (Fig 33A). In contrast, R was 0 until mid-June and variable thereafter (Fig 33B). NEP remained positive or 0 throughout May and June (Fig 33C) and fell through the remainder of the dataset. (Fig 33C). The mean (\pm SD) GPP in the whole lake was 0.14 (0.17) mg O₂ L⁻¹ day⁻¹, and across mesocosms the mean (\pm SD) was 0.18 (0.11) mg O₂ L⁻¹ day⁻¹. Mean R for the lake was -0.11 (0.18) mg O₂ L⁻¹ day⁻¹, and in the mesocosms mean (\pm SD) was -0.19 (0.15) mg O₂ L⁻¹ day⁻¹. Finally, mean (\pm SD) NEP in the whole lake was 0.03 (0.19) mg O₂ L⁻¹ day⁻¹ and -0.005 (0.10) mg O₂ L⁻¹ day⁻¹ in the mesocosms.

Patterns of N₂ showed differences between epilimnion and hypolimnion collected in the open water. The timeseries of N₂ showed that the measured N₂ concentration tended to be below saturation (Fig 32A), while in the hypolimnion the concentration of measured N₂ was above saturation (Fig 35B). We used ART to compare measured N₂ concentration and N₂ at saturation according to lake layer. We found a significant interaction between the type of N₂ measurement (directly measured or at saturation) and the lake layer (epilimnion or hypolimnion) (ART F₁=270.68 P<0.001; Table 19). Post-hoc tests revealed N₂ concentration at saturation was significantly higher than measured N₂ concentration in the epilimnion, suggesting the epilimnion was under saturated with N₂ (Fig 36A). In the hypolimnion, measured N₂ was significantly

higher than N_2 at saturation, suggesting over saturation of hypolimnion waters with N_2 (Fig 36A). Median abiotic N_2 flux in the epilimnion tended to be higher during the day than at night (Fig 36B), but this was not statistically significant (Wilcoxon rank sum, $W=81$ $P=0.312$). Biotic N_2 flux was not significantly different between the epilimnion and hypolimnion (2-way ANOVA, $F_1=0.003$ $P=0.960$) or daytime (2-way ANOVA, $F_1=3.44$ $P=0.072$; Table 19). Median biotic N_2 flux in the epilimnion was near 0 with similar variation both during the day and night (Fig 36C). Biotic N_2 flux at night in the hypolimnion was closer to 0 during the day and more positive and variable during the night (Fig 36C). The difference between measured N_2 and N_2 at saturation was significantly higher in the hypolimnion compared to the epilimnion (Wilcoxon rank sum, $W=552$ $P<0.001$; Fig 37).

Table 18. 1-way ANOVA results for ecosystem metabolism estimates, physical data in the mesocosm (MP = Microplastic, GPP = gross primary production, R = respiration, NEP = net ecosystem productivity, DO = dissolved oxygen, DO.Sat = dissolved oxygen at saturation, k.Gas = O_2 transfer velocity, Wtr = water temperature). Measured $N_2 - N_2$ at saturation refers to the difference between measured N_2 and N_2 at saturation. Values in bold indicate a significant p-value.

| Response | Term | Df | F value | Pr(>F) |
|----------|------------------|----|---------|------------------|
| GPP | MP Concentration | 8 | 0.87 | 0.543 |
| R | MP Concentration | 8 | 0.55 | 0.818 |
| NEP | MP Concentration | 8 | 0.58 | 0.796 |
| DO | MP Concentration | 8 | 837 | <0.001 |
| DO.Sat | MP Concentration | 8 | 5.35 | <0.001 |
| k.Gas | MP Concentration | 8 | 5.34 | <0.001 |

| | | | | |
|---|------------------|---|------|------------------|
| Wtr | MP Concentration | 8 | 5.52 | <0.001 |
| Measured N ₂ - Saturation N ₂ | MP Concentration | 2 | 0.34 | 0.715 |

Table 19. 2-way ANOVA results for mesocosm abiotic N₂ flux, mesocosm biotic N₂ flux, and open water biotic N₂ flux. ART results for mesocosm and open-water N₂ concentration. N₂ concentration refers to measured and at saturation N₂ concentrations. N₂ as a term has levels: measured and at saturation. Daytime as a term has levels: day and night. Lake layer as term has levels: epilimnion and hypolimnion. Values in bold indicate a significant p-value.

| Response | Term | DF | F value | Pr(>F) |
|------------------------------|------------------|----|----------|------------------|
| N ₂ Concentration | MP Concentration | 2 | 0.17 | 0.842 |
| | N ₂ | 1 | 377.97 | <0.001 |
| | Interaction | 1 | 0.01 | 0.990 |
| Abiotic N ₂ Flux | MP Concentration | 2 | 0.35 | 0.705 |
| | Daytime | 1 | 6.16 | 0.016 |
| | Interaction | 2 | 0.69 | 0.507 |
| Biotic N ₂ Flux | MP Concentration | 2 | 0.04 | 0.960 |
| | Daytime | 1 | 4.00E-03 | 0.948 |
| | Interaction | 2 | 0.03 | 0.967 |
| N ₂ Concentration | Lake layer | 1 | 284.27 | <0.001 |
| | N ₂ | 1 | 47.43 | <0.001 |
| | Interaction | 1 | 270.68 | <0.001 |
| Biotic N ₂ Flux | Lake layer | 1 | 3.00E-03 | 0.960 |
| | Daytime | 1 | 3.44 | 0.072 |
| | Interaction | 1 | 3.89 | 0.056 |

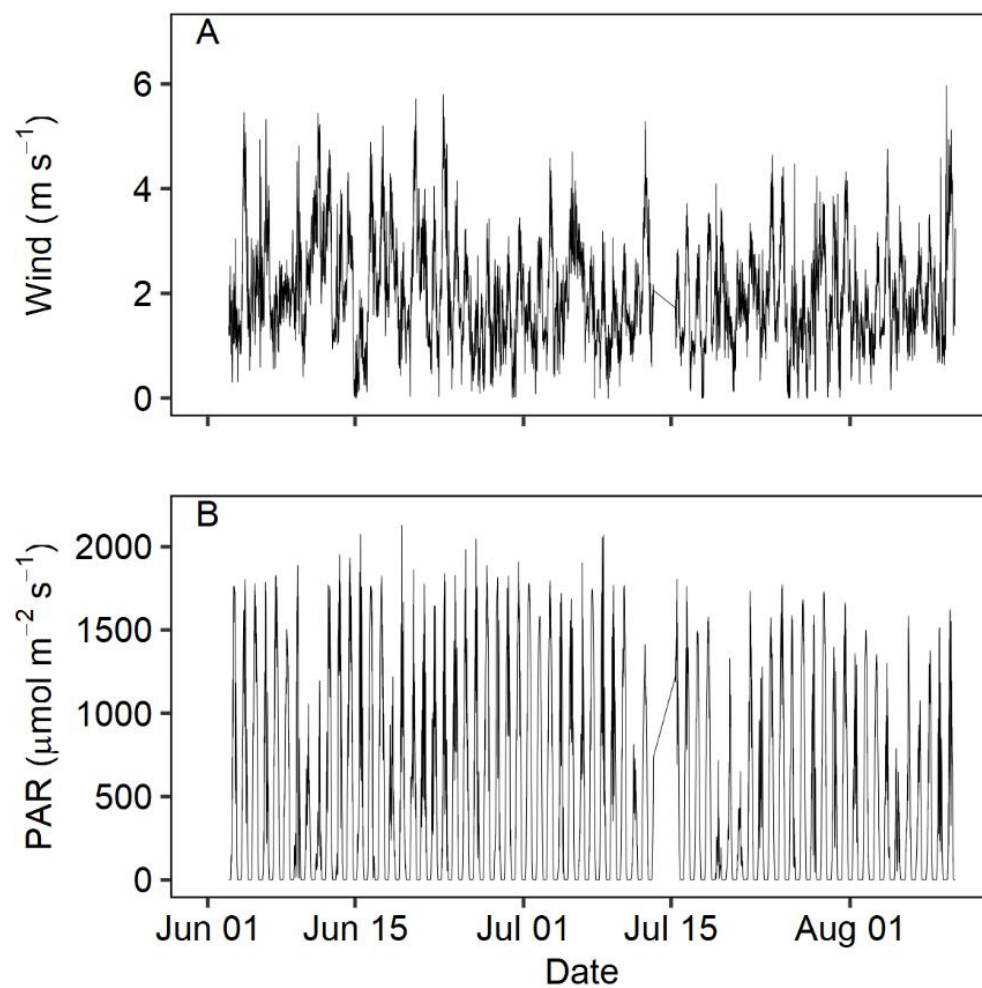


Figure 22. Timeseries from June 3 through August 10, 2021 of A) wind speed (m s^{-1}) and B) PAR ($\mu\text{mol m}^{-2} \text{s}^{-1}$). PAR = photosynthetically active radiation.

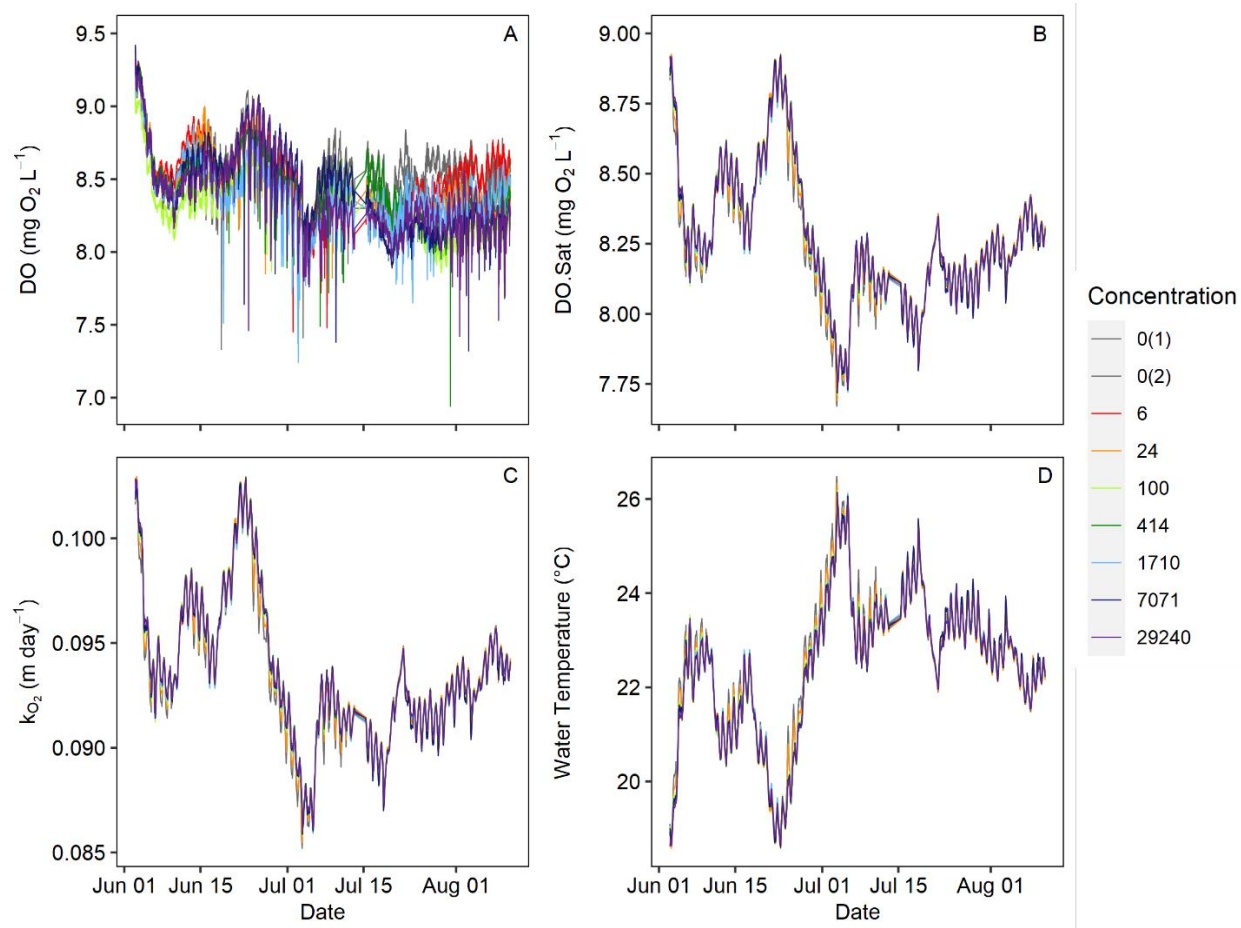


Figure 23. Timeseries of physical data from June 3 through August 10, 2021, in each mesocosm. A) observed DO (mg O₂ L⁻¹), B) DO at 100% saturation (mg O₂ L⁻¹), C) O₂ transfer velocity (m day⁻¹), and D) water temperature (°C). The legend indicates added microplastic concentration in the mesocosm, with 0(1) and 0(2) noting the control mesocosm B and H respectively.

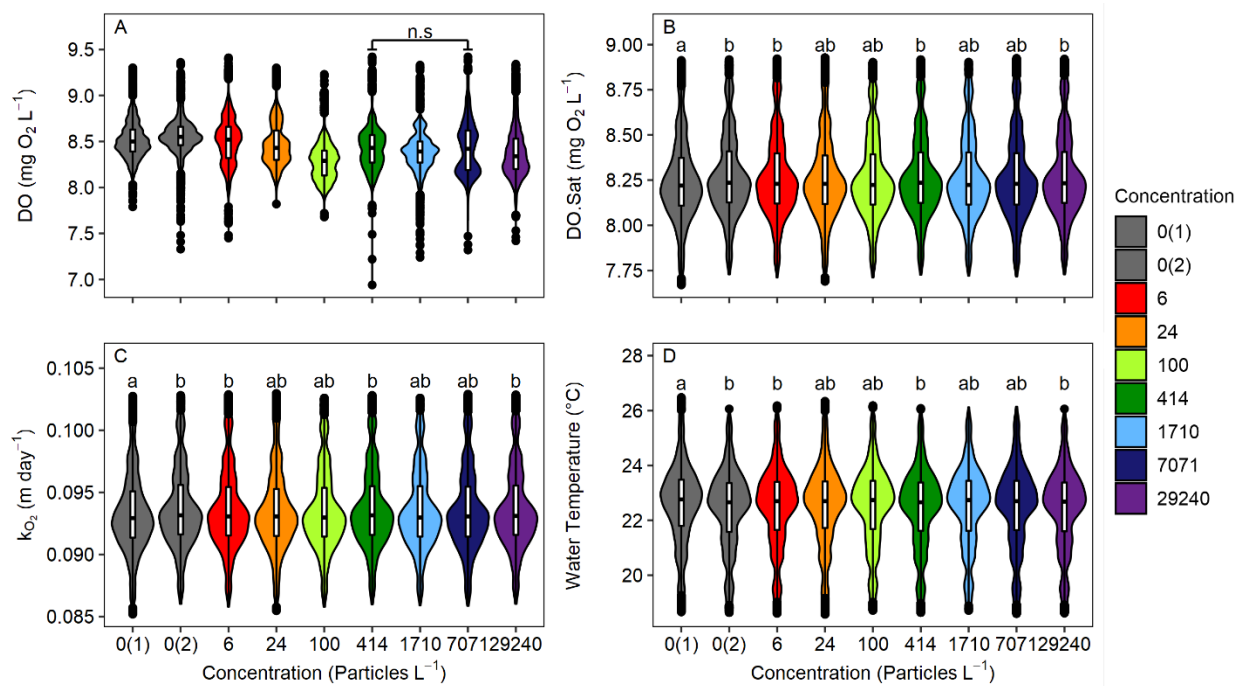


Figure 24. Violin plots with boxplots for each mesocosm of A) observed DO (mg O₂ L⁻¹), B) DO at 100% saturation (mg O₂ L⁻¹), C) O₂ transfer velocity (m day⁻¹), and D) water temperature (°C). Small letters over individual violin plots correspond to the results of Tukey's post hoc test. In panel A, mesocosms with 414 and 7071 particles L⁻¹ are not significantly different from each other while all other mesocosms are significantly different from each other. The legend indicates added microplastic concentration in the mesocosm, with 0(1) and 0(2) noting the two control mesocosms B and H respectively. The boxplot symbols are: center line = median, box edges = interquartile range, and dots = outliers).

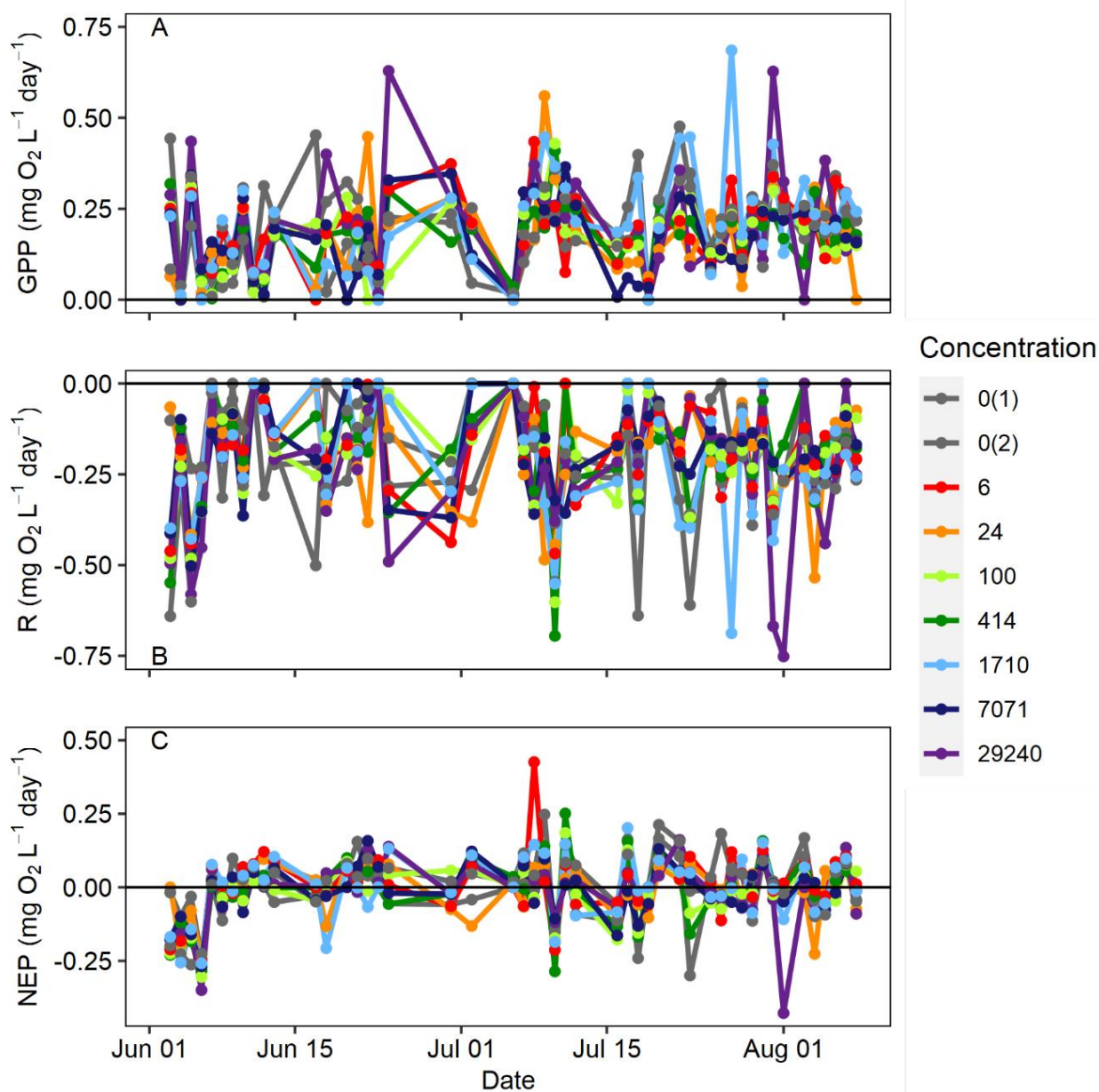


Figure 25. Timeseries from June 3 through August 10, 2021 of A) GPP ($\text{mg O}_2 \text{ L}^{-1} \text{ day}^{-1}$), B) R ($\text{mg O}_2 \text{ L}^{-1} \text{ day}^{-1}$), and C) NEP ($\text{mg O}_2 \text{ L}^{-1} \text{ day}^{-1}$). The legend indicates added microplastic concentration in the mesocosm, with 0(1) and 0(2) noting the two control mesocosm B and H respectively.

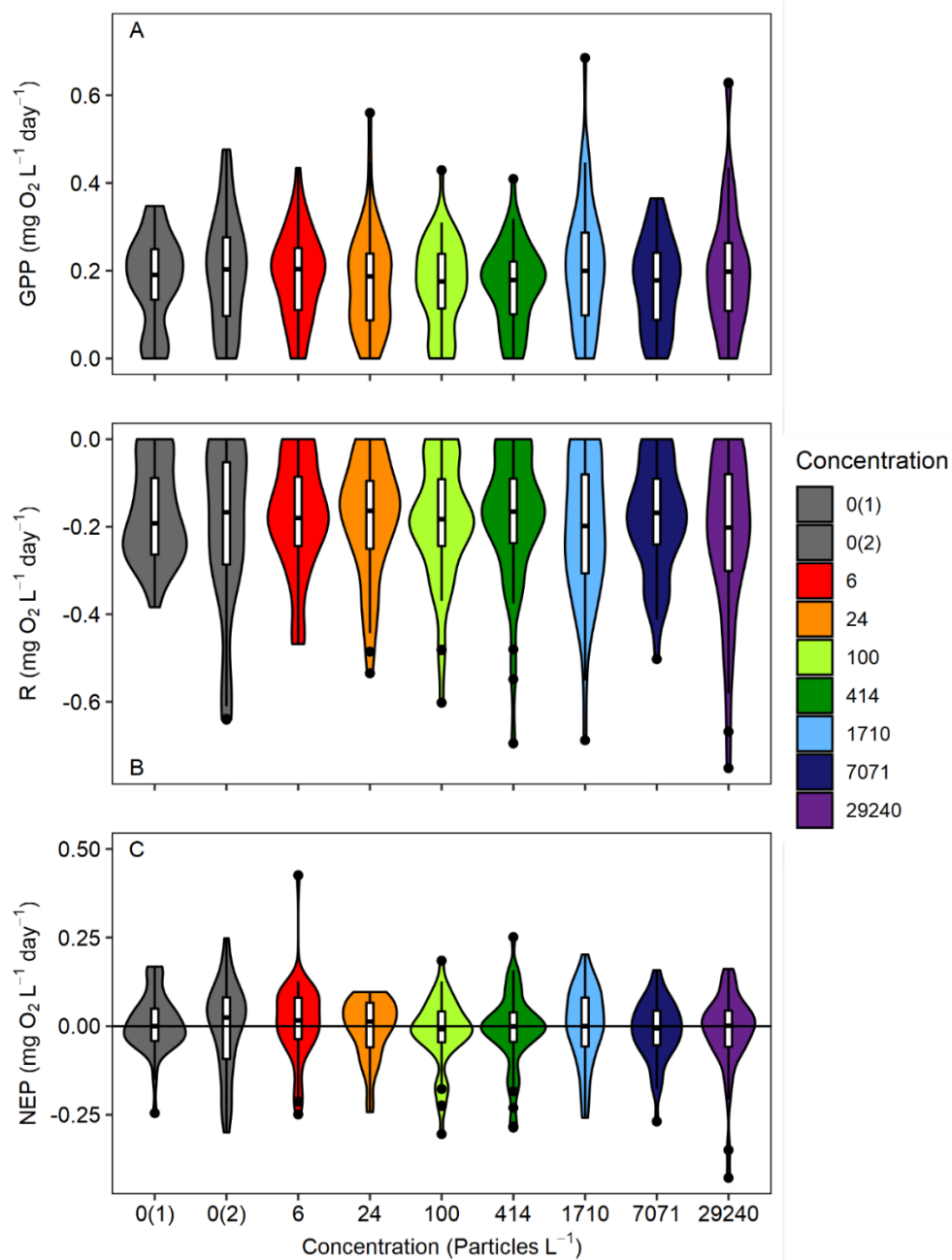


Figure 26. Violin plots with boxplots ecosystem metabolism estimates for each mesocosm. A) GPP (mg O₂ L⁻¹ day⁻¹), B) R (mg O₂ L⁻¹ day⁻¹), and C) NEP (mg O₂ L⁻¹ day⁻¹). The legend indicates added microplastic concentration in the mesocosm, with 0(1) and 0(2) noting the two control mesocosms B and H respectively. The boxplot symbols are: center line = median, box edges = interquartile range, and dots = outliers).

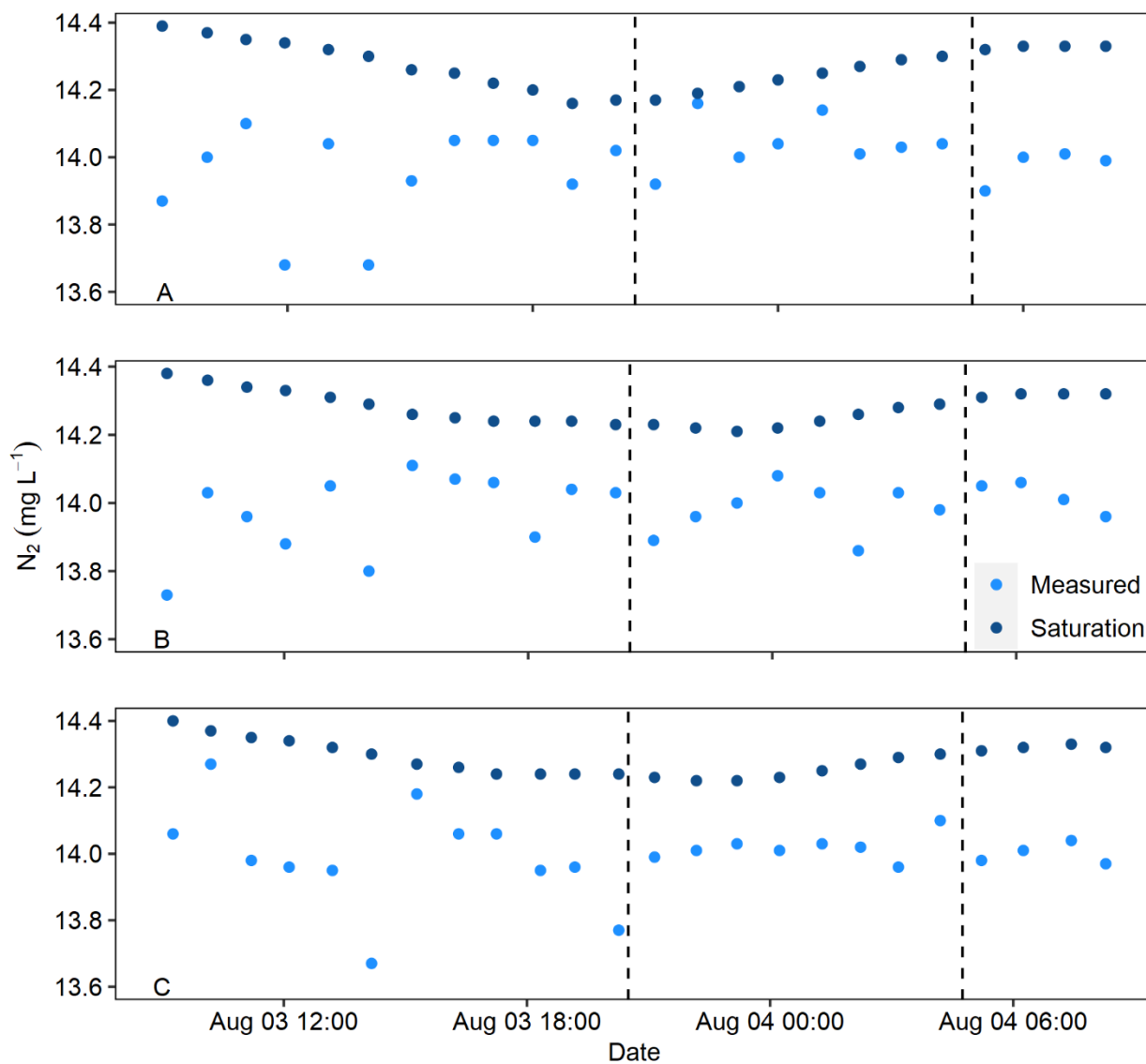


Figure 27. Timeseries of measured N_2 concentration and N_2 concentration at saturation (mg L^{-1}), recorded hourly from August 3, 9:00 through August 4, 2021 9:00 for three mesocosms. A) mesocosm B (0 particles L^{-1}), B) mesocosm I (1710 particles L^{-1}), and C) mesocosm D (29240 particles L^{-1}). The area between the dashed lines indicates night.

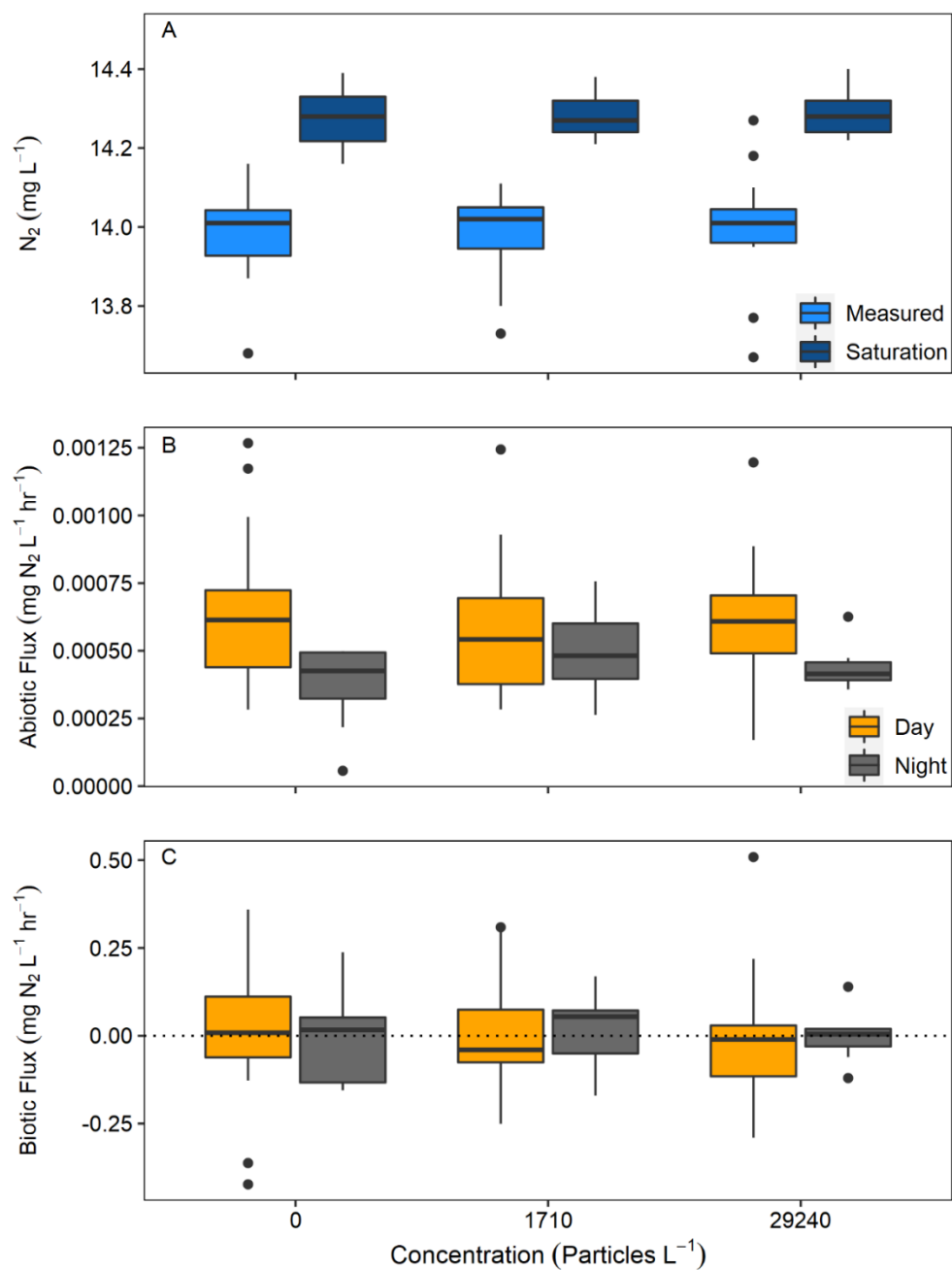


Figure 28. Boxplots of N_2 concentration and flux at three mesocosms. A) Measured N_2 concentration and N_2 concentration at saturation (mg L⁻¹), B) abiotic N_2 flux by day and night and, C) biotic N_2 flux by day and night (mg N₂ L⁻¹ hr⁻¹). Horizontal dashed lines indicate net 0 N_2 flux. The boxplot symbols are: center line = median, box edges = interquartile range, and dots = outliers).

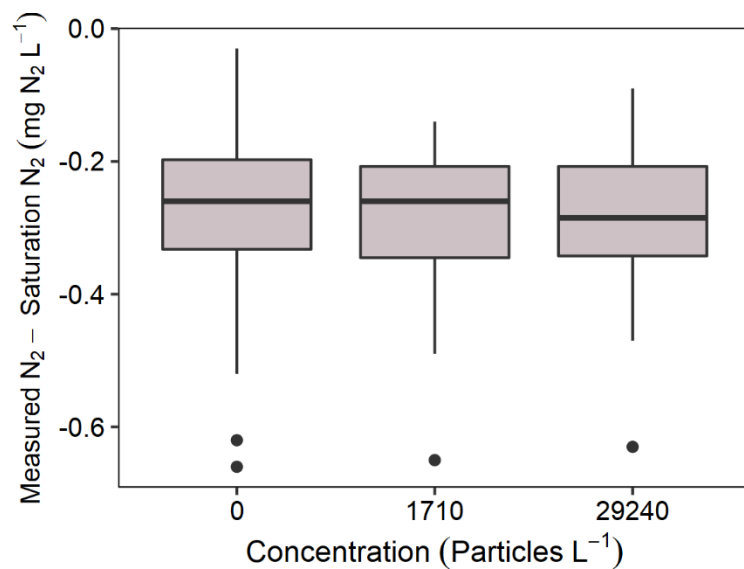


Figure 29. Boxplots of the difference between measured N₂ concentration and N₂ concentration at saturation (mg N₂ L⁻¹) in each mesocosm. The boxplot symbols are: center line = median, box edges = interquartile range, and dots = outliers).

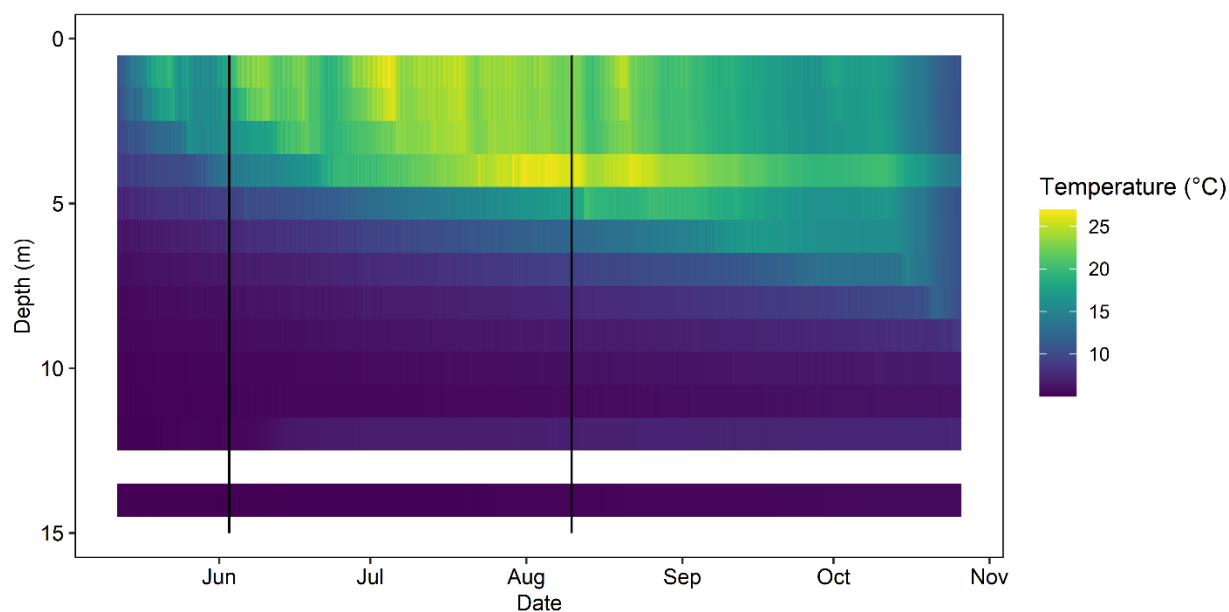


Figure 30. Temperature (°C) profile of lake 378 by 1 m depth increments from 1 m to 15 m from May 11 through October 26, 2021. The vertical black lines indicate the period for which ecosystem metabolism was estimated in the mesocosms: June 3, 2021 – August 10, 2021. The white space at 13 m is a result of the temperature logger at 13 m failing.

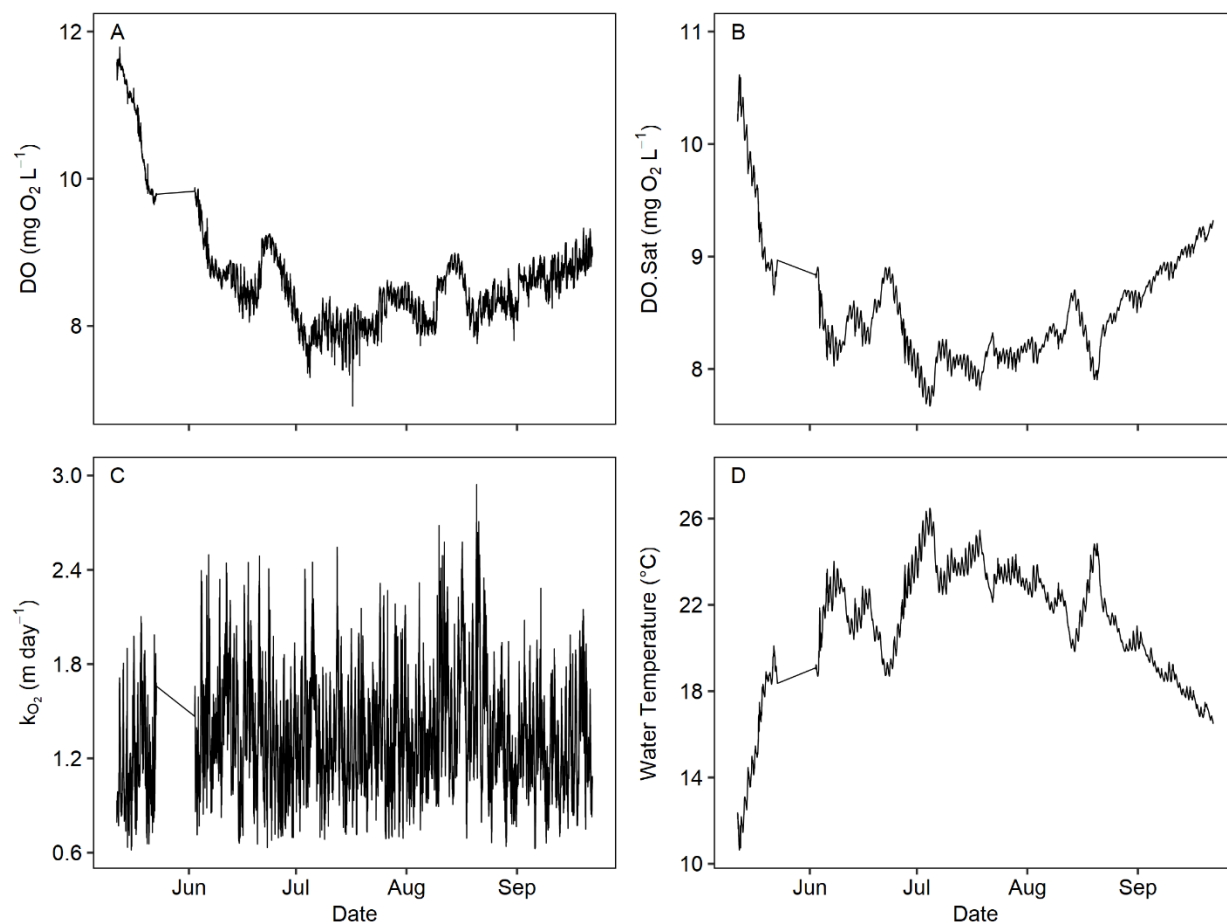


Figure 31. Whole-lake timeseries of physical data from May,11 through September 22, 2021 A) observed DO (mg O₂ L⁻¹), B) DO at 100% saturation (mg O₂ L⁻¹), C) O₂ transfer velocity (m day⁻¹), and D) water temperature (°C).

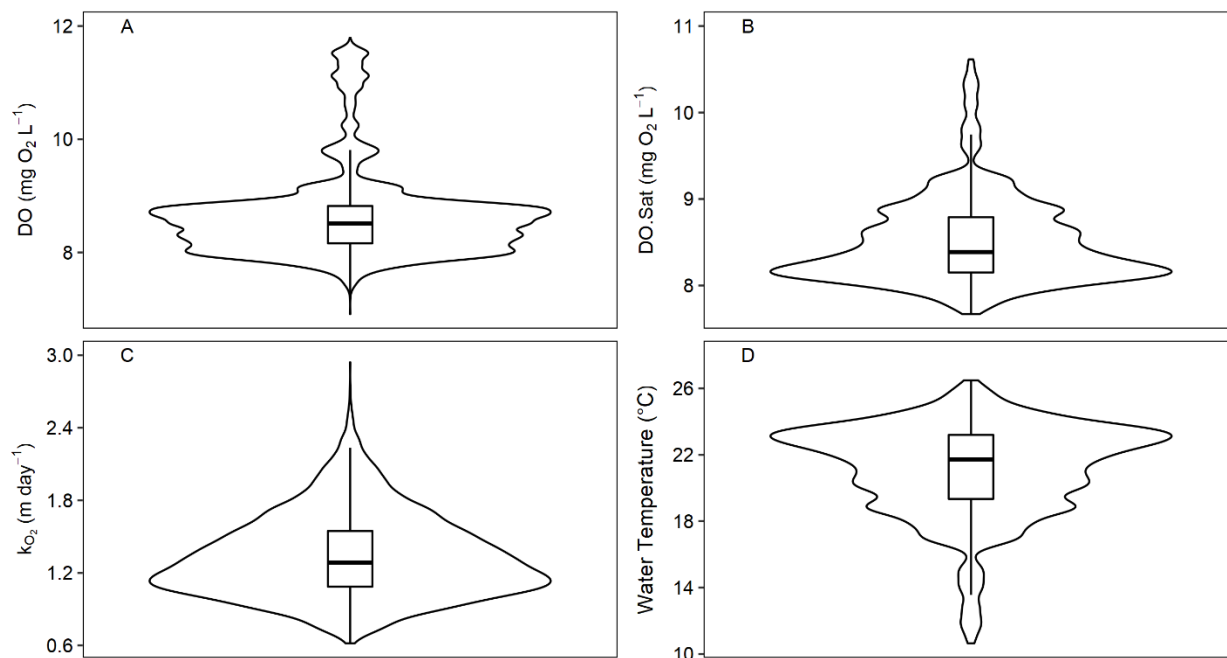


Figure 32. Violin plots with boxplots of physical data for the whole lake. A) observed DO (mg O₂ L⁻¹), B) DO at 100% saturation (mg O₂ L⁻¹), C) O₂ transfer velocity (m day⁻¹), and D) water temperature (°C). The boxplot symbols are: center line = median, box edges = interquartile range, and dots = outliers).

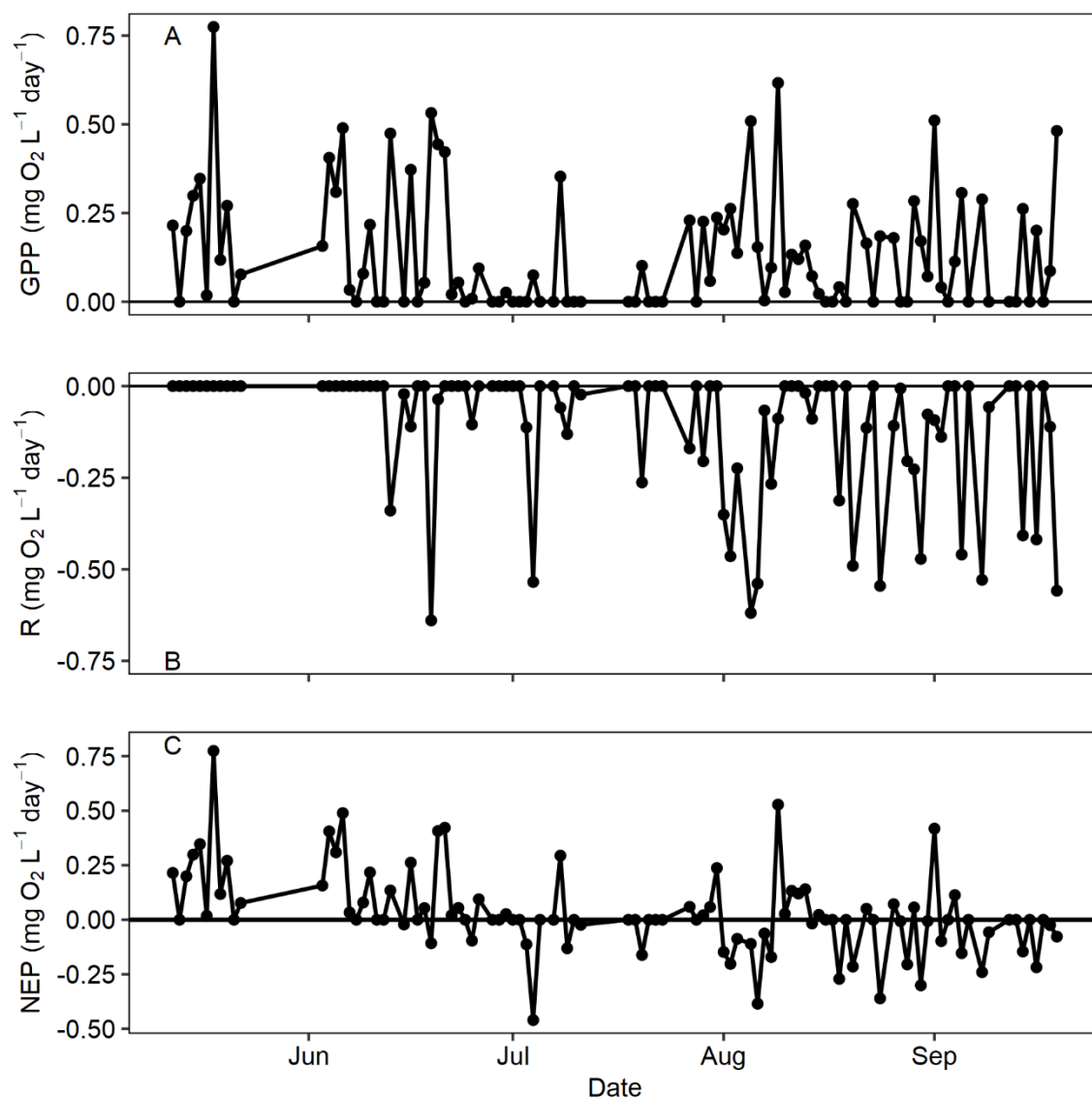


Figure 33. Whole-lake timeseries from May 12 through September 19, 2021 of A) GPP ($\text{mg O}_2 \text{ L}^{-1} \text{ day}^{-1}$), B) R ($\text{mg O}_2 \text{ L}^{-1} \text{ day}^{-1}$), and C) NEP ($\text{mg O}_2 \text{ L}^{-1} \text{ day}^{-1}$).

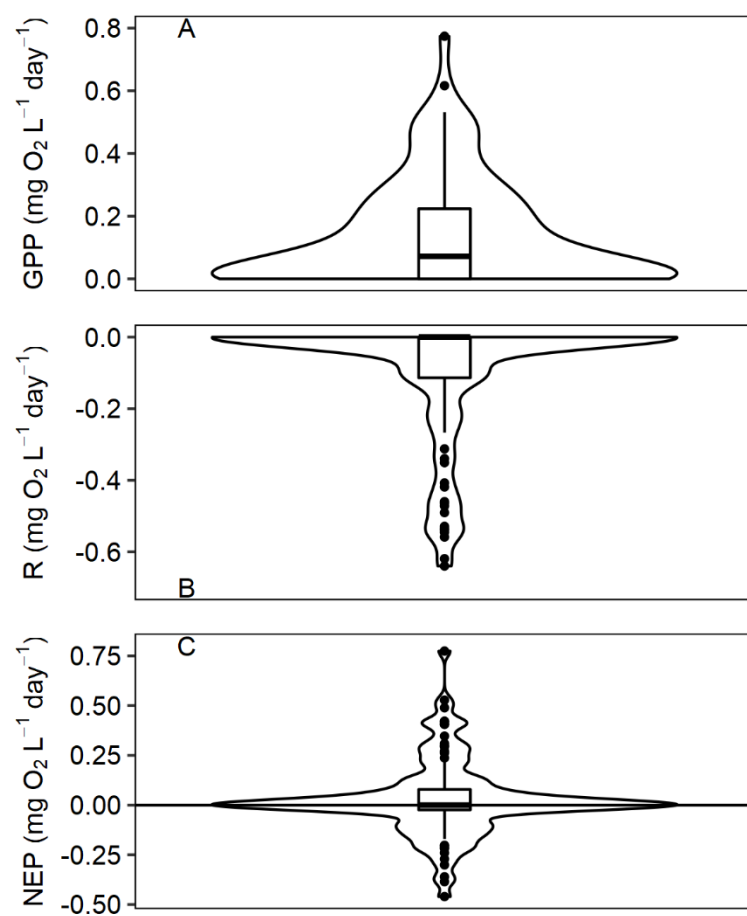


Figure 34. Violin plots with boxplots of ecosystem metabolism estimates for the whole lake. A) GPP ($\text{mg O}_2 \text{ L}^{-1} \text{ day}^{-1}$), B) R ($\text{mg O}_2 \text{ L}^{-1} \text{ day}^{-1}$), and C) NEP ($\text{mg O}_2 \text{ L}^{-1} \text{ day}^{-1}$). The boxplot symbols are: center line = median, box edges = interquartile range, and dots = outliers).

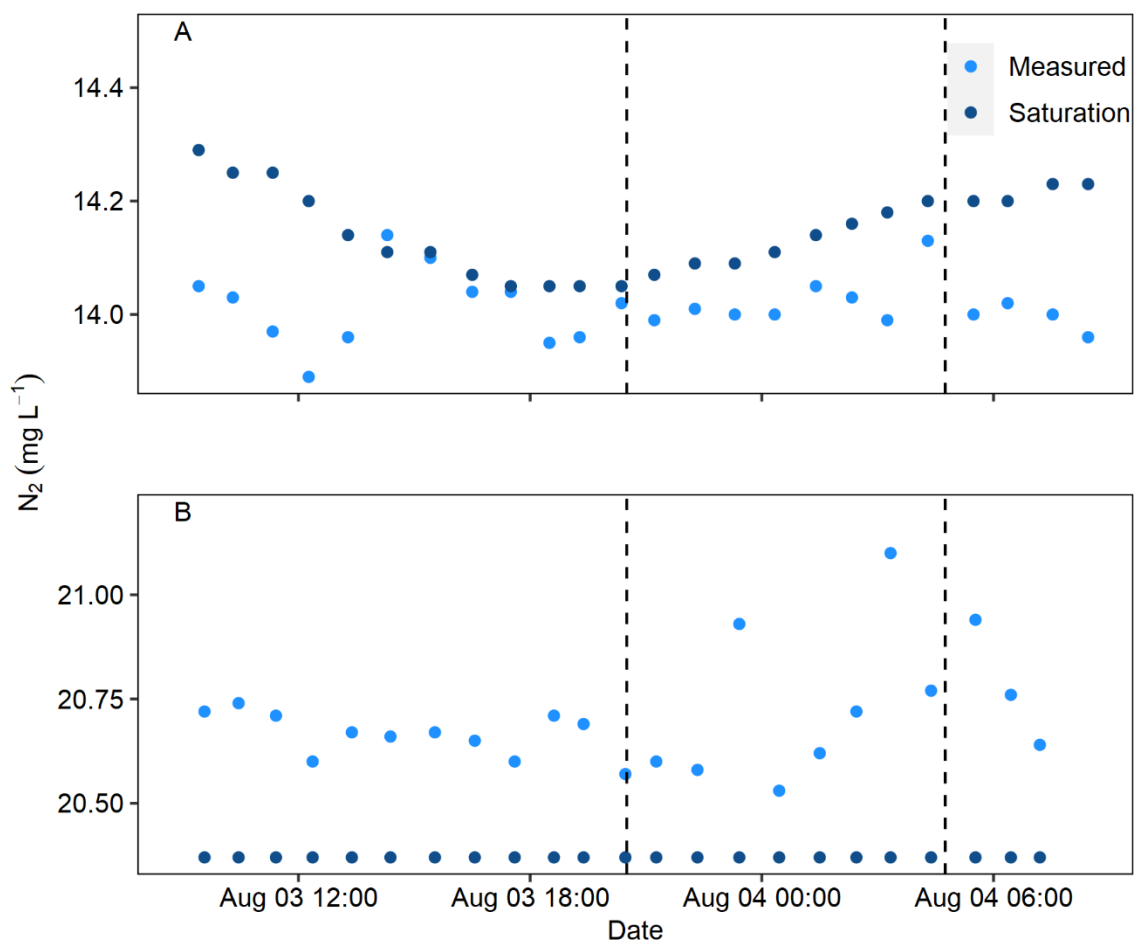


Figure 35. Timeseries of measured N_2 concentration and N_2 concentration at saturation (mg L^{-1}), recorded hourly from August 3 9:00 through August 4, 2021 9:00 in A) the epilimnion and B) the hypolimnion. The area within the dashed lines indicates night.

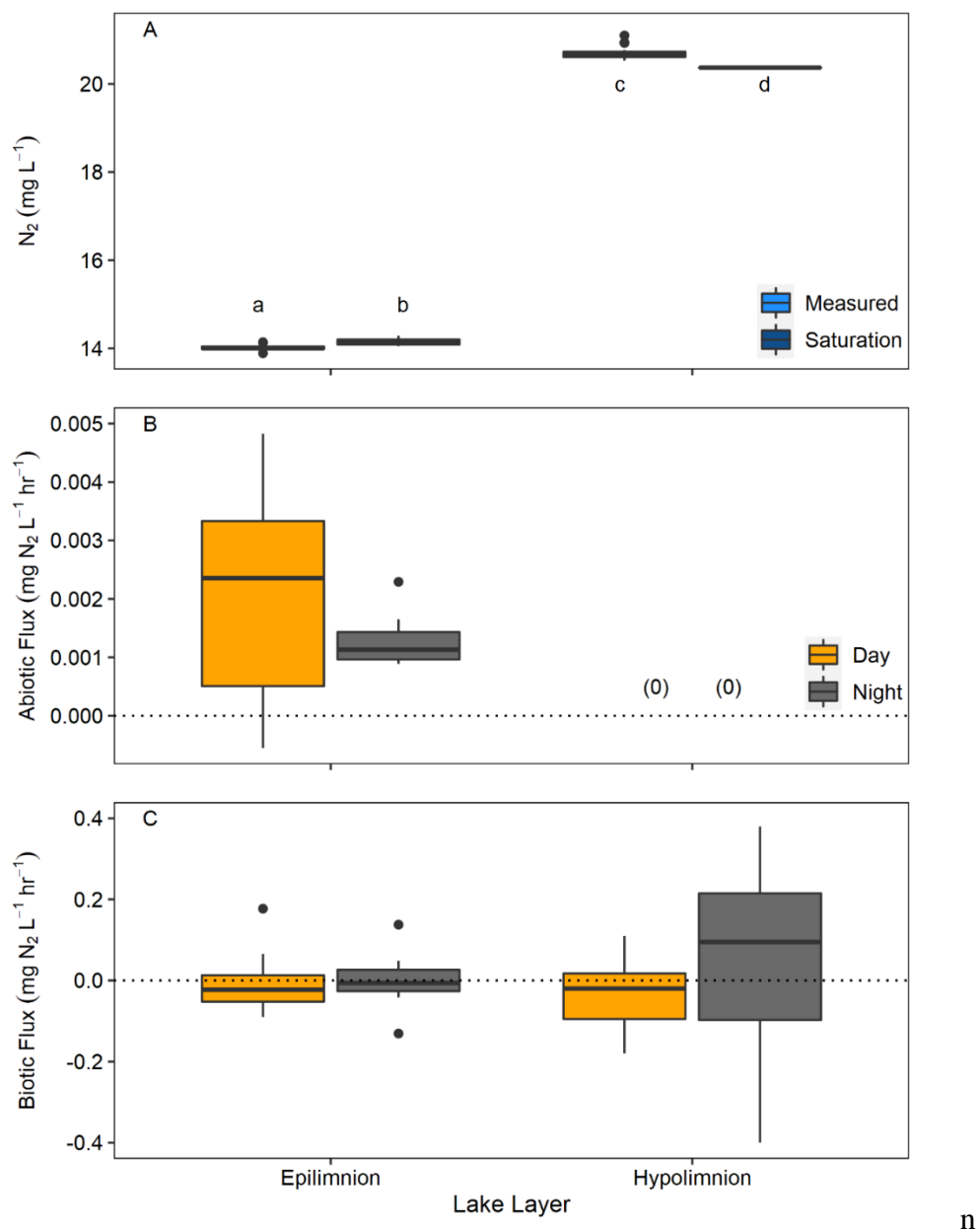


Figure 36. Boxplots of N_2 concentration and flux at the two lake layers. A) Measured N_2 concentration and N_2 concentration at saturation ($mg\ L^{-1}$), B) abiotic N_2 flux by day and night and, C) biotic N_2 flux by day and night ($mg\ N_2\ L^{-1}\ hr^{-1}$). Abiotic N_2 flux in the hypolimnion was 0 during both day and night which is indicated by the two zeros. Horizontal dashed lines indicate net 0 N_2 flux. The boxplot symbols are: center line = median, box edges = interquartile range, and dots = outliers).

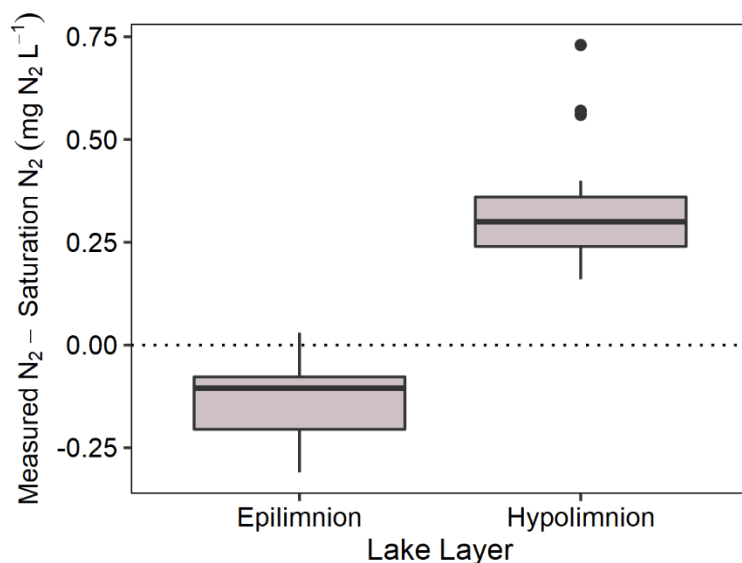


Figure 37. Boxplot of the difference between measured N₂ concentration and N₂ concentration at saturation (mg N₂ L⁻¹) at each lake layer. The horizontal dashed line indicates net 0 difference between measured N₂ concentration and N₂ concentration at saturation. The boxplot symbols are: center line = median, box edges = interquartile range, and dots = outliers).

Discussion

Contrary to our predictions, we did not find evidence for an impact of microplastic addition on the ecosystem processes of metabolism or N₂ flux. The lack of impact of microplastics on ecosystem processes is likely due to the oligotrophic nature of the study site and the duration of the project. Lakes that experience high microplastics are more commonly situated in areas of higher human population density and land-use modification relative to the remote, relatively pristine environment of the study site. Overall, the field of study into the environmental impacts of microplastic research is rapidly growing, and assessments are needed to address potential effects of plastic pollution at larger spatial scales and under different degrees of eutrophication. Our work contributes to that progress by assessing the ecological impacts of microplastics using large, in situ mesocosms and ecosystem-scale metrics.

Ecosystem metabolism rates were low, variable, and not impacted by microplastic addition

We found no difference in ecosystem metabolism across the microplastic treatments, suggesting that the potential for biofilm colonization of microplastic surfaces did not occur at levels high enough to impact ecosystem-scale rates. We expected surface area may be a limiting factor for biofilm growth and microplastics could serve as a substrate for biofilms which would increase overall biomass and thereby metabolic activity. Based on the trophic status of our study lake, however, nutrient limitation was likely the primary limiting factor, not surface area for colonization. In addition, ecosystem metabolism within the mesocosms may have been most strongly driven by planktonic organisms, rather than those which colonized the biofilms on the microplastic or mesocosm walls. This hypothesis is supported by the similarity between rates of metabolism among the mesocosms, and between the mesocosms and the whole-lake estimates. Calculating mean \pm SD metabolism rates for the whole lake for only June 3-August 8 (when the microplastic experiment was conducted) with the mesocosms showed very similar measurements for GPP (whole lake = 0.13 ± 0.17 mg O₂ L⁻¹ day⁻¹, mesocosms = 0.18 ± 0.11 mg O₂ L⁻¹ day⁻¹), R (whole lake = -0.10 ± 0.17 mg O₂ L⁻¹ day⁻¹, mesocosms = -0.19 ± 0.15 mg O₂ L⁻¹ day⁻¹), and NEP (whole lake = 0.03 ± 0.18 mg O₂ L⁻¹ day⁻¹, mesocosms = -0.005 ± 0.10 mg O₂ L⁻¹ day⁻¹). This similarity between metabolism metrics offers some support to the role of planktonic organisms in driving metabolism within mesocosms and the epilimnion sensor used for whole-lake metabolism. However, forthcoming analyses of microbes and algae in the water column, on the added microplastics, and on the mesocosm walls will reveal the amount of biofilm growth and organismal composition across the habitats.

Metabolism rates at this site were low and highly variable throughout the study period in all the experimental mesocosms and at the whole-lake scale, with no clear influence of seasonal patterns during our study. This is consistent with relatively low metabolism rates and minimal seasonal variation from other lakes within this broader geographic range. For example, previous measurements of ecosystem metabolism in 165 diverse lakes in the boreal region of Québec collected in late spring/summer estimated GPP: median = 0.463, IQR = 0.257-0.857 mg O₂ L⁻¹ day⁻¹; R: median = -0.506, IQR = 0.303-982 mg O₂ L⁻¹ day⁻¹; NEP: median = -0.048, IQR = -0.144-0.017 mg O₂ L⁻¹ day⁻¹ (Bogard et al., 2020). Ecosystem metabolism rates from this study are lower than the composite across 165 sites but are more similar if only lakes near the same latitude are considered (Bogard et al., 2020). When lakes were sampled in fall, early spring, and winter, metabolism metrics did not vary seasonally (Bogard et al., 2020). Our measurements also fall within the range of estimates for GPP, R and NEP of 3 northern Wisconsin lakes that also showed minimal seasonal variation (Solomon et al., 2013b). While ecosystem metabolism is an integrative metric that is valuable for quantifying impacts of environmental change, the relatively low rates and lack of seasonal pattern (at least during the June-August period represented here) may reduce its capacity for responding to microplastic pollution, at least without the addition of concurrent impacts such as excess nutrients.

Research at ELA is well known for establishing the role of nutrients as a primary structuring factor in lake ecosystems, including for rates of metabolism (Blanchfield et al., 2009; Findlay et al., 1994; Molot et al., 2021; Schindler, 1974, 1977). Earlier work at ELA has demonstrated the importance of phosphorus (P) in regulating biological activity within these lakes (Schindler, 1974, 1990). Addition of P can affect metabolism and N flux through changes

to phytoplankton. For example, fertilization with P-alone at two oligotrophic lakes at ELA in 2019 simulated a cyanobacterial bloom, which increased N-fixation, and thereby increased total N (Molot et al., 2021). In addition, low N and P water concentrations at ELA lakes have been related to slower leaf litter decomposition rates compared to other lakes in Ontario. Because ecosystem metabolism rates were low across mesocosms and at the whole-lake scale, we inferred that low activity of organisms in the mesocosms was not affected by the addition of microplastics as a surface for biofilm adhesion due to fundamental nutrient limitation (Costerton et al., 1995; Hunt et al., 2004; Jefferson, 2004; Sawyer & Hermanowicz, 1998).

Other studies at IISD-ELA have used ecosystem metabolism to quantify impacts of other pollutants or stressors, with mixed results for impacts on GPP, R, and NEP. Chronic or pulse additions of silver nanoparticles at a range of environmentally relevant concentrations had community level effects on plankton but no effect on ecosystem metabolism (Norman et al., 2019). Whole-lake fertilization with inorganic N and P resulted in decreased GPP (but not respiration), which was attributed to the influence of N:P stoichiometry on phytoplankton (Schindler, 1990). Finally, whole lake acidification with sulfuric acid had no impact on GPP, and R decreased only under extreme acidification (Schindler, 1990; Schindler et al., 1980). We note earlier manipulations quantified ecosystem metabolism through chamber incubations, under-ice respiration rates (Schindler, 1990), and ^{14}C (Hesslein et al., 1980), rather than the open-water metabolism method used for the present study.

Even though there was no difference in the metabolism rates among the microplastic treatments, individual mesocosms showed some differences in the measured DO concentration over time, which can offer some insight into factors that were controlling the DO signal we

recorded. Differences in DO concentration did not align with the microplastic addition gradient. This suggested that non-biological factors were the source of the observed variation in DO among the mesocosms. Physical factors that differed among mesocosms were likely the primary driver of DO signals, with our first 'suspects' being O₂ exchange between the water and atmosphere, as well as water temperature (Staeher et al., 2010). If DO variability was solely dependent on water temperature and O₂ transfer velocity we would expect the 1-way ANOVA results for DO, water temperature, and O₂ transfer velocity to be the same. However, when we compare patterns of water temperature, O₂ transfer velocity, and DO concentration among the mesocosms, the signals do not align. For example, DO was significantly different between the mesocosms '0(2) particles L⁻¹' and '6 particles L⁻¹', but those mesocosms showed no difference in water temperature or O₂ transfer velocity.

Ruling out O₂ transfer velocity and water temperature as the cause of differences in the DO concentration among mesocosms, one key factor remains that may account for the patterns: the 'A' term in the ecosystem metabolism equation $\frac{\Delta O_2}{\Delta t} = GPP - R - F - A$ (Shaehr et al., 2010). The term *A* includes several factors, including horizontal/vertical advection, photochemical oxidation of organic matter, anaerobic O₂ consumption, microstratification, and internal wave action (Hanson et al., 2008; Imberger, 1985; MacIntyre et al., 2002; Staeher et al., 2010). Nighttime increases in DO, which we observed as have others (McNair et al., 2013; Obertegger et al., 2017), are also commonly attributed to physical processes rather than biological changes (Hanson et al., 2008). Rapid changes in weather, wind speed, and precipitation can also cause rapid changes to diel O₂ (Hanson et al., 2008; Langman et al., 2010). These physical processes may have dominated the DO signal at times given the low biological

activity. Similar studies of microplastic addition in lakes with higher levels of metabolism (e.g., more eutrophic conditions) may offer more insight into its potential effect on ecosystem metabolism.

Flux of N₂ showed consistent under saturation and was not affected by microplastics

Like for ecosystem metabolism, dissolved N₂ dynamics were not affected by microplastics, suggesting the biofilm colonization of microplastic surfaces did not occur at levels high enough to impact N₂ concentration or flux, and that N₂ dynamics may be more strongly controlled by non-biofilm organisms or processes. Across all three of the microplastic treatments included in our analysis, measured N₂ concentration was at the same level of under saturation, suggesting that in each mesocosm losses of N₂ from the water were greater than sources of N₂ into the water across the 24-hour study period. Potential losses of dissolved N₂ include biological uptake (N-fixation) and abiotic diffusion due to differences in temperature and gas exchange (Bernhard, 2010; McCarthy et al., 2016; Weiss, 1970). Potential sources of dissolved N₂ include anaerobic respiration pathways that generate N₂ (denitrification and anammox) (Bernhard, 2010; McCarthy et al., 2016).

Previous studies have examined N₂ saturation levels in freshwaters, with variable patterns and driving factors isolated. For example, N₂ oversaturation was documented in Antarctic lakes (Craig et al., 1992; Wharton et al., 1987), aquaculture ponds (Boyd et al., 1994), and lakes in the upper Midwest of the USA (Loeks-Johnson & Cotner, 2020). In the latter case, N₂ saturation in lakes across Minnesota and Northern Iowa showed N₂ supersaturation throughout the year and across all lake layers, showing the lakes were net sources of N₂ (Loeks-Johnson & Cotner, 2020). The pattern was attributed to higher rates of denitrification and annamox compared to N-fixation,

especially because supersaturation was highest in summer when conditions for anaerobic respiratory processes were most favorable. The trophic statuses of the lakes were eutrophic, eutrophic-mesotrophic, mesotrophic, and mesotrophic-oligotrophic (Loeks-Johnson and Conter, 2020). Elsewhere, N_2 undersaturation has been reported in eutrophic lakes on a seasonal basis, attributed to high N-fixation (Wang et al., 2021; Zhao et al., 2022). Fewer studies have examined N_2 dynamics in oligotrophic lakes. However, Yang et al. (2015) recorded the mean N_2 saturation of 75 dimictic, low-productivity Swedish and Norwegian boreal lakes was 94.1% ($CV = 2.2\%$) with most lakes being undersaturated in N_2 consistent with the pattern observed at our oligotrophic site. Overall, there is relatively little literature on N_2 saturation levels, and more research on diel measurements, spanning a gradient of conditions, will generate insights into the relative importance of biological and physical drivers, and the potential impact of pollutants such as microplastics.

Our study measured N_2 flux on only a single date, but our results are consistent with previous work at the IISD-ELA lakes which suggest that P dynamics may drive dissolved N_2 patterns. This is supported by whole-lake P fertilization studies at ELA that have demonstrated P limitation (Schindler, 1974, 1977). In addition, N-fixation is driven by availability of P (Findlay et al., 1994; Molot et al., 2021). This can be attributed to N-fixation being very energetically costly, at least 16 ATP molecules are required to break the triple bond in N_2 (Bernhard, 2010) and therefore large amounts of P. Given the similar trophic status and N_2 saturation levels as low-productivity Swedish and Norwegian lakes (Yang et al., 2015), undersaturation of N_2 in low-productivity, P limited, boreal lakes could be a common condition, although this requires more study.

Our estimates of N₂ flux (mg N L⁻¹ d⁻¹) offer additional insight into the relative impact of biotic factors and abiotic factors in driving changes in dissolved N₂ over the diel study period. Our estimate of biotic N₂ flux showed rates were low, and there was no difference between day and night in any of the three mesocosms. We expected higher biotic uptake of N₂ during the day due to N₂ fixing cyanobacteria, but the consistent pattern suggests that organisms fix N at a constant rate. N-fixation is conducted by heterotrophs and autotrophs, greater insight into N-fixation could be generated by temporal measurement of nitrogenase (*nifH*) expression. In contrast we noted a higher abiotic N₂ flux during the day. We inferred that higher abiotic N₂ flux during the day was driven by warmer water temperatures which increase gas transfer velocity between the water and atmosphere (Jähne et al., 1987; Jähne & Haußecker, 1998).

The patterns for dissolved N₂ flux were different in the epilimnion compared to the patterns in the experimental mesocosms, which also help elucidate the role of physical drivers for dissolved N₂ patterns. The main difference in patterns between the epilimnion and the mesocosms was there was no difference in abiotic N₂ flux between day and night in the epilimnion, while there was for the mesocosms. Water temperature patterns in the epilimnion and mesocosms were the same, but the reaeration coefficient was different. We used a constant value for reaeration in the mesocosms ($k_{600} = 0.1056 \text{ m day}^{-1}$), but reaeration in the epilimnion was calculated using a method based on wind speed data collected at 15-minute intervals. The lack of diel dissolved N₂ flux pattern in the epilimnion suggest the values were driven by the wind data rather than the temperature data as the wind values show much higher temporal variation than temperature. Collectively, the data also support the role of abiotic factors in

driving N_2 flux over biological components at the whole-lake scales, and thereby the low impact of microplastics on dissolved N_2 dynamics in an oligotrophic setting.

The patterns of dissolved N_2 were different in the hypolimnion and epilimnion. As predicted, the hypolimnion was oversaturated with N_2 while the epilimnion was undersaturated. Oversaturation of N_2 indicated that in the hypolimnion, sources of N_2 via biological processes were greater than any potential losses of N_2 . The source of N_2 in the hypolimnion would be denitrification and anammox (Bernhard, 2010; McCarthy et al., 2016), especially in anoxic conditions. We did not measure dissolved oxygen in the hypolimnion or in sediments, however previous measurements of DO in Lake 378 taken August 14, 2019 showed DO was below 1.0 mg L^{-1} at 12 m and below 1.0 mg L^{-1} at 10 m on August 25, 2020 (IISD-ELA, unpublished data). There is also a physical component of the N_2 flux model that makes an important contribution to this outcome. The model of hypolimnion N_2 flux does not have an atmospheric gas exchange component, because N_2 is not transferred between the air and water in the hypolimnion. However, N_2 fluxes in the hypolimnion would still be attributed to biology because when N_2 was measured the lake was considerably stratified which greatly limits the diffusion and transport of gases and nutrients between the epilimnion and hypolimnion (Bédard & Knowles, 1991; Deemer et al., 2011).

Oversaturation of N_2 in the hypolimnion in our dataset is consistent with other studies. Oversaturation of N_2 in the hypolimnion, attributed to denitrification, has been observed in eutrophic lakes (Beaulieu et al., 2014; Deemer et al., 2011; Grantz et al., 2012). The anoxic zone of the Black Sea has also been demonstrated to be oversaturated with N_2 due to denitrification and anammox (Fuchsman et al., 2008). Last, the hypolimnion of boreal, humic lakes were

oversaturated in N_2 , and ^{15}N tracers revealed denitrification as the source (Tirola et al., 2011).

The same study found lakes with N_2 undersaturation in the hypolimnion occurred via physical impacts of ebullition generated by high methane (CH_4) production in the hypolimnion (Tirola et al., 2011).

Ongoing analyses and suggestions for future studies

Additional forthcoming data generated by this large, interdisciplinary research collaboration will enhance the interpretation and understanding of our results for the impacts of microplastics on ecosystem processes and place the data within the larger context of the study. Data on total dissolved N, particulate N, NO_2 , NO_3 , and NH_3 will enhance our understanding of ecosystem metabolism and N_2 fluxes and show whether individual N pools were affected by microplastic addition. Analysis of dissolved inorganic C, particulate C, dissolved organic carbon (DOC), and chlorophyll will also enhance our understanding of how well the metabolism model captured C dynamics. Measurements of total dissolved P and particulate P, along with their proportional abundance to N pools may offer an explanation for the low rates we observed. Other data will demonstrate whether the effects of microplastic were constrained to particular organisms relevant to ecosystem processes. For example, analysis on biofilm biomass on microplastics will indicate if microplastic served as a substrate for biofilm. Results from light-dark incubations of microplastic, wall-attached periphyton, and phytoplankton will show us how the activity of individual constituents of the microbial community were affected by microplastic exposure. Differences in community composition may be generated by microplastics, but not reflected in our ecosystem-scale measurements. The composite data will reveal the effects of

microplastic on all levels of biological organization and could show critical patterns that were not revealed by the highly integrated our measurements of ecosystem-scale processes.

We did not find an effect of microplastics on ecosystem processes in this study, but more analyses are needed to understand the potential for microplastics to affect ecosystem processes across a gradient of conditions. Future studies should study the effect of a combination of stressors on ecosystem processes. For example, the effects on ecosystem processes could be compared between P fertilization and P fertilization with microplastic additions. Future studies may consider microplastic addition studies in eutrophic lakes or wetlands where the biological signals may be more readily impacted. Measuring concentrations of greenhouse gasses such as CH₄ and nitrous oxide (N₂O) following mesocosm microplastic additions could also inform the potential effects of microplastic pollution on climate change. Finally, studies that conduct whole-lake additions of microplastics, and analyze the data over longer time scales will be critical to examining their potential impact on ecosystem dynamics.

REFERENCE LIST

- Altman, D. G., & Bland, M. J. (1995). The normal distribution. *BMJ*, *310*, 298.
- Amaral-Zettler, L. A., Zettler, E. R., Mincer, T. J., Klaassen, M. A., & Gallager, S. M. (2021). Biofouling impacts on polyethylene density and sinking in coastal waters: A macro/micro tipping point? *Water Research*, *201*, 117289. <https://doi.org/10.1016/j.watres.2021.117289>
- Amaral-Zettler, L. A., Zettler, E. R., Slikas, B., Boyd, G. D., Melvin, D. W., Morrall, C. E., Proskurowski, G., & Mincer, T. J. (2015). The biogeography of the Plastisphere: Implications for policy. *Frontiers in Ecology and the Environment*, *13*(10), 541–546. <https://doi.org/10.1890/150017>
- Amaral-Zettler, L. A., Zettler, E. R., & Mincer, T. J. (2020). Ecology of the plastisphere. *Nature Reviews Microbiology*, *18*(3), 139–151.
- Ammar, Y., Swailes, D., Bridgens, B., & Chen, J. (2015). Influence of surface roughness on the initial formation of biofilm. *Surface and Coatings Technology*, *284*, 410–416. <https://doi.org/10.1016/j.surfcoat.2015.07.062>
- Andrady, A. L., & Neal, M. A. (2009). Applications and societal benefits of plastics. *Philosophical Transactions of the Royal Society B: Biological Sciences*, *364*(1526), 1977–1984. <https://doi.org/10.1098/rstb.2008.0304>
- Barnes, D. K. A., Galgani, F., Thompson, R. C., & Barlaz, M. (2009). Accumulation and fragmentation of plastic debris in global environments. *Philosophical Transactions of the Royal Society B: Biological Sciences*, *364*(1526), 1985–1998. <https://doi.org/10.1098/rstb.2008.0205>
- Barros, J., & Seena, S. (2021). Plastisphere in freshwaters: An emerging concern. *Environmental Pollution*, *290*(September), 118123. <https://doi.org/10.1016/j.envpol.2021.118123>
- Battin, T. J., Besemer, K., Bengtsson, M. M., Romani, A. M., & Packmann, A. I. (2016). The ecology and biogeochemistry of stream biofilms. *Nature Reviews Microbiology*, *14*(4), 251–263. <https://doi.org/10.1038/nrmicro.2016.15>
- Battin, T. J., Kaplan, L. A., Newbold, J. D., & Hansen, C. M. E. (2003). Contributions of microbial biofilms to ecosystem processes in stream mesocosms. *Nature*, *426*(6965), 439–442. <https://doi.org/10.1038/nature02152>

- Beaulieu, J. J., Smolenski, R. L., Nietch, C. T., Townsend-Small, A., Elovitz, M. S., & Schubauer-Berigan, J. P. (2014). Denitrification alternates between a source and sink of nitrous oxide in the hypolimnion of a thermally stratified reservoir. *Limnology and Oceanography*, *59*(2), 495–506. <https://doi.org/10.4319/lo.2014.59.2.0495>
- Bédard, C., & Knowles, R. (1991). Denitrification, and Methanogenesis in a Thermally Stratified Lake. *Canadian Journal of Fisheries and Aquatic Sciences*, *48*(6), 1048–1054. www.nrcresearchpress.com
- Bernhard, A. (2010). The nitrogen cycle: processes. *Nature Education Knowledge*, *2*(2), 1–8. [http://128.143.22.36/blandy/blandy_web/education/Bay/The Nitrogen Cycle_ Processes, Players, and Human Impact _ Learn Science at Scitable.pdf](http://128.143.22.36/blandy/blandy_web/education/Bay/The%20Nitrogen%20Cycle_%20Processes,%20Players,%20and%20Human%20Impact_%20Learn%20Science%20at%20Scitable.pdf)
- Blanchfield, P. J., Paterson, M. J., Shearer, J. A., & Schindler, D. W. (2009). Johnson and Vallentyne's legacy: 40 years of aquatic research at the Experimental Lakes Area. *Canadian Journal of Fisheries and Aquatic Sciences*, *66*(11), 1831–1836. <https://doi.org/10.1139/F09-14>
- Blettler, M. C. M., & Wantzen, K. M. (2019). Threats Underestimated in Freshwater Plastic Pollution: Mini-Review. *Water, Air, and Soil Pollution*, *230*(7). <https://doi.org/10.1007/s11270-019-4220-z>
- Bogard, M. J., St-Gelais, N. F., Vachon, D., & del Giorgio, P. A. (2020). Patterns of Spring/Summer Open-Water Metabolism Across Boreal Lakes. *Ecosystems*, *23*(8), 1581–1597. <https://doi.org/10.1007/s10021-020-00487-7>
- Boyd, C. E., Watten, B. J., Goubier, V., & Wu, R. (1994). Gas supersaturation in surface waters of aquaculture ponds. *Aquacultural Engineering*, *13*(1), 31–39. [https://doi.org/10.1016/0144-8609\(94\)90023-X](https://doi.org/10.1016/0144-8609(94)90023-X)
- Brentrup, J. A., Richardson, D. C., Carey, C. C., Ward, N. K., Bruesewitz, D. A., & Weathers, K. C. (2021). Under-ice respiration rates shift the annual carbon cycle in the mixed layer of an oligotrophic lake from autotrophy to heterotrophy. *Inland Waters*, *11*(1), 114–123. <https://doi.org/10.1080/20442041.2020.1805261>
- Brothers, S., Kazanjian, G., Köhler, J., Scharfenberger, U., & Hilt, S. (2017). Convective mixing and high littoral production established systematic errors in the diel oxygen curves of a shallow, eutrophic lake. *Limnology and Oceanography: Methods*, *15*(5), 429–435. <https://doi.org/10.1002/lom3.10169>
- Burton, E., Yakandawala, N., LoVetri, K., & Madhyastha, M. S. (2007). A microplate spectrofluorometric assay for bacterial biofilms. *Journal of Industrial Microbiology and Biotechnology*, *34*(1), 1–4. <https://doi.org/10.1007/s10295-006-0086-3>

- Cabrol, L., Thalasso, F., Gandois, L., Sepulveda-Jauregui, A., Martinez-Cruz, K., Teisserenc, R., Tananaev, N., Tveit, A., Svenning, M. M., & Barret, M. (2020). Anaerobic oxidation of methane and associated microbiome in anoxic water of Northwestern Siberian lakes. *Science of the Total Environment*, 736, 139588. <https://doi.org/10.1016/j.scitotenv.2020.139588>
- Cai, L., Gong, X., Sun, X., Li, S., & Yu, X. (2018). Comparison of chemical and microbiological changes during the aerobic composting and vermicomposting of green waste. *PLoS ONE*, 13(11), 1–16. <https://doi.org/10.1371/journal.pone.0207494>
- Callahan, B. J., McMurdie, P. J., Rosen, M. J., Han, A. W., Johnson, A. J. A., & Holmes, S. P. (2016). DADA2: High resolution sample inference from Illumina amplicon data. *Nature Methods*, 13(7), 581–583. https://doi.org/10.1007/978-1-4614-9209-2_118-1
- Caporaso, J. G., Lauber, C. L., Walters, W. A., Berg-Lyons, D., Huntley, J., Fierer, N., Owens, S. M., Betley, J., Fraser, L., Bauer, M., Gormley, N., Gilbert, J. A., Smith, G., & Knight, R. (2012). Ultra-high-throughput microbial community analysis on the Illumina HiSeq and MiSeq platforms. *ISME Journal*, 6(8), 1621–1624. <https://doi.org/10.1038/ismej.2012.8>
- Carrareto Alves, L. M., Marcondes de Souza, J. A., de Mello Varani, A., & de Macedo Lemos, E. G. (2014). The family rhizobiaceae. In *The Prokaryotes* (pp. 419–437). <https://doi.org/10.1007/978-3-642-30197-1>
- Cazzaniga, G., Ottobelli, M., Ionescu, A., Garcia-Godoy, F., & Brambilla, E. (2015). Surface properties of resin-based composite materials and biofilm formation: A review of the current literature. *American Journal of Dentistry*, 28(6), 311–320.
- Chamas, A., Moon, H., Zheng, J., Qiu, Y., Tabassum, T., Jang, J. H., Abu-Omar, M., Scott, S. L., & Suh, S. (2020). Degradation Rates of Plastics in the Environment. *ACS Sustainable Chemistry and Engineering*, 8(9), 3494–3511. <https://doi.org/10.1021/acssuschemeng.9b06635>
- Chaudhary, A., Dunn, S. T., Kelly, J., & Hoellein, T. J. (n.d.). *PERIPHYTON AND 'PLASTIC'-PHYTON IN AN URBAN STREAM: MICROBIAL BIOFILM SUCCESSION ON PLASTIC LITTER SURFACES*.
- Chen, Q., Zhang, X., Xie, Q., Lee, Y. H., Lee, J. S., & Shi, H. (2021). Microplastics habituated with biofilm change decabrominated diphenyl ether degradation products and thyroid endocrine toxicity. *Ecotoxicology and Environmental Safety*, 228, 112991. <https://doi.org/10.1016/j.ecoenv.2021.112991>

- Chen, X., Chen, X., Zhao, Y., Zhou, H., Xiong, X., & Wu, C. (2020). Effects of microplastic biofilms on nutrient cycling in simulated freshwater systems. *Science of the Total Environment*, 719, 137276. <https://doi.org/10.1016/j.scitotenv.2020.137276>
- Chen, X., Xiong, X., Jiang, X., Shi, H., & Wu, C. (2019). Sinking of floating plastic debris caused by biofilm development in a freshwater lake. *Chemosphere*, 222, 856–864. <https://doi.org/10.1016/j.chemosphere.2019.02.015>
- Choy, C. A., & Drazen, J. C. (2013). Plastic for dinner? Observations of frequent debris ingestion by pelagic predatory fishes from the central North Pacific. *Marine Ecology Progress Series*, 485, 155–163. <https://doi.org/10.3354/meps10342>
- Cole, J. J., & Caraco, N. F. (1998). Atmospheric exchange of carbon dioxide in a low-wind oligotrophic lake measured by the addition of SF₆. *Limnology and Oceanography*, 43(4), 647–656. <https://doi.org/10.4319/lo.1998.43.4.0647>
- Costerton, W. J., Lewandowski, Z., Caldwell, D. E., Korber, D. R., & Lappin-Scott, H. M. (1995). Microbial biofilms. *Annual Review of Microbiology*, 49(1), 711–745. <https://doi.org/10.1201/9780203500224>
- Craig, H., Wharton, R. A., & McKay, C. P. (1992). Oxygen supersaturation in ice-covered antarctic lakes: Biological versus physical contributions. *Science*, 255(5042), 318–321. <https://doi.org/10.1126/science.11539819>
- Crusius, J., & Wanninkhof, R. (2003). Gas transfer velocities measured at low wind speed over a lake. *Limnology and Oceanography*, 48(3), 1010–1017. <https://doi.org/10.4319/lo.2003.48.3.1010>
- Dai, W., Wang, N., Wang, W., Ye, X., Cui, Z., Wang, J., Yao, D., Dong, Y., & Wang, H. (2021). Community profile and drivers of predatory myxobacteria under different compost manures. *Microorganisms*, 9(11), 1–15. <https://doi.org/10.3390/microorganisms9112193>
- Davis, N. M., Proctor, D. M., Holmes, S. P., Relman, D. A., & Callahan, B. J. (2018). Simple statistical identification and removal of contaminant sequences in marker-gene and metagenomics data. *Microbiome*, 6(1), 1–14. <https://doi.org/10.1186/s40168-018-0605-2>
- Debroas, D., Anne, M., & Alexandra, T. H. (2017). Plastics in the North Atlantic garbage patch: A boat-microbe for hitchhikers and plastic degraders. *Science of the Total Environment*, 599–600, 1222–1232. <https://doi.org/10.1016/j.scitotenv.2017.05.059>
- Deemer, B. R., Harrison, J. A., & Whitling, E. W. (2011). Microbial dinitrogen and nitrous oxide production in a small eutrophic reservoir: An in situ approach to quantifying hypolimnetic

- process rates. *Limnology and Oceanography*, 56(4), 1189–1199. <https://doi.org/10.4319/lo.2011.56.4.1189>
- Donlan, R. M. (2016). Biofilms: Microbial Life on Surfaces. *Emerging Infectious Diseases*, 82(5), 108–126.
- Doronina, N., Kaparullina, E., & Trotsenko, Y. (2014). The Family Methylophilaceae. In *The Prokaryotes: Alphaproteobacteria and Betaproteobacteria* (pp. 869–880). Springer. <https://doi.org/10.1007/978-3-642-30197-1>
- Elkin, L. A., Kay, M., Higgins, J. J., & Wobbrock, J. O. (2021). *An Aligned Rank Transform Procedure for Multifactor Contrast Tests*. <https://doi.org/10.1145/3472749.3474784>
- Engel, F., Attermeyer, K., Ayala, A. I., Fischer, H., Kirchesch, V., Pierson, D. C., & Weyhenmeyer, G. A. (2019). Phytoplankton gross primary production increases along cascading impoundments in a temperate, low-discharge river: Insights from high frequency water quality monitoring. *Scientific Reports*, 9(1), 1–13. <https://doi.org/10.1038/s41598-019-43008-w>
- Fazey, F. M. C., & Ryan, P. G. (2016). Biofouling on buoyant marine plastics: An experimental study into the effect of size on surface longevity. *Environmental Pollution*, 210, 354–360. <https://doi.org/10.1016/j.envpol.2016.01.026>
- Findlay, D. L., Hecky, R. E., Hendzel, L. L., Stainton, M. P., & Regehr, G. W. (1994). Relationship between N₂-fixation and heterocyst abundance and its relevance to the nitrogen budget of Lake 227. *Canadian Journal of Fisheries and Aquatic Sciences*, 51(10), 2254–2266. <https://doi.org/10.1139/f94-229>
- Finlay, J. A., Callow, M. E., Ista, L. K., Lopez, G. P., & Callow, J. A. (2002). The influence of surface wettability on the adhesion strength of settled spores of the green alga *Enteromorpha* and the diatom *Amphora*. *Integrative and Comparative Biology*, 42(6), 1116–1122. <https://doi.org/10.1093/icb/42.6.1116>
- Flemming, H. C., & Wingender, J. (2010). The biofilm matrix. *Nature Reviews Microbiology*, 8(9), 623–633. <https://doi.org/10.1038/nrmicro2415>
- Foley, C. J., Feiner, Z. S., Malinich, T. D., & Höök, T. O. (2018). A meta-analysis of the effects of exposure to microplastics on fish and aquatic invertebrates. *Science of the Total Environment*, 631–632, 550–559. <https://doi.org/10.1016/j.scitotenv.2018.03.046>
- Frère, L., Maignien, L., Chalopin, M., Huvet, A., Rinnert, E., Morrison, H., Kerninon, S., Cassone, A. L., Lambert, C., Reveillaud, J., & Paul-Pont, I. (2018). Microplastic bacterial

- communities in the Bay of Brest: Influence of polymer type and size. *Environmental Pollution*, 242, 614–625. <https://doi.org/10.1016/j.envpol.2018.07.023>
- Frias, J. P. G. L., & Nash, R. (2019). Microplastics : Finding a consensus on the definition. *Marine Pollution Bulletin*, 138(November 2018), 145–147. <https://doi.org/10.1016/j.marpolbul.2018.11.022>
- Friends of the Chicago River. (n.d.). About the River. Friends of the Chicago River. Retrieved September 3, 2022, from <https://www.chicagoriver.org/about-the-river/where-is-the-chicago-river>
- Fu, B., Wang, S., Su, C., & Forsius, M. (2013). Linking ecosystem processes and ecosystem services. *Current Opinion in Environmental Sustainability*, 5(1), 4–10. <https://doi.org/10.1016/j.cosust.2012.12.002>
- Fuchsman, C. A., Murray, J. W., & Konovalov, S. K. (2008). Concentration and natural stable isotope profiles of nitrogen species in the Black Sea. *Marine Chemistry*, 111(1–2), 90–105. <https://doi.org/10.1016/j.marchem.2008.04.009>
- Galbally, I. E., & Kirstine, W. (2002). The production of methanol by flowering plants and the global cycle of methanol. *Journal of Atmospheric Chemistry*, 43(3), 195–229. <https://doi.org/10.1023/A:1020684815474>
- Gewert, B., Plassmann, M. M., & Macleod, M. (2015). Pathways for degradation of plastic polymers floating in the marine environment. *Environmental Sciences: Processes and Impacts*, 17(9), 1513–1521. <https://doi.org/10.1039/c5em00207a>
- Geyer, R., Jambeck, J. R., & Law, K. L. (2017). Production, uses, and fate of all plastics ever made. *Science Advances*, 3(7), 5. <https://doi.org/10.1126/sciadv.1700782>
- Ghasemi, A., & Zahediasl, S. (2012). Normality tests for statistical analysis: A guide for non-statisticians. *International Journal of Endocrinology and Metabolism*, 10(2), 486–489. <https://doi.org/10.5812/ijem.3505>
- Gigault, J., Halle, A. ter, Baudrimont, M., Pascal, P. Y., Gauffre, F., Phi, T. L., el Hadri, H., Grassl, B., & Reynaud, S. (2018). Current opinion: What is a nanoplastic? *Environmental Pollution*, 235, 1030–1034. <https://doi.org/10.1016/j.envpol.2018.01.024>
- Gil-Delgado, J. A., Guijarro, D., Gosálvez, R. U., López-Iborra, G. M., Ponz, A., & Velasco, A. (2017). Presence of plastic particles in waterbirds faeces collected in Spanish lakes. *Environmental Pollution*, 220, 732–736. <https://doi.org/10.1016/j.envpol.2016.09.054>

- Grantz, E. M., Kogo, A., & Thad Scott, J. (2012). Partitioning whole-lake denitrification using in situ dinitrogen gas accumulation and intact sediment core experiments. *Limnology and Oceanography*, 57(4), 925–935. <https://doi.org/10.4319/lo.2012.57.4.0925>
- Gregory, M. R. (2009). Environmental implications of plastic debris in marine settings-entanglement, ingestion, smothering, hangers-on, hitch-hiking and alien invasions. *Philosophical Transactions of the Royal Society B: Biological Sciences*, 364(1526), 2013–2025. <https://doi.org/10.1098/rstb.2008.0265>
- Hanson, P. C., Carpenter, S. R., Kimura, N., Wu, C., Cornelius, S. P., & Kratz, T. K. (2008). Evaluation of metabolism models for free-water dissolved oxygen methods in lakes. *Limnology and Oceanography: Methods*, 6(9), 454–465. <https://doi.org/10.4319/lom.2008.6.454>
- Harrison, J. P., Hoellein, T. J., Sapp, M., Tagg, A. S., Ju-Nam, Y., & Ojeda, J. J. (2018). Microplastic-associated biofilms: a comparison of freshwater and marine environments. In *Freshwater microplastics* (pp. 181–201). Springer, Cham.
- Hesslein, R. H., Broecker, W. S., Quay, P. D., & Schindler, D. W. (1980). Whole-Lake Radiocarbon Experiment in an Oligotrophic Lake at the Experimental Lakes Area, Northwestern Ontario. *Canadian Journal of Fisheries and Aquatic Sciences*, 37(3), 454–463. <https://doi.org/10.1139/f80-059>
- Hoellein, T. J., McCormick, A. R., Hittie, J., London, M. G., Scott, J. W., & Kelly, J. J. (2017a). Longitudinal patterns of microplastic concentration and bacterial assemblages in surface and benthic habitats of an urban river. *Freshwater Science*, 36(3), 491–507. <https://doi.org/10.1086/693012>
- Hoellein, T. J., McCormick, A. R., Hittie, J., London, M. G., Scott, J. W., & Kelly, J. J. (2017b). Longitudinal patterns of microplastic concentration and bacterial assemblages in surface and benthic habitats of an urban river. *Freshwater Science*, 36(3), 491–507. <https://doi.org/10.1086/693012>
- Hoellein, T. J., & Rochman, C. M. (2021). The “plastic cycle”: a watershed-scale model of plastic pools and fluxes. *Frontiers in Ecology and the Environment*, 19(3), 176–183. <https://doi.org/10.1002/fee.2294>
- Hoellein, T. J., Rojas, M., Pink, A., Gasior, J., & Kelly, J. (2014). Anthropogenic litter in urban freshwater ecosystems: Distribution and microbial interactions. *PLoS ONE*, 9(6). <https://doi.org/10.1371/journal.pone.0098485>

- Hoellein, T. J., Shogren, A. J., Tank, J. L., Risteca, P., & Kelly, J. J. (2019). Microplastic deposition velocity in streams follows patterns for naturally occurring allochthonous particles. *Scientific Reports*, 9(1), 1–11. <https://doi.org/10.1038/s41598-019-40126-3>
- Hoellein, T. J., & Zarnoch, C. B. (2014). Effect of eastern oysters (*Crassostrea virginica*) on sediment carbon and nitrogen dynamics in an urban estuary. *Ecological Applications*, 24(2), 271–286. [https://doi.org/https://doi.org/10.1890/12-1798.1](https://doi.org/10.1890/12-1798.1)
- Holland, E. R., Mallory, M. L., & Shutler, D. (2016). Plastics and other anthropogenic debris in freshwater birds from Canada. *Science of the Total Environment*, 571, 251–258. <https://doi.org/10.1016/j.scitotenv.2016.07.158>
- Holland, R., Dugdale, T. M., Wetherbee, R., Brennan, A. B., Finlay, J. A., Callow, J. A., & Callow, M. E. (2004). Adhesion and motility of fouling diatoms on a silicone elastomer. *Biofouling*, 20(6), 323–329. <https://doi.org/10.1080/08927010400029031>
- Holtgrieve, G. W., Arias, M. E., Irvine, K. N., Lamberts, D., Ward, E. J., Kumm, M., Koponen, J., Sarkkula, J., & Richey, J. E. (2013). Patterns of Ecosystem Metabolism in the Tonle Sap Lake, Cambodia with Links to Capture Fisheries. *PLoS ONE*, 8(8). <https://doi.org/10.1371/journal.pone.0071395>
- Honious, S. A. S., Hale, R. L., Guilinger, J. J., Crosby, B. T., & Baxter, C. v. (2021). Turbidity Structures the Controls of Ecosystem Metabolism and Associated Metabolic Process Domains Along a 75-km Segment of a Semiarid Stream. *Ecosystems*. <https://doi.org/10.1007/s10021-021-00661-5>
- Hornbach, D. J., Schilling, E. G., & Kundel, H. (2020). Ecosystem metabolism in small ponds: The effects of floating-leaved macrophytes. *Water (Switzerland)*, 12(5), 1–25. <https://doi.org/10.3390/w12051458>
- Horton, A. A., Walton, A., Spurgeon, D. J., Lahive, E., & Svendsen, C. (2017). Microplastics in freshwater and terrestrial environments: Evaluating the current understanding to identify the knowledge gaps and future research priorities. *Science of the Total Environment*, 586, 127–141. <https://doi.org/10.1016/j.scitotenv.2017.01.190>
- Hunt, S. M., Werner, E. M., Huang, B., Hamilton, M. A., & Stewart, P. S. (2004). Hypothesis for the role of nutrient starvation in biofilm detachment. *Applied and Environmental Microbiology*, 70(12), 7418–7425. <https://doi.org/10.1128/AEM.70.12.7418-7425.2004>
- Imberger, J. (1985). The diurnal mixed layer. *Limnology and Oceanography*, 30(4), 737–770. <https://doi.org/10.4319/lo.1985.30.4.0737>

- Jackson, C. R. (2003). Changes in community properties during microbial succession. *Oikos*, 101(2), 444–448.
- Jähne, B., & Haußecker, H. (1998). AIR-WATER GAS EXCHANGE. *Annual Review of Fluid Mechanics*, 30(1), 443–468.
- Jähne, B., Münnich, K. O., Bössinger, R., Dutzi, A., Huber, W., & Libner, P. (1987). On the Parameters Influencing Air-Water Gas Exchange of magnitude lower in the water than in the air, information, which in turn has also hindered transfer in the water $k +$. *Journal of Geophysical Research*, 92(C2), 1937–1949.
- Jane, S. F., & Rose, K. C. (2018). Carbon quality regulates the temperature dependence of aquatic ecosystem respiration. *Freshwater Biology*, 63(11), 1407–1419. <https://doi.org/10.1111/fwb.13168>
- Jankowski, K. J., Mejia, F. H., Blaszcak, J. R., & Holtgrieve, G. W. (2021). Aquatic ecosystem metabolism as a tool in environmental management. *Wiley Interdisciplinary Reviews: Water*, 8(4), 1–27. <https://doi.org/10.1002/wat2.1521>
- Jefferson, K. K. (2004). What drives bacteria to produce a biofilm? *FEMS Microbiology Letters*, 236(2), 163–173. <https://doi.org/10.1016/j.femsle.2004.06.005>
- Jepsen, E. M., & de Bruyn, P. J. N. (2019). Pinniped entanglement in oceanic plastic pollution: A global review. *Marine Pollution Bulletin*, 145(December 2018), 295–305. <https://doi.org/10.1016/j.marpolbul.2019.05.042>
- Kaiser, D., Kowalski, N., & Waniek, J. J. (2017). Effects of biofouling on the sinking behavior of microplastics. *Environmental Research Letters*, 12(12). <https://doi.org/10.1088/1748-9326/aa8e8b>
- Kalyuzhnaya, M. G., Martens-Habbena, W., Wang, T., Hackett, M., Stolyar, S. M., Stahl, D. A., Lidstrom, M. E., & Chistoserdova, L. (2009). Methylophilaceae link methanol oxidation to denitrification in freshwater lake sediment as suggested by stable isotope probing and pure culture analysis. *Environmental Microbiology Reports*, 1(5), 385–392. <https://doi.org/10.1111/j.1758-2229.2009.00046.x>
- Kana, T. M., Darkangelo, C., Hunt, M. D., Oldham, J. B., Bennett, G. E., & Cornwell, J. C. (1994). Membrane Inlet Mass Spectrometer for Rapid High-Precision Determination of N₂, O₂, and Ar in Environmental Water Samples. *Analytical Chemistry*, 66(23), 4166–4170. <https://doi.org/10.1021/ac00095a009>

- Kana, T. M., Sullivan, M. B., Cornwell, J. C., & Groszkowski, K. M. (1998). Denitrification in estuarine sediments determined by membrane inlet mass spectrometry. *Limnology and Oceanography*, 43(2), 334–339. <https://doi.org/10.4319/lo.1998.43.2.0334>
- Katsikogianni, M., Missirlis, Y. F., Harris, L., & Douglas, J. (2004). Concise review of mechanisms of bacterial adhesion to biomaterials and of techniques used in estimating bacteria-material interactions. *European Cells and Materials*, 8, 37–57. <https://doi.org/10.22203/eCM.v008a05>
- Kesy, K., Oberbeckmann, S., Kreikemeyer, B., & Labrenz, M. (2019). Spatial Environmental Heterogeneity Determines Young Biofilm Assemblages on Microplastics in Baltic Sea Mesocosms. *Frontiers in Microbiology*, 10(August), 1–18. <https://doi.org/10.3389/fmicb.2019.01665>
- Kettner, M. T., Oberbeckmann, S., Labrenz, M., & Grossart, H.-P. (2019). The eukaryotic life on microplastics in brackish ecosystems. *Frontiers in Microbiology*, 10(MAR). <https://doi.org/10.3389/fmicb.2019.00538>
- Langman, O., Hanson, P., Carpenter, S., & Hu, Y. (2010). Control of dissolved oxygen in northern temperate lakes over scales ranging from minutes to days. *Aquatic Biology*, 9(2), 193–202. <https://doi.org/10.3354/ab00249>
- Lebreton, L. C. M., van der Zwet, J., Damsteeg, J. W., Slat, B., Andrady, A., & Reisser, J. (2017). River plastic emissions to the world's oceans. *Nature Communications*, 8, 1–10. <https://doi.org/10.1038/ncomms15611>
- Li, W., Zhang, Y., Wu, N., Zhao, Z., Xu, W., Ma, Y., & Niu, Z. (2019). Colonization Characteristics of Bacterial Communities on Plastic Debris Influenced by Environmental Factors and Polymer Types in the Haihe Estuary of Bohai Bay, China. *Environmental Science and Technology*, 53(18), 10763–10773. <https://doi.org/10.1021/acs.est.9b03659>
- Liu, S., Huang, Y., Luo, D., Wang, X., Wang, Z., Ji, X., Chen, Z., Dahlgren, R. A., Zhang, M., & Shang, X. (2022). Integrated effects of polymer type, size and shape on the sinking dynamics of biofouled microplastics. *Water Research*, 220(May), 118656. <https://doi.org/10.1016/j.watres.2022.118656>
- Lobelle, D., & Cunliffe, M. (2011). Early microbial biofilm formation on marine plastic debris. *Marine Pollution Bulletin*, 62(1), 197–200. <https://doi.org/10.1016/j.marpolbul.2010.10.013>
- Loeks-Johnson, B. M., & Cotner, J. B. (2020). Upper Midwest lakes are supersaturated with N₂. *Proceedings of the National Academy of Sciences of the United States of America*, 117(29), 17063–17067. <https://doi.org/10.1073/pnas.1921689117>

- López-Rojo, N., Pérez, J., Basaguren, A., Pozo, J., Rubio-Ríos, J., Casas, J. J., & Boyero, L. (2020). Effects of two measures of riparian plant biodiversity on litter decomposition and associated processes in stream microcosms. *Scientific Reports*, *10*(1), 1–10. <https://doi.org/10.1038/s41598-020-76656-4>
- Lyautey, E., Jackson, C. R., Cayrou, J., Rols, J.-L., & Garabetian, F. (2005). Bacterial Community Succession in Natural River Biofilm Assemblages. *Microbial Ecology*, *50*, 589–601. <https://doi.org/10.1007/s00248-005-5032-9>
- Lyons, K. G., Brigham, C. A., Traut, B. H., & Schwartz, M. W. (2005). Rare species and ecosystem functioning. *Conservation Biology*, *19*(4), 1019–1024. <https://doi.org/10.1111/j.1523-1739.2005.00106.x>
- MacIntyre, S., Romero, J. R., & Kling, G. W. (2002). Spatial-temporal variability in surface layer deepening and lateral advection in an embayment of Lake Victoria, East Africa. *Limnology and Oceanography*, *47*(3), 656–671. <https://doi.org/10.4319/lo.2002.47.3.0656>
- Mai, L., Sun, X. F., Xia, L. L., Bao, L. J., Liu, L. Y., & Zeng, E. Y. (2020). Global Riverine Plastic Outflows. *Environmental Science and Technology*, *54*(16), 10049–10056. <https://doi.org/10.1021/acs.est.0c02273>
- Matthews, C. J. D., St. Louis, V. L., & Hesslein, R. H. (2003). Comparison of three techniques used to measure diffusive gas exchange from sheltered aquatic surfaces. *Environmental Science and Technology*, *37*(4), 772–780. <https://doi.org/10.1021/es0205838>
- McCarthy, M. J., Gardner, W. S., Lehmann, M. F., Guindon, A., & Bird, D. F. (2016). Benthic nitrogen regeneration, fixation, and denitrification in a temperate, eutrophic lake: Effects on the nitrogen budget and cyanobacteria blooms. *Limnology and Oceanography*, *61*(4), 1406–1423. <https://doi.org/10.1002/lno.10306>
- McCarthy, M. J., Lavrentyev, P. J., Yang, L., Zhang, L., Chen, Y., Qin, B., & Gardner, W. S. (2007a). Nitrogen dynamics and microbial food web structure during a summer cyanobacterial bloom in a subtropical, shallow, well-mixed, eutrophic lake (Lake Taihu, China). *Hydrobiologia*, *581*(1), 195–207. <https://doi.org/10.1007/s10750-006-0496-2>
- McCarthy, M. J., Lavrentyev, P. J., Yang, L., Zhang, L., Chen, Y., Qin, B., & Gardner, W. S. (2007b). Nitrogen dynamics and microbial food web structure during a summer cyanobacterial bloom in a subtropical, shallow, well-mixed, eutrophic lake (Lake Taihu, China). *Hydrobiologia*, *581*(1), 195–207. <https://doi.org/10.1007/s10750-006-0496-2>
- McCormick, A. R., & Hoellein, T. J. (2016). Anthropogenic litter is abundant, diverse, and mobile in urban rivers: Insights from cross-ecosystem analyses using ecosystem and community ecology tools. *Limnology and Oceanography*. <https://doi.org/10.1002/lno.10328>

- McCormick, A. R., Hoellein, T. J., London, M. G., Hittie, J., Scott, J. W., & Kelly, J. J. (2016). Microplastic in surface waters of urban rivers: Concentration, sources, and associated bacterial assemblages. *Ecosphere*, 7(11). <https://doi.org/10.1002/ecs2.1556>
- McGivney, E., Cederholm, L., Barth, A., Hakkarainen, M., Hamacher-Barth, E., Ogonowski, M., & Gorokhova, E. (2020). Rapid Physicochemical Changes in Microplastic Induced by Biofilm Formation. *Frontiers in Bioengineering and Biotechnology*, 8(March), 1–14. <https://doi.org/10.3389/fbioe.2020.00205>
- McMurdie, P. J., & Holmes, S. (2013). Phyloseq: An R Package for Reproducible Interactive Analysis and Graphics of Microbiome Census Data. *PLoS ONE*, 8(4). <https://doi.org/10.1371/journal.pone.0061217>
- McNair, J. N., Gereaux, L. C., Weinke, A. D., Sesselmann, M. R., Kendall, S. T., & Biddanda, B. A. (2013). New methods for estimating components of lake metabolism based on free-water dissolved-oxygen dynamics. *Ecological Modelling*, 263, 251–263. <https://doi.org/10.1016/j.ecolmodel.2013.05.010>
- Metropolitan Water Reclamation District of Greater Chicago. (2019, March 3). Terrence J. O'Brien Water Reclamation Plant. Metropolitan Water Reclamation District of Greater Chicago. Retrieved September 3, 2022, from https://mwrdd.org/sites/default/files/documents/Fact_Sheet_O%27Brien.pdf
- Miao, L., Wang, P., Hou, J., Yao, Y., Liu, Z., Liu, S., & Li, T. (2019). Distinct community structure and microbial functions of biofilms colonizing microplastics. *Science of the Total Environment*, 650, 2395–2402. <https://doi.org/10.1016/j.scitotenv.2018.09.378>
- Mills, L. J., & Chichester, C. (2005). Review of evidence: Are endocrine-disrupting chemicals in the aquatic environment impacting fish populations? *Science of the Total Environment*, 343(1–3), 1–34. <https://doi.org/10.1016/j.scitotenv.2004.12.070>
- Min, K., Cuiffi, J. D., & Mathers, R. T. (2020). Ranking environmental degradation trends of plastic marine debris based on physical properties and molecular structure. *Nature Communications*, 11(1), 1–11. <https://doi.org/10.1038/s41467-020-14538-z>
- Molot, L. A., Higgins, S. N., Schiff, S. L., Venkiteswaran, J. J., Paterson, M. J., & Baulch, H. M. (2021). Phosphorus-only fertilization rapidly initiates large nitrogen-fixing cyanobacteria blooms in two oligotrophic lakes. *Environmental Research Letters*, 16(6). <https://doi.org/10.1088/1748-9326/ac0564>
- Mulholland, P. J., Helton, A. M., Poole, G. C., Hall, R. O., Hamilton, S. K., Peterson, B. J., Tank, J. L., Ashkenas, L. R., Cooper, L. W., Dahm, C. N., Dodds, W. K., Findlay, S. E. G.,

- Gregory, S. v., Grimm, N. B., Johnson, S. L., McDowell, W. H., Meyer, J. L., Valett, H. M., Webster, J. R., ... Thomas, S. M. (2008). Stream denitrification across biomes and its response to anthropogenic nitrate loading. *Nature*, *452*(7184), 202–205. <https://doi.org/10.1038/nature06686>
- Murali, A., Bhargava, A., & Wright, E. S. (2018). IDTAXA: A novel approach for accurate taxonomic classification of microbiome sequences. *Microbiome*, *6*(1), 1–14. <https://doi.org/10.1186/s40168-018-0521-5>
- Muthukrishnan, T., al Khaburi, M., & Abed, R. M. M. (2019). Fouling Microbial Communities on Plastics Compared with Wood and Steel: Are They Substrate- or Location-Specific? *Microbial Ecology*, *78*(2), 361–374. <https://doi.org/10.1007/s00248-018-1303-0>
- Nakashima, E., Isobe, A., Kako, S., Itai, T., & Takahashi, S. (2012). Quantification of toxic metals derived from macroplastic litter on Ookushi Beach, Japan. *Environmental Science and Technology*, *46*(18), 10099–10105. <https://doi.org/10.1021/es301362g>
- Napper, I. E., & Thompson, R. C. (2020). Plastic Debris in the Marine Environment: History and Future Challenges. *Global Challenges*, *4*(6), 1900081. <https://doi.org/10.1002/gch2.201900081>
- Nauendorf, A., Krause, S., Bigalke, N. K., Gorb, E. v., Gorb, S. N., Haeckel, M., Wahl, M., & Treude, T. (2016). Microbial colonization and degradation of polyethylene and biodegradable plastic bags in temperate fine-grained organic-rich marine sediments. *Marine Pollution Bulletin*, *103*(1–2), 168–178. <https://doi.org/10.1016/j.marpolbul.2015.12.024>
- Norman, B. C., Frost, P. C., Blakelock, G. C., Higgins, S. N., Hoque, M. E., Vincent, J. L., Cetinic, K., & Xenopoulos, M. A. (2019). Muted responses to Ag accumulation by plankton to chronic and pulse exposure to silver nanoparticles in a boreal lake. *Facets*, *2019*(4), 566–583. <https://doi.org/10.1139/facets-2018-0047>
- Oberbeckmann, S., Bartosik, D., Huang, S., Werner, J., Hirschfeld, C., Wibberg, D., Heiden, S. E., Bunk, B., Overmann, J., Becher, D., Kalinowski, J., Schweder, T., Labrenz, M., & Markert, S. (2021). Genomic and proteomic profiles of biofilms on microplastics are decoupled from artificial surface properties. *Environmental Microbiology*, *23*(6), 3099–3115. <https://doi.org/10.1111/1462-2920.15531>
- Oberbeckmann, S., Kreikemeyer, B., & Labrenz, M. (2018). Environmental factors support the formation of specific bacterial assemblages on microplastics. *Frontiers in Microbiology*, *8*(JAN), 1–12. <https://doi.org/10.3389/fmicb.2017.02709>

- Oberbeckmann, S., & Labrenz, M. (2020). Marine Microbial Assemblages on Microplastics: Diversity, Adaptation, and Role in Degradation. *Annual Review of Marine Science*, 12, 209–232. <https://doi.org/10.1146/annurev-marine-010419-010633>
- Obertegger, U., Obrador, B., & Flaim, G. (2017). Dissolved oxygen dynamics under ice: Three winters of high-frequency data from Lake Tovel, Italy. *Water Resources Research*, 53(8), 7234–7246. <https://doi.org/10.1002/2017WR020599>
- Odum, Howard, T. (1956). Primary Production in Flowing Waters. *Limnology and Oceanography*, 1(2), 102–117. <https://doi.org/10.4319/lo.1956.1.2.0102>
- Oksanen, A. J., Blanchet, F. G., Friendly, M., Kindt, R., Legendre, P., Mcglinn, D., Minchin, P. R., Hara, R. B. O., Simpson, G. L., Solymos, P., Stevens, M. H. H., & Szoecs, E. (2020). *Vegan: community ecology package* (pp. 2395–2396). https://doi.org/10.1007/978-94-024-1179-9_301576
- Pace, M. L., Buelo, C. D., & Carpenter, S. R. (2021). Phytoplankton biomass, dissolved organic matter, and temperature drive respiration in whole lake nutrient additions. *Limnology and Oceanography*, 66(6), 2174–2186. <https://doi.org/10.1002/lno.11738>
- Parrish, K., & Fahrenfeld, N. L. (2019). Microplastic biofilm in fresh- And wastewater as a function of microparticle type and size class. *Environmental Science: Water Research and Technology*, 5(3), 495–505. <https://doi.org/10.1039/c8ew00712h>
- Pettersen, R. C. (1984). The chemical composition of wood. In *The Chemistry of Solid Wood* (Vol. 207, pp. 57–126). <https://doi.org/10.1038/116610a0>
- Plastics Europe. (2021). *Plastics - the Facts 2021*. Plastics Europe Market Research Group (PEMRG) and Conversio Market & Strategy GmbH. <https://plasticseurope.org/>
- Quast, C., Pruesse, E., Yilmaz, P., Gerken, J., Schweer, T., Yarza, P., Peplies, J., & Glöckner, F. O. (2013). The SILVA ribosomal RNA gene database project: Improved data processing and web-based tools. *Nucleic Acids Research*, 41(D1), 590–596. <https://doi.org/10.1093/nar/gks1219>
- R Core Team (2021). R: A language and environment for statistical computing. R Foundation for Statistical Computing, Vienna, Austria. URL <https://www.R-project.org/>.
- Rabaey, J. S., Domine, L. M., Zimmer, K. D., & Cotner, J. B. (2021). Winter Oxygen Regimes in Clear and Turbid Shallow Lakes. *Journal of Geophysical Research: Biogeosciences*, 126(3), 1–15. <https://doi.org/10.1029/2020JG006065>

- Read, J. S., Hamilton, D. P., Jones, I. D., Muraoka, K., Winslow, L. A., Kroiss, R., Wu, C. H., & Gaiser, E. (2011). Derivation of lake mixing and stratification indices from high-resolution lake buoy data. *Environmental Modelling and Software*, 26(11), 1325–1336. <https://doi.org/10.1016/j.envsoft.2011.05.006>
- Reisinger, A. J., Tank, J. L., Hoellein, T. J., & Hall, R. O. (2016). Sediment, water column, and open-channel denitrification in rivers measured using membrane-inlet mass spectrometry. *Journal of Geophysical Research: Biogeosciences*, 121(5), 1258–1274. <https://doi.org/10.1002/2015JG003261>
- Renner, L. D., & Weibel, D. B. (2011). Physicochemical regulation of biofilm formation. *MRS Bulletin*, 36(5), 347–355. <https://doi.org/10.1557/mrs.2011.65.Physicochemical>
- Richardson, D. C., Carey, C. C., Bruesewitz, D. A., & Weathers, K. C. (2017). Intra- and inter-annual variability in metabolism in an oligotrophic lake. *Aquatic Sciences*, 79(2), 319–333. <https://doi.org/10.1007/s00027-016-0499-7>
- Rochman, C. M., Brookson, C., Bikker, J., Djuric, N., Earn, A., Bucci, K., Athey, S., Huntington, A., McIlwraith, H., Munno, K., Frond, H. de, Kolomijeca, A., Erdle, L., Grbic, J., Bayoumi, M., Borrelle, S. B., Wu, T., Santoro, S., Werbowski, L. M., ... Hung, C. (2019). Rethinking microplastics as a diverse contaminant suite. *Environmental Toxicology and Chemistry*, 38(4), 703–711. <https://doi.org/10.1002/etc.4371>
- Rochman, C. M., Hoh, E., Kurobe, T., & Teh, S. J. (2013). Ingested plastic transfers hazardous chemicals to fish and induces hepatic stress. *Scientific Reports*, 3, 1–7. <https://doi.org/10.1038/srep03263>
- Rose, K. C., Winslow, L. A., Read, J. S., Read, E. K., Solomon, C. T., Adrian, R., & Hanson, P. C. (2014). Improving the precision of lake ecosystem metabolism estimates by identifying predictors of model uncertainty. *Limnology and Oceanography: Methods*, 12(MAY), 303–312. <https://doi.org/10.4319/lom.2014.12.303>
- Royer, S.-J., Ferron, S., Wilson, S. T., & Karl, D. M. (2018). Production of methane and ethylene from plastic in the environment. *Journal of Computational and Applied Mathematics*, 13(8), e0200574. <https://doi.org/10.1016/j.cam.2010.07.024>
- Rummel, C. D., Lechtenfeld, O. J., Kallies, R., Benke, A., Herzsprung, P., Rynek, R., Wagner, S., Potthoff, A., Jahnke, A., & Schmitt-Jansen, M. (2021). Conditioning Film and Early Biofilm Succession on Plastic Surfaces. *Environmental Science and Technology*, 55(16), 11006–11018. <https://doi.org/10.1021/acs.est.0c07875>
- Ryan, P. G., Moore, C. J., van Franeker, J. A., & Moloney, C. L. (2009). Monitoring the abundance of plastic debris in the marine environment. *Philosophical Transactions of the*

Royal Society B: Biological Sciences, 364(1526), 1999–2012.
<https://doi.org/10.1098/rstb.2008.0207>

- Sanchez, W., Bender, C., & Porcher, J. M. (2014). Wild gudgeons (*Gobio gobio*) from French rivers are contaminated by microplastics: Preliminary study and first evidence. *Environmental Research*, 128, 98–100. <https://doi.org/10.1016/j.envres.2013.11.004>
- Sartory, D. P., & Grobbelaar, J. U. (1984). Extraction of chlorophyll a from freshwater phytoplankton for spectrophotometric analysis. *Hydrobiologia*, 114(3), 177–187. <https://doi.org/10.1007/BF00031869>
- Saunders, L. J., Rodriguez-Gil, J. L., Stoyanovich, S. S., Kimpe, L. E., Hanson, M. L., Hollebhone, B. P., Orihel, D. M., & Blais, J. M. (2022). Effect of spilled diluted bitumen on chemical air-water exchange in boreal lake limnocorrals. *Chemosphere*, 291(P1), 132708. <https://doi.org/10.1016/j.chemosphere.2021.132708>
- Sawyer, L. K., & Hermanowicz, S. W. (1998). Detachment of biofilm bacteria due to variations in nutrient supply. *Water Science and Technology*, 37(4–5), 211–214. [https://doi.org/10.1016/S0273-1223\(98\)00108-5](https://doi.org/10.1016/S0273-1223(98)00108-5)
- Schindler, D. W. (1974). Eutrophication and recovery in experimental lakes: Implications for lake management. *Science*, 184(4139), 897–899. <https://doi.org/10.1126/science.184.4139.897>
- Schindler, D. W. (1977). Evolution of phosphorus limitation in lakes. *Science*, 195(4275), 260–262. <https://doi.org/10.1126/science.195.4275.260>
- Schindler, D. W. (1988). Experimental studies of chemical stressors on whole lake ecosystems. *SIL Proceedings, 1922-2010*, 23(1), 11–41. <https://doi.org/10.1080/03680770.1987.11897899>
- Schindler, D. W. (1990). Experimental Perturbations of Whole Lakes as Tests of Hypotheses concerning Ecosystem Structure and Function Published by : Wiley on behalf of Nordic Society Oikos Stable URL : <http://www.jstor.org/stable/3565733> REFERENCES Linked ref. *Oikos*, 57(1), 25–41. <http://www.jstor.org/myaccess.library.utoronto.ca/stable/pdf/3565733.pdf>
- Schindler, D. W., Wagemann, R., Cook, R. B., Rusczyński, T., & Prokopowich, J. (1980). Experimental Acidification of Lake 223, Experimental Lakes Area: Background Data and the First Three Years of Acidification. *Canadian Journal of Fisheries and Aquatic Sciences*, 37(3), 342–354. <https://doi.org/10.1139/f80-048>

- Schuyler, Q., Hardesty, B. D., Wilcox, C., & Townsend, K. (2014). Global Analysis of Anthropogenic Debris Ingestion by Sea Turtles. *Conservation Biology*, 28(1), 129–139. <https://doi.org/10.1111/cobi.12126>
- Seeley, M. E., Song, B., Passie, R., & Hale, R. C. (2020). Microplastics affect sedimentary microbial communities and nitrogen cycling. *Nature Communications*, 11(1), 1–10. <https://doi.org/10.1038/s41467-020-16235-3>
- Shen, C., Huang, L., Xie, G., Wang, Y., Ma, Z., Yao, Y., & Yang, H. (2021). Effects of plastic debris on the biofilm bacterial communities in lake water. *Water (Switzerland)*, 13(11), 1–13. <https://doi.org/10.3390/w13111465>
- Sherwood, A. R., & Presting, G. G. (2007). Universal primers amplify a 23S rDNA plastid marker in eukaryotic algae and cyanobacteria. *Journal of Phycology*, 43(3), 605–608. <https://doi.org/10.1111/j.1529-8817.2007.00341.x>
- Solomon, C. T., Bruesewitz, D. A., Richardson, D. C., Rose, K. C., van de Bogert, M. C., Hanson, P. C., Kratz, T. K., Larget, B., Adrian, R., Leroux Babin, B., Chiu, C. Y., Hamilton, D. P., Gaiser, E. E., Hendricks, S., Istvá, V., Laas, A., O'Donnell, D. M., Pace, M. L., Ryder, E., ... Zhu, G. (2013a). Ecosystem respiration: Drivers of daily variability and background respiration in lakes around the globe. *Limnology and Oceanography*, 58(3), 849–866. <https://doi.org/10.4319/lo.2013.58.3.0849>
- Solomon, C. T., Bruesewitz, D. A., Richardson, D. C., Rose, K. C., van de Bogert, M. C., Hanson, P. C., Kratz, T. K., Larget, B., Adrian, R., Leroux Babin, B., Chiu, C. Y., Hamilton, D. P., Gaiser, E. E., Hendricks, S., Istvá, V., Laas, A., O'Donnell, D. M., Pace, M. L., Ryder, E., ... Zhu, G. (2013b). Ecosystem respiration: Drivers of daily variability and background respiration in lakes around the globe. *Limnology and Oceanography*, 58(3), 849–866. <https://doi.org/10.4319/lo.2013.58.3.0849>
- Staehr, P. A., Bade, D., van de Bogert, M. C., Koch, G. R., Williamson, C., Hanson, P., Cole, J. J., & Kratz, T. (2010). Lake metabolism and the diel oxygen technique: State of the science. *Limnology and Oceanography: Methods*, 8(NOV), 628–644. <https://doi.org/10.4319/lom.2010.8.0628>
- Stefanidis, K., & Dimitriou, E. (2019). Differentiation in aquatic metabolism between littoral habitats with floating-leaved and submerged macrophyte growth forms in a shallow eutrophic lake. *Water (Switzerland)*, 11(2). <https://doi.org/10.3390/w11020287>
- Tirola, M. A., Rissanen, A. J., Sarpakunnas, M., Arvola, L., & Nykänen, H. (2011). Stable isotope profiles of nitrogen gas indicate denitrification in oxygen-stratified humic lakes. *Rapid Communications in Mass Spectrometry*, 25(11), 1497–1502. <https://doi.org/10.1002/rcm.4917>

- Ulseth, A. J., Bertuzzo, E., Singer, G. A., Schelker, J., & Battin, T. J. (2018). Climate-Induced Changes in Spring Snowmelt Impact Ecosystem Metabolism and Carbon Fluxes in an Alpine Stream Network. *Ecosystems*, 21(2), 373–390. <https://doi.org/10.1007/s10021-017-0155-7>
- Vachon, D., & Prairie, Y. T. (2013). The ecosystem size and shape dependence of gas transfer velocity versus wind speed relationships in lakes. *Canadian Journal of Fisheries and Aquatic Sciences*, 70(12), 1757–1764. <https://doi.org/10.1139/cjfas-2013-0241>
- Vincent, A. E. S., Chaudhary, A., Kelly, J. J., & Hoellein, T. J. (2022). Biofilm assemblage and activity on plastic in urban streams at a continental scale: Site characteristics are more important than substrate type. *Science of The Total Environment*, 835(February), 155398. <https://doi.org/10.1016/j.scitotenv.2022.155398>
- Vincent, A. E. S., & Hoellein, T. J. (2021). Distribution and transport of microplastic and fine particulate organic matter in urban streams. *Ecological Applications*, 0(0), 1–16. <https://doi.org/10.1002/eap.2429>
- Wang, T.-H., Huang, C.-C., & Hung, J.-H. (2021). EARRINGS: an efficient and accurate adapter trimmer entails no a priori adapter sequences. *Bioinformatics*, January, 1–7. <https://doi.org/10.1093/bioinformatics/btab025>
- Webster, J. R., Benfield, E. F., Ehrman, T. P., Schaeffer, M. A., Tank, J. E., Hutchens, J. J., & D'Angelo, D. J. (1999). What happens to allochthonous material that falls into streams? A synthesis of new and published information from Coweeta. *Freshwater Biology*, 41(4), 687–705. <https://doi.org/10.1046/j.1365-2427.1999.00409.x>
- Weiss, R. F. (1970). The solubility of nitrogen, oxygen and argon in water and seawater. *Deep-Sea Research and Oceanographic Abstracts*, 17(4), 721–735. [https://doi.org/10.1016/0011-7471\(70\)90037-9](https://doi.org/10.1016/0011-7471(70)90037-9)
- Wharton, R. A. J., McKay, C. P., Mancinelli, R. L., & Simmons, G. M. J. (1987). Perennial N₂ supersaturation in an Antarctic lake. *Nature*, 325(22), 343–345.
- Wilson, E. O., & MacArthur, R. H. (1967). *The theory of island biogeography* (Vol. 1). Princeton University Press.
- Windsor, F. M., Durance, I., Horton, A. A., Thompson, R. C., Tyler, C. R., & Ormerod, S. J. (2019). A catchment-scale perspective of plastic pollution. *Global Change Biology*, 25(4), 1207–1221. <https://doi.org/10.1111/gcb.14572>

- Winslow, L. A., Zwart, J. A., Batt, R. D., Dugan, H. A., Woolway, R. I., Corman, J. R., Hanson, P. C., & Read, J. S. (2016). LakeMetabolizer: an R package for estimating lake metabolism from free-water oxygen using diverse statistical models. *Inland Waters*, 6(4), 622–636. <https://doi.org/10.1080/iw-6.4.883>
- Wobbrock, Jacob O., Findlater, Leah., Gergle, Darren., Higgins, J. J. (2011). The Aligned Rank Transform for Nonparametric Factorial Analyses Using Only ANOVA Procedures. *Proceedings of the SIGCHI Conference on Human Factors in Computing Systems*, 143–146. <https://doi.org/10.1145/1978942.1978963>
- Wright, R. J., Erni-Cassola, G., Zadjelovic, V., Latva, M., & Christie-Oleza, J. A. (2020). Marine Plastic Debris: A New Surface for Microbial Colonization. *Environmental Science and Technology*, 54(19), 11657–11672. <https://doi.org/10.1021/acs.est.0c02305>
- Wright, R. J., Langille, M. G. I., & Walker, T. R. (2021). Food or just a free ride? A meta-analysis reveals the global diversity of the Plastisphere. *ISME Journal*, 15(3), 789–806. <https://doi.org/10.1038/s41396-020-00814-9>
- Yang, H., Andersen, T., Dörsch, P., Tominaga, K., Thrane, J. E., & Hessen, D. O. (2015). Greenhouse gas metabolism in Nordic boreal lakes. *Biogeochemistry*, 126(1–2), 211–225. <https://doi.org/10.1007/s10533-015-0154-8>
- Zhao, F., Zhan, X., Xu, H., Zhu, G., Zou, W., Zhu, M., Kang, L., Guo, Y., Zhao, X., Wang, Z., & Tang, W. (2022). New insights into eutrophication management: Importance of temperature and water residence time. *Journal of Environmental Sciences (China)*, 111, 229–239. <https://doi.org/10.1016/j.jes.2021.02.033>
- Zhu, B. K., Fang, Y. M., Zhu, D., Christie, P., Ke, X., & Zhu, Y. G. (2018). Exposure to nanoplastics disturbs the gut microbiome in the soil oligochaete *Enchytraeus crypticus*. *Environmental Pollution*, 239, 408–415. <https://doi.org/10.1016/j.envpol.2018.04.017>
- Zobell, C. E. (1943). The Effect of Solid Surfaces Upon Bacterial Activity. *Journal of Bacteriology*, 204, 39–56.
- Zobell, C. E., & Allen, E. C. (1935). The Significance of Marine Bacteria in the Fouling of Submerged Surfaces. *Journal of Bacteriology*, 29(3), 239–251. <https://doi.org/10.1128/membr.22.1.1-19.1958>

VITA

Mr. Raúl Lazcano González was born and raised in Appleton, Wisconsin. In 2016 Mr. Lazcano graduated from Appleton East High School and enrolled in Loyola University Chicago. At Loyola University Chicago Mr. Lazcano earned a Bachelor of Science degree in Biology with an emphasis in Molecular Biology and graduated *summa cum laude* in 2020. As a graduate student Mr. Lazcano was a teaching assistant for Conservation Biology and Microbiology.